UNIVERSITÀ DEGLI STUDI DI PADOVA

DIPARTIMENTO DI BIOLOGIA

SCUOLA DI DOTTORATO DI RICERCA IN BIOSCIENZE E BIOTECNOLOGIE
INDIRIZZO: BIOLOGIA CELLULARE
XXVI CICLO

THE ENDOPLASMIC RETICULUM-MITOCHONDRIA COUPLING: ROLE OF PRESENILIN-2

Direttore della scuola: Ch.mo Prof. Giuseppe Zanotti
Coordinatore: Ch.mo Prof. Paolo Bernardi
Supervisori: Ch.mo Prof. Tullio Pozzan
Dott.ssa Paola Pizzo

Dottorando: Riccardo Filadi

INDEX

SUMMARY

Alzheimer's Disease (AD) is the most frequent form of dementia. A small percentage of cases is inherited (Familial AD, FAD) and is due to dominant mutations on three genes, coding for Amyloid Precursor Protein (APP), Presenilin-1 (PS1) and Presenilin-2 (PS2).

Mutations in these proteins cause alterations in the cleavage of APP by a PS1- or PS2-containing enzyme, named γ-secretase, thus leading to an increase in the ratio between Aβ42 and Aβ40, the two main peptides finally derived from APP maturation. This in turn would increase the deposition of the "Amyloid Plaques", one of the main histopathological feature of AD. To date, the generation of Aβ42 peptides, its oligomers and finally amyloid plaques is the core of the most widely accepted pathogenic hypothesis for AD, the "Amyloid Cascade Hypothesis".

PS1 and PS2 are ubiquitous "9 trans-membrane domains" homologous proteins localized mainly in the membranes of Endoplasmic Reticulum (ER), Golgi apparatus, endosomes and plasma membrane. Despite being the catalytic core of γ-secretase, PSs display also some specialized, γ-secretase independent activities. On this line, numerous studies reported a role for FAD-linked PS mutations in cellular calcium (Ca^{2+}) alterations.

Ca^{2+} is a key second messenger in living cells and it regulates a multitude of cell functions; thus, alterations in its signaling cascade can be detrimental for cell fate. Ca^{2+} mishandling has been proposed as a causative mechanism for different neurodegenerative diseases and in particular for AD. Although supported by several groups for many years, the Ca^{2+} hypothesis for AD pathogenesis has never been undisputedly accepted, since some data were clearly in contrast, especially those considering PS2 mutations.

In our lab, it was previously shown that several FAD PS2 mutants, but not PS1, reduce ER and Golgi apparatus Ca^{2+} content, mainly by interfering with SERCA activity.

Over the last decade, evidence has accumulated on the existence of continuous flux of information between the ER and mitochondria, two organelles whose privileged interplay modulate key aspects of cell pathophysiology, ranging from lipid metabolism and Ca^{2+} homeostasis to cell death.

Several proteins have been suggested to be involved in keeping the ER and mitochondria at a given distance, allowing the correct organization, their mutual interactions and Ca^{2+} cross-talk. Among them, mitofusin 2 (Mfn2), which is located on both the outer mitochondrial membrane (OMM) and the ER surface, has been shown to take part in

homotypic interactions that contribute to the tethering at the level of mitochondria-associated-membranes (MAMs).
Interestingly, also PS1 and PS2 are enriched in MAMs: we have recently demonstrated that PS2, but not PS1, is able to modulate ER-mitochondria tethering and their Ca^{2+} cross-talk, with PS2-FAD mutants more potent than their wt counterpart in this novel function.

We here investigate the molecular mechanism by which PS2 favours ER-mt tethering, taking into consideration the possibility that PS2 effect depends on the presence of Mfn2.

By crossed genetic complementation and ablation experiments, we found that, in order to modulate ER-mitochondria coupling, PS2 requires the expression of Mfn2 and *viceversa*. In contrast, their homologues PS1 and Mitofusin 1 (Mfn1) are completely dispensable for these functions. Functional and biochemical evidence indicates that PS2 (wt and FAD) needs to physically interact, via its big cytosolic loop, with Mfn2 at both sides of MAM domains, likely forming, or stabilizing, a triple complex made by itself, ER and mitochondrial Mfn2.

Our results clearly suggest that PS2 and Mfn2 cooperate and need one each other to promote ER-mitochondria apposition. On the contrary, their homologues PS1 and Mfn1 are completely dispensable in this function.

In order to explain the stronger effect of FAD-PS2 compared to wt, we performed protein subcellular fractionation from mouse brains, and we observed that in transgenic (tg) mice, carrying FAD-PS2-N141I mutation, PS2 is strongly enriched in MAMs, compared to controls. Moreover, in tg mice also Mfn2 levels are slightly increased in MAMs, thus possibly explaining the stronger tethering in presence of FAD mutations.

We proposed a model in which, being FAD-PS2 more enriched in MAMs compared to wt, it could here recruit more Mfn2 (by physically interacting with it both in *cis* and in *trans)* and form more PS2-Mfn2 complexes critical for determining the apposition between the two organelles.

Finally, the increase in ER-mitochondria coupling was observed not only in FAD-models over-expressing the mutated form of PS2, but also in human fibroblasts from patient carrying the PS2-N141I mutation, thus a condition in which the mutated protein exerts its function independently of any artefact due to its over-expression.

Further investigations will be focused to highlight the mechanism that promotes accumulation into MAMs of FAD-PS2 and whether these stronger FAD-PS2-linked effects on ER-mitochondria coupling are involved in the pathogenesis of AD.

RIASSUNTO

La malattia di Alzheimer (AD) è la forma più frequente di demenza. Una piccola percentuale dei casi è ereditaria (Familial AD, FAD) ed è dovuta a mutazioni autosomiche dominanti in tre geni, che codificano per la Proteina Precursore dell'Amiloide (APP), per Presenilina-1 (PS1) e per Presenilina-2 (PS2).

Le mutazioni in queste proteine causano alterazioni nella maturazione di APP da parte di un enzima (detto γ-secretasi) che contiene alternativamente PS1 o PS2, portando così ad un aumento del rapporto tra Aβ42 e Aβ40, che sono i due principali peptidi prodotti in seguito al taglio di APP. Questo a sua volta induce un aumento della deposizione delle "placche amiloidi", uno dei principali marcatori isto-patologici dell'AD. La generazione del peptide Aβ42, dei suoi oligomeri e delle placche amiloidi costituisce il *core* dell'ipotesi patogenica ad oggi più accreditata per spiegare l'insorgenza della malattia di Alzheimer, ossia "l'ipotesi della cascata amiloide".

PS1 e PS2 sono proteine omologhe ubiquitarie con 9 domini trans-membrana, principalmente localizzate nelle membrane del reticolo endoplasmatico (ER), dell'apparato del Golgi, degli endosomi e in membrana plasmatica. Oltre a costituire il nucleo catalitico della γ-secretasi, le presenilline possiedono anche delle attività specializzate γ-secretasi indipendenti, talvolta non ridondanti tra le due proteine. Per esempio, molti studi hanno evidenziato un ruolo per alcune mutazioni nelle Presenilline associate a FAD nell'alterazione dell'omeostasi del calcio (Ca^{2+}) intracellulare.

Il Ca^{2+} è un secondo messaggero chiave per le cellule e regola numerose funzioni cellulari; pertanto, alterazioni nelle dinamiche di questo ione possono essere estremamente dannose per le cellule e sono state proposte essere alla base di diverse patologie neurodegenerative, tra cui in particolare l'AD. Sebbene sia stata ampiamente supportata da vari gruppi, l'ipotesi dell'alterazione dell'omeostasi del Ca^{2+} alla base dell'insorgenza dell'AD non è mai stata completamente accettata, dal momento che alcuni dati sono chiaramente discordanti, soprattutto per quanto riguarda alcune mutazioni in PS2.

Nel nostro laboratorio, è stato in precedenza dimostrato che diverse mutazioni associate a FAD in PS2, ma non in PS1, riducono il contenuto di Ca^{2+} nell'ER e nell'apparato del Golgi, principalmente attraverso una inibizione della pompa SERCA.

Negli ultimi anni, crescenti evidenze hanno dimostrato l'esistenza di un continuo flusso di informazioni tra l'ER e i mitocondri, due organelli la cui interrelazione modula aspetti chiave nella pato-fisiologia delle cellule, dal metabolismo lipidico alla regolazione dell'omeostasi del Ca^{2+}, fino alla morte cellulare.

Diverse proteine sono state coinvolte nel mantenimento di una appropriata distanza tra l'ER e i mitocondri, permettendo così una corretta organizzazione delle loro reciproche interazioni e dello scambio di Ca^{2+} tra di essi. Tra queste è stato proposto che Mitofusina-2 (Mfn2), localizzata sia sulla membrana mitocondriale esterna (OMM) che, in minore percentuale, sulla superficie dell'ER, moduli il *tethering* fisico tra i due organelli, attraverso delle interazioni di tipo omotipico a livello delle "membrane associate ai mitocondri" (MAM).

Anche PS1 e PS2 sono arricchite a livello delle MAM: nel nostro laboratorio abbiamo recentemente dimostrato che PS2, ma non PS1, modula la vicinanza fisica tra l'ER e i mitocondri, influenzando così lo scambio di Ca^{2+} tra di essi.

Nel lavoro presentato in questa tesi, abbiamo studiato attraverso quale meccanismo molecolare PS2 è in grado di influenzare il *tethering*, prendendo in considerazione la possibilità che l'effetto di PS2 dipenda in qualche modo dalla presenza di Mfn2.

Attraverso esperimenti incrociati di ablazione e ricostituzione genetica, abbiamo dimostrato che per modulare l'accoppiamento tra i due organelli PS2 necessita dell'espressione di Mfn2, e viceversa. Al contrario, le loro proteine omologhe PS1 e Mitofusina-1 (Mfn1) non sembrano essere coinvolte in queste funzioni. Evidenze funzionali e biochimiche indicano che PS2 (wt e FAD) interagisce fisicamente attraverso il suo esteso dominio citosolico con Mfn2 presente in entrambi i lati delle MAM, probabilmente formando o stabilizzando un triplice complesso formato da PS2, da Mfn2 sull'ER e da Mfn2 sulla OMM.

I risultati qui esposti suggeriscono che PS2 e Mfn2 cooperano e necessitano reciprocamente una dell'altra per mantenere il *tethering* tra ER e mitocondri, mentre invece PS1 e Mfn1 non sono necessarie.

Per spiegare l'effetto potenziato sull'accoppiamento tra i due organelli delle forme mutate di PS2 associate a FAD, rispetto alla proteina wt, abbiamo effettuato dei sub-frazionamenti proteici a partire da cervelli di topi. Ciò che abbiamo osservato è che nei topi transgenici (tg),

che portano la mutazione associata a FAD PS2-N141I, PS2 è fortemente arricchita a livello delle MAM, rispetto ai controlli. Inoltre, nei topi transgenici anche Mfn2 è leggermente arricchita nelle MAM, il che potrebbe forse spiegare l'effetto più forte sul *tethering* delle mutazioni FAD. Il modello che proponiamo è che, essendo la PS2 mutata più arricchita nelle MAM rispetto alla forma wt, recluti più Mfn2 (interagendo con essa sia in *cis* che in *trans*) e formi più complessi PS2-Mfn2, i quali sono fondamentali per determinare l'accoppiamento tra i due organelli.

Infine, l'aumentato *tethering* tra ER e mitocondri è stato osservato anche in fibroblasti di un paziente FAD con la mutazione PS2-N141I, ossia una condizione in cui la proteina mutata esercita la sua funzione indipendentemente da qualsiasi possibile artefatto legato alla sua sovra-espressione.

Ulteriori studi saranno necessari per capire quale meccanismo favorisce l'accumulo di PS2 mutata nelle MAM e se l'aumentata vicinanza tra ER e mitocondri, osservata in presenza delle mutazioni in PS2 associate a FAD, sia in qualche modo coinvolta nell'insorgenza o, quantomeno, nella progressione della malattia di Alzheimer.

1. INTRODUCTION

ALZHEIMER'S DISEASE

Alzheimer's disease (AD) is an irreversible neurodegenerative disorder of the central nervous system. From the clinical point of view, the features of the early stage of the pathology usually include a mild impairment in cognitive function (such as acquiring new information), some behavioral alterations and slight short-term memory deficits. Later, personality disorders, severe recent memory and learning impairments, progressive decline in lexical abilities and spatial disorientation appear. Finally, usually after 5-10 years from the first symptoms, also long-term memory is severely impaired, the ability to recognize familial faces is lost, hallucinations, aggressive behavior and aphasia are common, language is reduced to single words and patients became completely non self-sufficient (Förstl H. and Kurz A., 1999).

AD counts more that 20 million cases worldwide and is the most common cause of dementia. Old age is closely linked to AD, but environmental factors and enrichment, diet and hyperlipidemia has been proposed to have an additional role in the onset of the pathology (Förstl H. and Kurz A., 1999). AD is distinguished between the most common "late onset" cases, that affect people > 65 years old, and a small percentage (< 5%) of "early onset" cases. Among the latter, around 15% (*i.e.*, less than 1% of total AD cases) is autosomal, dominantly inherited and represents the familial forms of AD (FAD). The three genes whose mutations are responsible for FAD were identified in the middle of the 90s and are those encoding for Presenilin 1 (PS1, 80% of FAD cases with the most aggressive phenotype and the earliest onset that sometimes can appear at 30-35 years of age), Amyloid Precursor Protein (APP, the 14% of FAD cases) and Presenilin 2 (PS2, 6% of FAD) (Ertekin-Taner N., 2007; Geodert M. and Spillantini M.G., 2006) (See below for more details on these proteins).

Alois Alzheimer first pointed out in 1907 that the disease which would later bear his name has distinct and recognizable neuropathological characteristics. In particular, the two primary cardinal lesions associated with AD are the neurofibrillary tangles and the senile plaques (Perl P.D., 2010; Parihar M.S. and Hemnani T., 2004). From a macroscopic point of view, brain specimens obtained from most AD cases show a modest degree of cerebral cortical atrophy, especially at the level of the frontotemporal cortex and the parietal lobe, and a more significant atrophy of the hippocampus. The loss of brain tissue is generally associated to a dilation of the lateral ventricles (Fig.1). However, among advanced age

subjects, there is considerable overlap between brain morphology of normal individuals and age-matched AD patients. In early onset AD cases, instead, comparisons with age-matched controls reveals a clear difference upon gross inspection of the brain (Perl P.D., 2010). Studies using new neuroimaging techniques (such as ^{18}F-FDG PET that is able to reveal regional hypometabolism of glucose in the brain) and fluid biomarkers suggest that AD could be detected pre-clinically, although to date there is not yet consensus on their diagnostic use (Perrin R.J. et al., 2009).

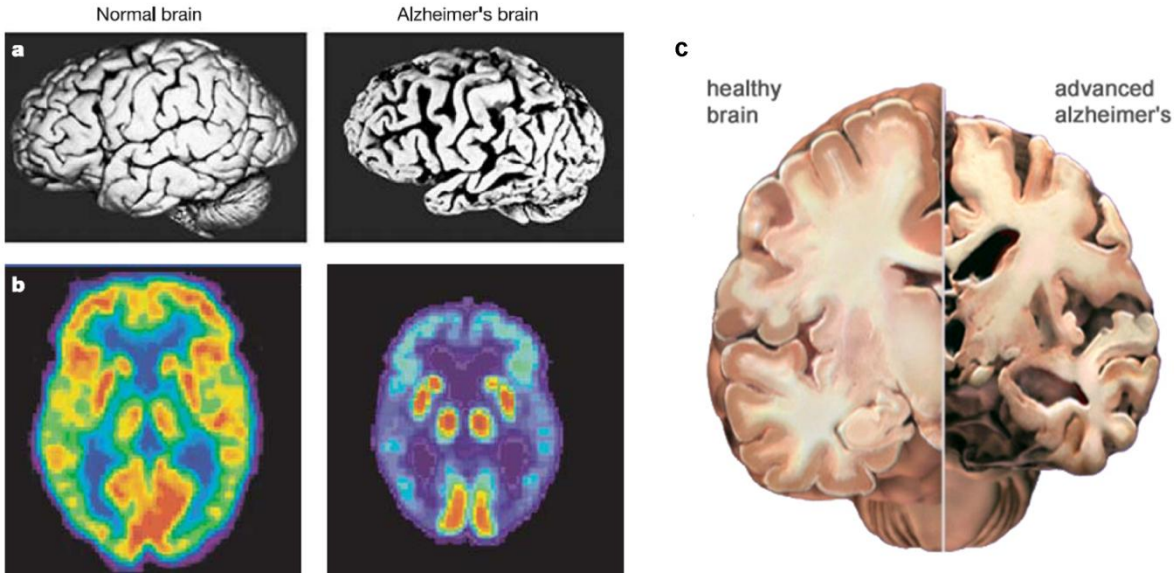

Fig.1: a) and c) Macroscopic alterations observed in AD brain; b) PET scans reveal a lower glucose utilization in AD brain (modified from Mattson M.P., 2004 and from alz.org web site).

On the other hand, as anticipated above, the main microscopic alterations are neurofibrillary tangles (NFT) and senile plaques (Fig.2). The tangles are abnormal fibrous inclusions within the perikaryal cytoplasm of some neurons and in the dystrophic axons that surround the plaques. Ultrastructurally, they are composed of abnormal fibrils measuring 10 nm in diameter that occur in pairs and are wound in a helical fashion with a regular periodicity of 80 nm. The primary constituent of the NFT is the abnormally phosphorylated microtubule-associated protein *tau*, although a number of other proteins have been found to be associated with the tangles, such as ubiquitin, cholinesterases, and beta-amyloid (Perl P.D., 2010). The senile (amyloid) plaques are extracellular structures characterized by a central core mainly constituted by the amyloid beta peptide (Aβ), that forms insoluble fibrils. This peptide derives from the maturation of the aforementioned APP (see below for details on APP maturation), and assumes a typical β-sheet configuration that enables it to bind the Congo Red dye, although other immuno-istochemical techniques are now preferred to better

visualize the plaques. The central cores of senile plaques have been shown to contain several other proteins, such as heparan sulfate glycoproteins, apolipoprotein E, complement proteins, and alpha-1-antichymotrypsin (Perl P.D., 2010). The plaques are often surrounded by dystrophic neurites, microglia and reactive astrocytes. Whether these microglial cells are actively involved in a neuroinflammatory pathogenic cascade, or are reacting to the presence of constituents within these lesions, remains a matter of intense debate.

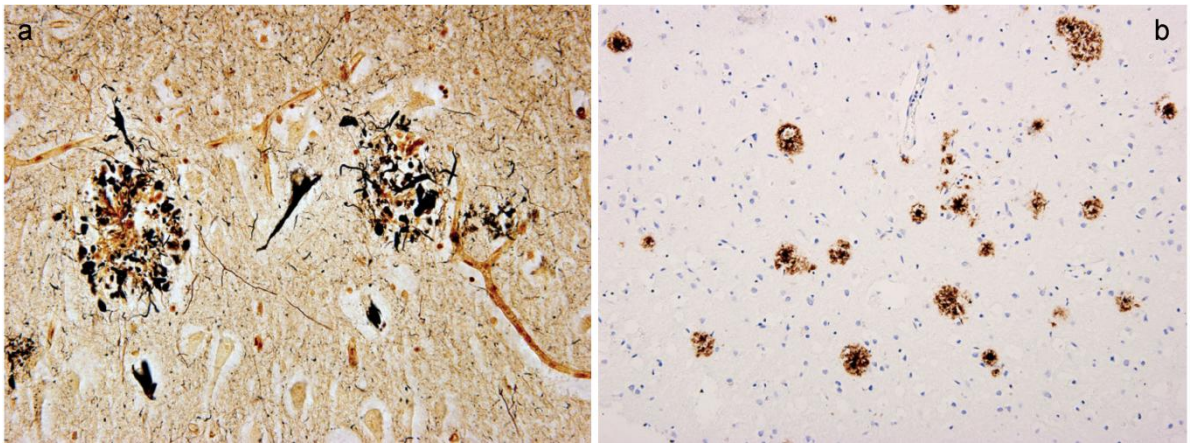

Fig.2: a) Two amyloid plaques surrounded by dystrophic neurites and a neurofibrillary tangle between them in the cortex of an AD patient; b) Immuno-histochemical techniques allow to visualize amyloid plaques (modified from Perl P.D., 2010).

However, it must be underlined that all the macro- and micro-alterations that can be observed in AD accumulate within the brain over a period of many years and could be observed, to some degree, also in brains of normal old-age subjects. For this reason, the presence of these alterations is not sufficient, alone, to diagnose AD.

γ-SECRETASE

γ–secretase is a large enzymatic complex composed of four different integral membrane proteins, responsible for the generation of the amyloid beta peptide (Aβ) from the C-terminal fragment of APP. The peculiar ability of γ–secretase to mediate an intra-membrane protein cleavage is shared with only few other enzymes, called I-CLiPs (intramembrane-cleaving proteases). In particular γ–secretase is an aspartyl protease and can cleave a lot of different substrates, with few specificity and requiring few common features, like being type I transmembrane proteins (Tolia A. and De Strooper B., 2009). Among them there are APP, Notch, Delta1, E- and N- cadherins, CD44, Nectina-1α, ErbB4 and the β2 subunit of the voltage dependent Na^+ channel (McCarthy J.V. et al., 2009).

The four γ–secretase components that have been shown to be necessary and sufficient for the enzymatic activity are Presenilin (either PS1 or PS2), Nicastrin (NCT), Antherior Pharynx-defective 1 (Aph-1) and Presenilin Enhancer-2 (Pen-2), with a stoichiometry that seems to be 1:1:1:1. Additional proteins might, however, be involved in the regulation of the activity or subcellular localization of the complex (De Strooper B. et al., 2012).

While Presenilin (1 or 2) constitutes the catalytic core of the enzyme, the other three proteins seem to have a more structural function (Tolia A. and De Strooper B., 2009).

Nicastrin is a 709aa type I glycoprotein (80-130 kDa, depending on the glycosilation state), with the TM domain which is the main site for the interaction with Aph-1 and PS. The large extra-cellular domain undergoes significant post-translational modifications during the incorporation into the γ–secretase complex and contain a DAP domain that is thought to be critical for the initial binding of the enzyme to the substrates (Fig.3).

Aph-1 is a 7 TM domains, 30 kDa protein with the N- and C-terminus protruding in the lumen or in the cytosol, respectively. In humans there are two genes encoding for Aph-1, *i.e.*, *Aph-1a* and *Aph-1b*. In the TM4 domain there is a GxxxG motif necessary for the interaction with Pen-2 and PS, but not with NCT. Its role is not completely understood, but it seems to work like an initial scaffold for the proper assembly of the complex (Fig.3).

Pen-2 is a small protein (101aa) with two TM domains and both the N- and C-termini toward the luminal side. The N-term is important for the interaction with PS, while the C-term and the TM1 domain are necessary for the endo-proteolysis and the following activation of PS, although the mechanism is not known yet (Fig.3).

NCT and Aph-1 form an initial subcomplex in the endoplasmic reticulum (ER), with a role of the multiple TMDs of Aph-1 in the binding to NCT (De Strooper B. et al., 2012). The NCT/Aph-1 subcomplex then interacts with the PS and Pen-2 subcomplex. Incorporation of Pen-2 results in the maturation/proteolytic cleavage of PS to its active structure. This tetrameric state has been reported to assemble immediately before or within COPII vesicles, protein transport carriers that exit the ER (Kim J. et al., 2007). A large amount of these complexes cycles between the ER and Golgi apparatus, but only a small percentage is thought to proceed through the Golgi where NCT is further glycosilated before reaching the endosomes and plasma membrane. Indeed, only a minor fraction of total γ-secretase complexes seems to be active (probably less than 10% of the total) and is located at the

plasma membrane or in endosomes, while the remaining is present in endomembranes but in an inactive state (Kaether C. et al., 2006a and b; Chyung G.H. et al., 2005).

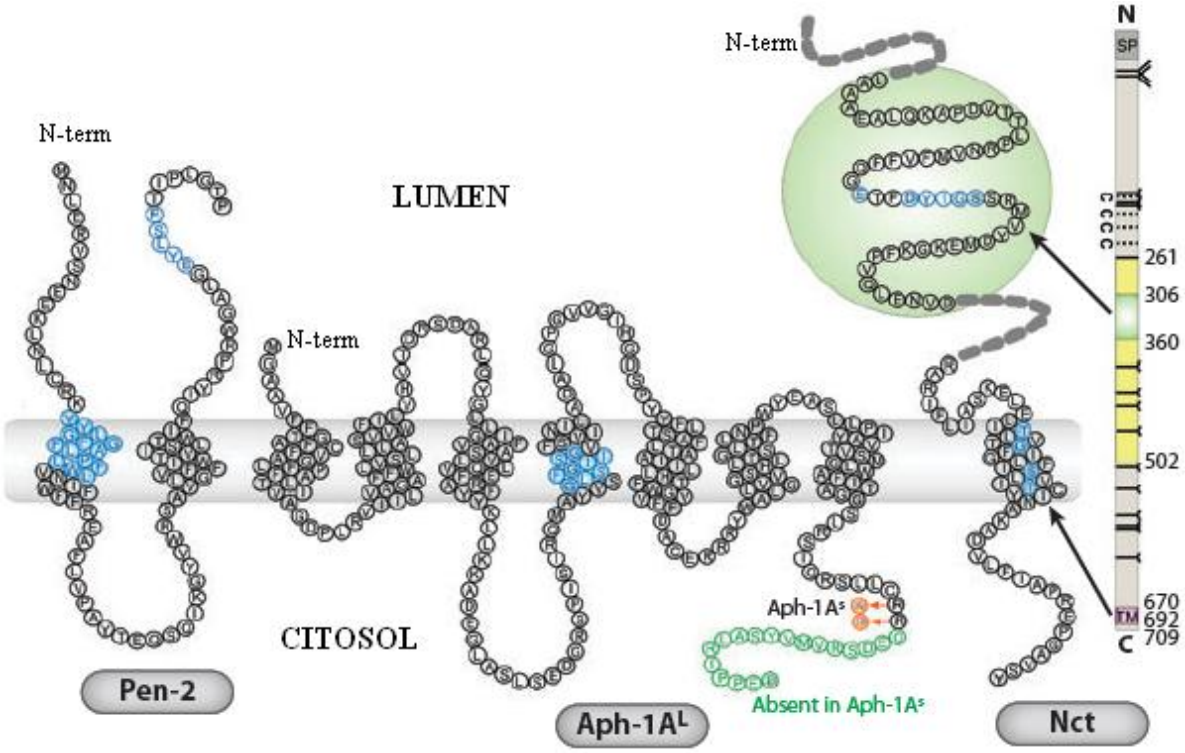

Fig.3: Schematic representation of the sequence and the topology of NCT, Pen-2 and Aph-1. In blue the regions important for protein-protein interaction, while the green circle indicates the DAP domain of NCT. From De Strooper B. and Annaert W., 2010.

Despite the great efforts to determine the precise γ-secretase structure, because of the unique features of being a membrane-embedded protein complex harboring at least 19 membrane-spanning domains and executing intramembrane hydrolysis of substrates, crystallization of the purified γ-secretase complex has not been obtained yet. However, human γ-secretase complexes have been purified and analyzed by EM and 3D reconstruction (Ogura T. et al. 2006). The resultant three-dimensional structure of γ-secretase at 48 A° resolution occupied a volume of 560 x 320 x 240 A° with a low-density space containing multiple pores, which may house the catalytic site (for a review, see De Strooper B. et al., 2012). The most intriguing aspect in the structure-function relationship of γ-secretase is how it executes the proteolytic cleavage of substrate proteins within the hydrophobic environment of the lipid bilayer. Further analysis of the γ-secretase complex structure by cryoelectron microscopy and single-particle image reconstruction at 12 A° resolution revealed several domains on the extracellular side, three low-density cavities, and a surface groove in the transmembrane region of the complex (Osenkowski P. et al., 2009). Moreover, TM domains

6 and 7 of PS (that contains the two aspartate residues critical for the enzymatic activity) were found to partly face a hydrophilic environment (*i.e.*, in a catalytic pore structure) that enables the intramembrane proteolysis (De Strooper B. et al., 2012).

Because γ-secretase plays an essential role in producing the Aβ peptide, which is considered the main pathogenic factor responsible for AD, many studies have tried to discover and develop inhibitors as potential therapeutics for AD. Due to the large variety of γ-secretase substrates, however, most of the molecules have displayed toxicity consequently to a non–substrate-specific enzymatic inhibition. Although the impairment of Notch signalling has been demonstrated to be critical for the majority of them, molecules that display a more specific effect on APP cleavage have been recently obtained and are currently under investigation (for a review, see De Strooper B. et al., 2012).

PRESENILINS

Presenilin-1 (PS1) and Presenilin-2 (PS2) are homologous membrane proteins 467 and 448aa long, respectively, with a MW around 50 kDa. The sequence identity between them is around 65% and they are considered the catalitic core of γ-secretase, since its enzymatic activity is abolished in MEF KO for both PS1 and PS2 (Herreman A. et al., 2000). The catalitic core of the enzyme is constituted by either PS1 or PS2, and the two are never present together within the same complex. Thus, considering that also two different Aph-1 genes exist in humans (*Aph-1a* and *Aph-1b*), there are at least four different type of γ-secretase, whose recognizing/cleaving specificity however is unknown (De Strooper B. et al., 2012).

PS1 and PS2 have 10 hydrophobic domains and 9 TM domains, with the N-term spanning in the cytosol and the C-term in the lumen (Fig.4). As for the other members of the γ-secretase, they are found predominantly in the ER and Golgi apparatus, just a few in the plasma membrane. They are highly expressed in the brain, although their expression is detectable in most adult human tissues (Brunkan A.L. and Goate A.M., 2005). The immature holoprotein undergoes an autocatalytic cleavage at the level of the 7th hydrophobic domain (which is part of a large cytosolic loop) once it is incorporated into the enzyme, generating an N-terminal fragment of 30 kDa (NTF) and a C-terminal fragment of 20 kDa (CTF): the dimer NTF/CTF is considered the catalytically active form of PS, with two critical aspartate residues into the TM domains 6 and 7, whose mutation leads to the complete inactivation of the enzyme (Fig.4) (Kimberly W.T. et al., 2000). Thus, PS maturation needs other partners

and is saturable; the full length (FL) PS has a very short half life (1.5 h) compared to the mature form (24 h), since it undergoes proteasomal degradation (Kim T.W. et al., 1997).

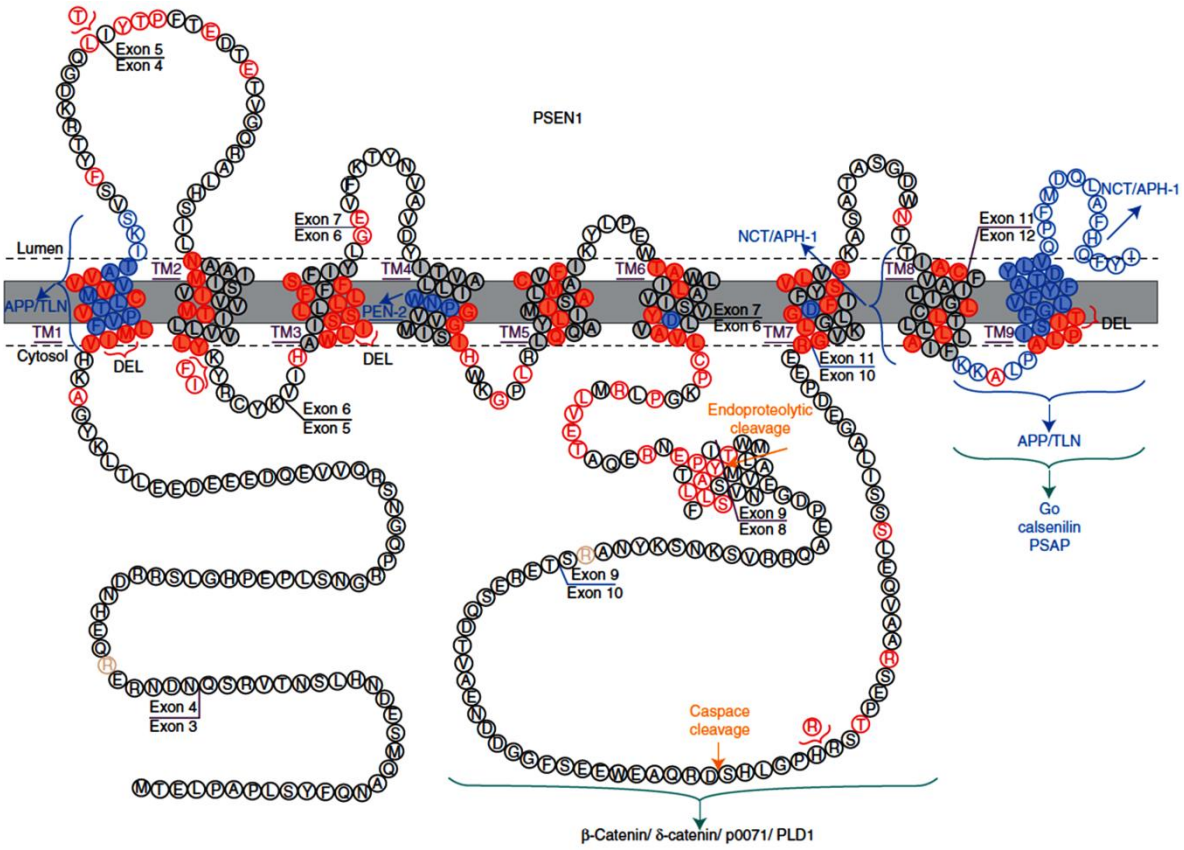

Fig.4: Schematic representation of PS1 sequence and topology. In red, the aa whose mutations are associated to FAD; in blue, those involved in protein-protein interactions. From De Strooper B. et al., 2012.

More than 150 autosomal dominant mutations in PS1 (Fig.4, red aa) and around 12 in PS2 have been associated to the onset of FAD. Since PS are the catalytic core of the γ-secretase, that cleaves APP generating the toxic Aβ peptide, the initial consensus was that FAD mutations in PS result in an increased production of Aβ. This was initially reported in different cell models and in transgenic mice carrying FAD-PS mutations, especially for Aβ42 (Scheuner D. et al., 1996; Citron M. et al., 1997). These results however have been recently challenged by other studies reporting an increase in the Aβ42/Aβ40 ratio in FAD-PS expressing models, but consequently to a drop in the production of Aβ40, suggesting an overall decreased activity of the γ-secretase (Florean C. et al., 2008; Walker E.S. et al., 2005; Shimojo M. et al., 2007). Although this is still matter of intense debate, the initial idea of gain-of-function FAD-PS mutations has been revised in a loss-of-function hypothesis, with a resulting decreased total production of Aβ associated with a less precise cleavage of APP, shifting the product balance from Aβ40 to Aβ42 and thus increasing the ratio Aβ42/Aβ40

(De Strooper B., 2007). This point is quite important because, as discussed below, Aβ42 is thought to initiate the oligomerization of all the Aβ species.

Despite their well established role in γ-secretase activity, PS have also pleiotropic, γ-secretase independent functions, ranging from regulation of Ca^{2+} homeostasis (a matter that will be extensively discussed below), protein trafficking, cell adhesion and autophagy (for recent reviews see De Strooper B. and Annaert W., 2010; De Strooper B. et al., 2012).

APP

The amyloid precursor protein (APP) is a member of the family of type I trans-membrane proteins, with a single TM domain. In mammals this family includes APP and the APP like protein 1 and 2 (APLP1/2). These proteins have different well conserved domains, particularly the extracellular domains E1 and E2 and the intracellular domain. The Aβ containing domain is not conserved, being present only in APP, but the function of the proteins are redundant, as demonstrated by combined KO studies (Wolfe M.S. and Guènette S.Y., 2007).

The APP encoding gene is localized on the long arm of chromosome 21, it consists of 18 exons and undergoes tissue-specific splicing, generating different isoforms, ranging from 365 to 770 aa. APP is abundantly expressed in the brain and the APP695 isoform is predominant in neurons.

In the passage from the ER to Golgi apparatus, APP undergoes post-translational modifications that include O- and N-glycosilations, with only 10% of the protein being found in the plasma membrane (the protein is also recycled through endocytosis; Thinakaran G. and Koo E.H., 2008).

Different roles have been proposed for APP, although its trophic one and its involvement in cellular adesion have obtained the major consensus (Zheng H. and Koo E.H., 2006; Thinakaran G. and Koo E.H., 2008). The first is mediated by the extracellular soluble domain (APPsα), generated upon α-secretase-mediated cleavage of APP. APPsα promotes neurites growth and synaptogenesis, in addition to the growth of other cell types, such as fibroblasts. The second one is mediated by particular protein domains that interact with some extracellular matrix components, such as laminin and collagen. Among other possible functions, APP plays a role in (Thinakaran G. and Koo E.H., 2008):

a) cell signaling, as a membrane receptor, a function proposed on the basis of structural similarities with Notch (a well known trans-membrane receptor involved in a large variety of cellular pathways, such as neurogenesis), although only recently a specific ligand has been found (TAG-1, involved in cell adhesion; Ma Q.H. et al., 2008);

b) axonal transport, since APP interacts with kinesin-1;

c) transcriptional regulation mediated by the APP intra-cellular domain (AICD, released after APP cleavage by the γ-secretase) and by the adaptor Fe65;

d) cell migration.

APP can undergo two distinct and competitive maturation pathways, one amyloidogenic and the other non-amyloidogenic (Fig.5; for reviews, see Zheng H. and Koo E.H., 2006; Thinakaran G. and Koo E.H., 2008). The latter is predominant and, in this case, APP is firstly cleaved by the α-secretase within the sequence that contain Aβ peptide, thus preventing its formation. A soluble N-terminal fragment is released in the extracellular space (APPsα) and a C-terminal fragment (C83) remains bound to the membrane. Conversely, in the amyloidogenic pathway APP is firstly cleaved by the β-secretase at the level of the future Aβ peptide, generating a soluble N-terminal fragment released in the extracellular environment (APPsβ) and a C-terminal domain bound to the membrane (C99). C83 and C99 can be further processed by γ-secretase inside the TM domain of APP: C83 cleavage produces the release of the extracellular, non-pathogenic peptide p3 and the intracellular AICD (that may migrate to the nucleus to regulate transcription); on the other hand, from C99 are generated the amyloidogenic Aβ peptide (released in the extracellular space) and again AICD.

However, γ-secretase has not a unique site of cleavage and can produce in sequence Aβ peptides of different length (from 49 to 38 aa). The most abundant is Aβ40 and about 10% is represented by Aβ42, more hydrophobic and more susceptible to oligomerization.

FAD linked APP mutations are mainly localized near the sites of cleavage by α/β/γ secretase and promote the amyloidogenic pathway, favoring the APP processing mediated by the β and γ secretases. This observation, together with the facts that mutations inside the Aβ peptide favor its aggregation and APP overexpression (for example in Down Syndrome, due to trisomy 21) is associated to an early onset of symptoms compatible with AD, gives strong genetic support to the amyloid cascade hypothesis for AD pathogenesis.

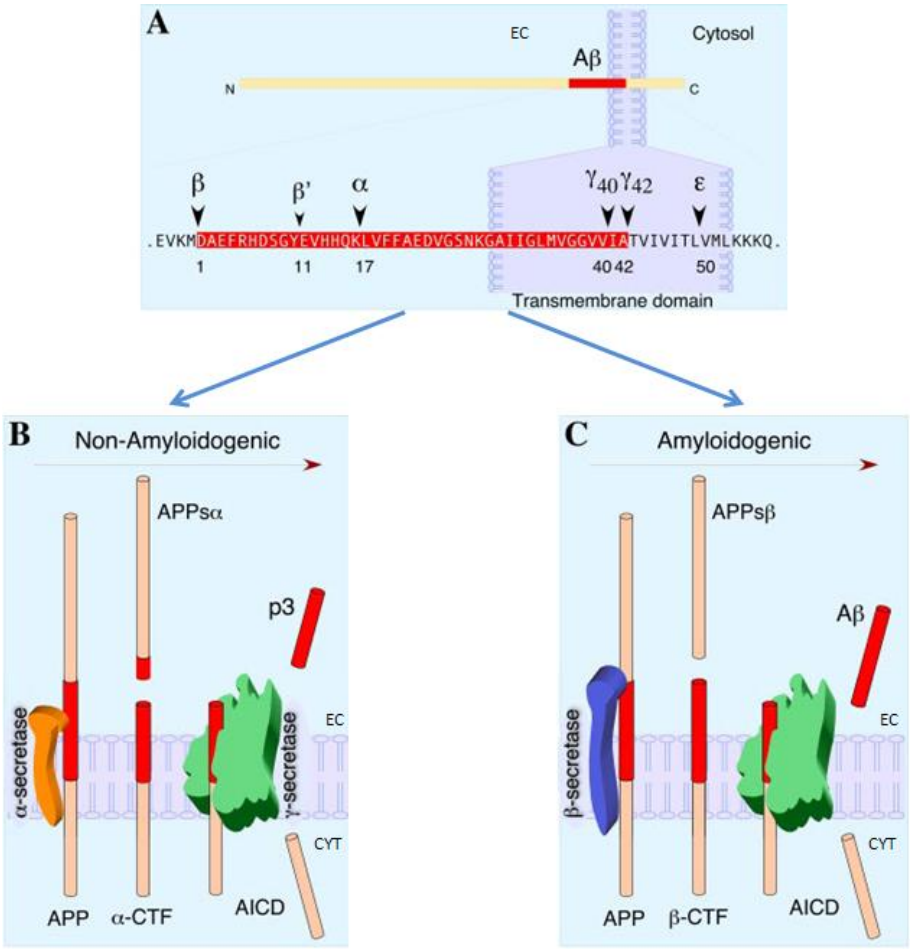

Fig.5: The two alternative pathways for APP maturation. From Thinakaran G. and Koo E.H., 2008.

THE AMYLOID CASCADE HYPOTHESIS

The amyloid cascade hypothesis proposes that the neurodegeneration observed in AD is due to a series of events that could be attributed to an alteration in the processing of APP and the subsequent production of the Aβ peptide (Fig.6) (Hardy J. and Selkoe D.J., 2002). The hypothesis is supported by a set of genetic studies, that have associated FAD to autosomal dominant mutations in three genes (codifying for APP, PS1, PS2), all involved in the production of Aβ peptide. These mutations seem to be able to increase the production of the Aβ42 peptide or, at least, the Aβ42/Aβ40 ratio (Haass, C. and Selkoe, D.J., 2007). Indeed, different studies have demonstrated that Aβ42 is more susceptible to oligomerization and could form the initial nucleus for subsequent Aβ40 deposition and formation of fibrils found in amyloid plaques (Chen Y.R. and Glabe, C.G., 2006).

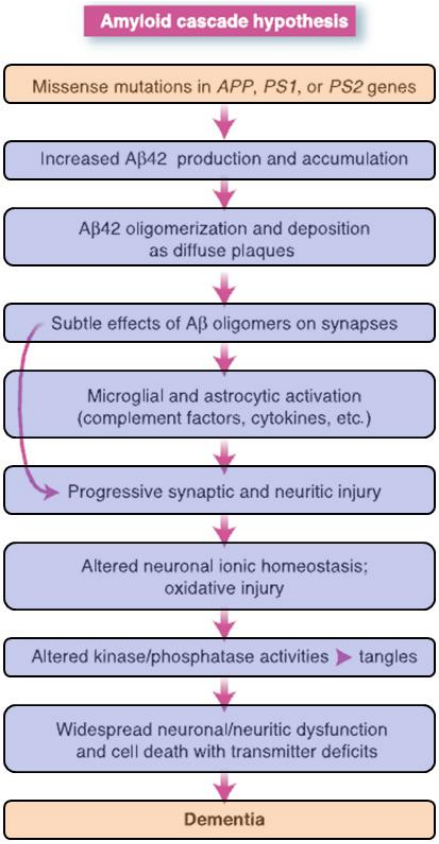

Fig.6: The amyloid cascade hypothesis. From Hardy J. and Selkoe D.J., 2002.

However, the observation that the number of amyloid plaques does not correlate with the degree of dementia and that some plaques can be found also in the brain of normal old people argues against this hypothesis. It has been also proposed that Aβ soluble oligomers are the toxic form at the basis of synaptic dysfunctions and not the insoluble fibrils or the monomer that are observed in the plaques (Haass, C. and Selkoe, D.J., 2007). Indeed, the levels of soluble forms of Aβ better correlate with the degree of cognitive impairment, compared to the number of plaques. On this line, the soluble oligomers have been demonstrate to inhibit the maintenance of the long term potentiation (LTP) in the hippocampus, a phenomenon involved in memory formation (Walsh D.M. et al., 2002). This suggests that plaques could represent inert aggregates of Aβ, although the possibility that they form a reservoir of smaller, soluble species or even a protective mechanism that sequesters these oligomers has not been elucidated yet.

Different mechanisms have been proposed to explain the pathogenic activity of Aβ (Parihar M.S. and Hemnani T., 2004; Fiala J.C, 2007; LaFerla F.M. et al., 2007; Gandy S., 2005; Querfurth H.W. and LaFerla F.M, 2010). Among them, must be pointed out an

alteration of Ca^{2+} homeostasis, mitochondrial and energy metabolism dysfunctions, the formation of cationic channels on plasma membrane, cellular oxidative stress due to ROS over-production, cytoskeletal and axonal transport alterations, inflammatory processes, increase susceptibility to pro-apoptotic and pro-necrotic stimuli. All these processes can be considered as a cascade of events that might be due to initial, small perturbations in specific cell signaling pathways.

It is not completely clear whether Aβ oligomers can bind specifically to some cell receptors (causing a specific toxicity in cholinergic neurons), or they can bind, in an unspecific manner, to a large variety of channels/receptors, causing different negative cellular effects. It has been propose that the Prion protein (PrP) is an Aβ receptor (Laurén J. et al., 2009), although recently this conclusion has been challenged (Kessels H.W. et al., 2010). There are however compelling evidence that Aβ oligomers could interfere with some pathways downstream NMDA and AMPA receptors, impairing their endocytosis and affecting LTP (Fig.7) (Haass, C. and Selkoe, D.J., 2007; Querfurth H.W. and LaFerla F.M, 2010), since these receptors are widely expressed at synaptic level and play a fundamental role in the modulation of LTP and synaptic plasticity, by modulating Ca^{2+} entry through the plasma membrane. Aβ oligomers could also form cationic channels in plasma membrane (PM), increasing the entry of Ca^{2+}. In turn, Ca^{2+} homeostasis alterations can severely damage cells, modulating the activity of kinases/phosphatases (note that tau is hyper-phosphorylated in AD) and their downstream signaling pathways. All these alterations could eventually lead to synaptic dysfunction/neuronal loss, responsible for the dementia observed in AD patients.

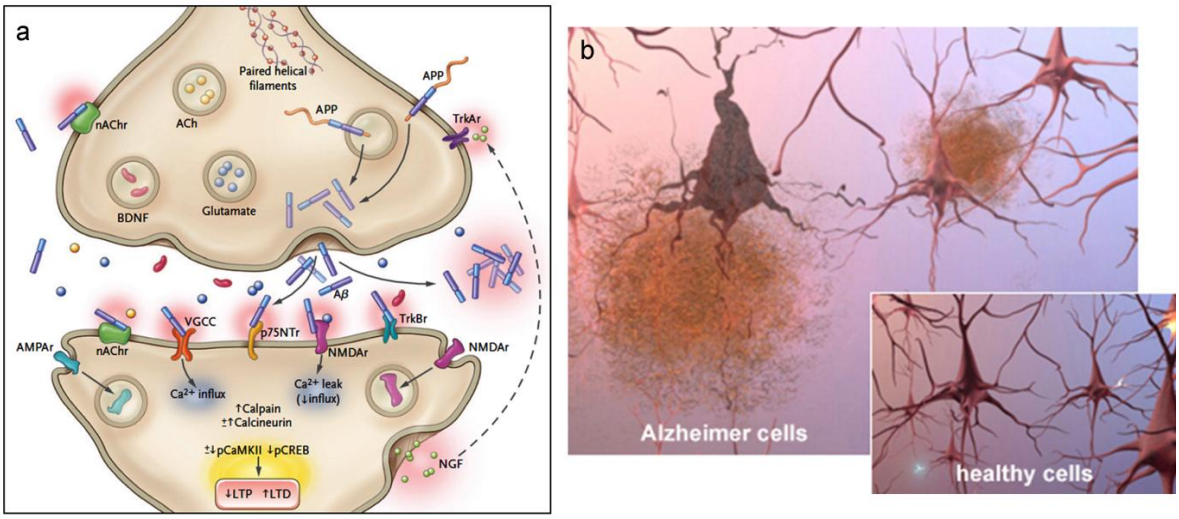

Fig.7: a) Schematic representation of the pleiotropic effects of Aβ at the synaptic level and b) plaques (and tangles) could damage neurons, being a reservoir of Aβ. From a) Haass C. and Selkoe D.J., 2007; b) alz.org. web site.

THE Ca^{2+} HYPOTHESIS

Ca^{2+} is one of the most important intracellular second messenger and have an essential role in different cellular processes, ranging from fertilization, active secretion, muscular contraction, cell differentiation to cell death (Fig.8) (Berridge M.J. et al., 2000).

The high versatility of Ca^{2+} allows the generation of signals that can be deciphered on the basis of their spatial and temporal extension, the amplitude and the frequency, thus rendering Ca^{2+} an universal messenger. The deciphering of these signals depends from some Ca^{2+} binding proteins and some signaling proteins downstream of them, that in turn transmit the message to the cellular effectors.

This key role is particularly important at neuronal level, where processes like excitability, neurotransmitters release, long term synaptic plasticity and the transcription of some genes depend from the intracellular [Ca^{2+}] (Berridge M.J., 1998).

The observation that different FAD-PS mutations are associated to alterations in Ca^{2+} homeostasis, and that Aβ levels (particularly the number of amyloid plaques) do not correlate with the degree of dementia, suggested an alternative hypothesis to the "amyloid-cascade" one in order to explain the pathogenesis of AD. This hypothesis proposes that the neurodegeneration observed in AD patients is due to a sequence of events linked to alterations in intracellular Ca^{2+} handling. Before to discuss this aspect, a brief introduction on the major players in the maintenance of Ca^{2+} homeostasis is presented.

Ca^{2+} HOMEOSTASIS

In resting conditions, the cytosolic [Ca^{2+}]c is maintained low, at around 100nM (beyond differences due to the specific cell type). Upon different stimuli, cytosolic [Ca^{2+}] rapidly increases until the low micromolar range. This increase in both excitable and non-excitable cells is due to the release of Ca^{2+} from the intracellular stores (mainly endo/sarcoplasmic reticulum ER/SR, where [Ca^{2+}] can reach 200-500μM) and/or the entry of Ca^{2+} from the extracellular environment (where [Ca^{2+}] is around 1.8 mM). In the first case, the predominant mechanism in the majority of tissues (but not in muscle cells) is the activation of phospholipase C (PLC), that results in the production of inositol 1,4,5 trisphosphate (IP_3) and diacylglycerol (DAG). IP_3 interacts with Ca^{2+} releasing channels located in the ER and Golgi apparatus, causing their opening and the release of Ca^{2+} into the cytosol. The subsequent Ca^{2+} depletion into the stores often induces also a Ca^{2+} influx through PM channels

(Capacitative Ca^{2+} Entry, CCE), whose nature was recently elucidated (Wang Y. et al., 2010; Lewis R.S., 2007). As far as Ca^{2+} entry is concerned, the mechanism is more cell-specific, with tens of different isoforms of PM Ca^{2+} channels, whose nature depends from the cell type and the PM sub-domain (Fig.8).

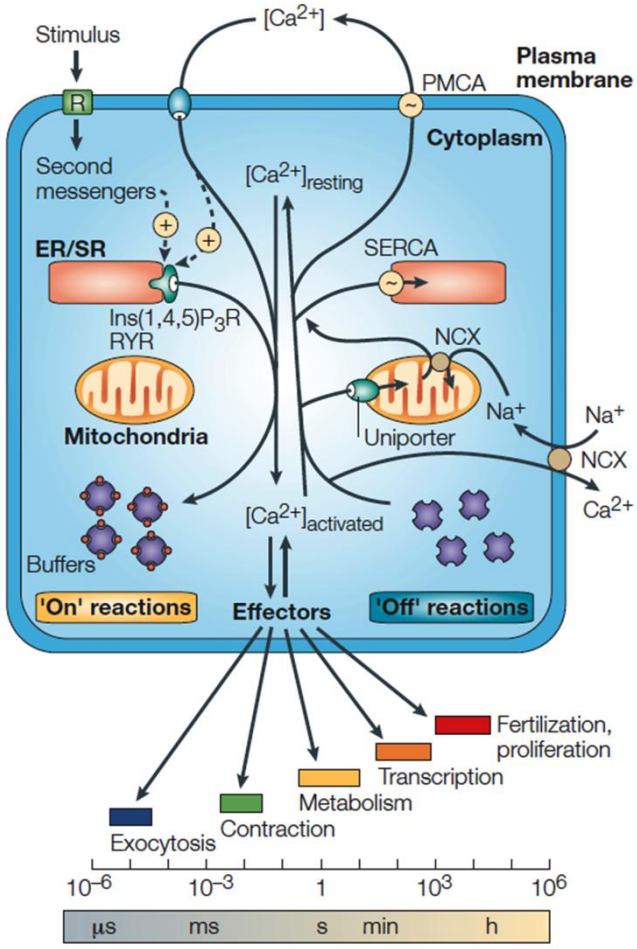

Fig.8: A schematic representation of Ca^{2+} homeostasis and Ca^{2+}-regulated processes. From Berridge M.J. et al., 2003.

Once generated, intracellular Ca^{2+} signal must be properly turned off, to ensure the specificity required to control cell function and to avoid excessive, dangerous stimulation. Two are the main mechanisms to terminate a Ca^{2+} signal: extrusion from the cytosol into the extracellular space or re-accumulation into intracellular Ca^{2+} stores (for reviews, see Zampese E. and Pizzo P., 2012; Clapham D.E., 2007). Moreover, in the generation and propagation of cytosolic Ca^{2+} signals must be take into account also the buffering capacity not only of specific organelles within the cytosol (such as mitochondria), but also the buffering capacity of the cytosol itself. Indeed, in the cytosol are present different Ca^{2+} binding proteins, capable to shape the signal. These proteins usually contain conserved EF-

hands domains specialized in Ca^{2+} binding, composed of two α-helixes and a 12 aa loop. Among these EF-hand containing proteins, several have a buffering function and they are mostly involved in chelating Ca^{2+} ions, such as Parvalbumin, Calbindin and Calretinin (Schwaller B., 2009). Others, such as Calmodulin (CaM), are instead Ca^{2+} sensor and are characterized by profound structural changes upon Ca^{2+} binding to their EF-hands, with exposure of hydrophobic domains that allows their interaction with, and the modulation of different proteins, the effectors. Thus, this buffering capacity contributes to finely tune and shape cellular Ca^{2+} signals, in both their spatial (compartimentalization) and temporal extension (limiting Ca^{2+} diffusion rate) (Rizzuto R. and Pozzan T., 2006).

It appears clear that PM and different intracellular organelles cooperate in the maintenance of intracellular Ca^{2+} homeostasis (Fig.9). The key features of Ca^{2+} handling by PM, ER, Golgi apparatus and mitochondria are summarized below, with particular attention to mitochondria. Although other organelles contribute to Ca^{2+} homeostasis (such as nucleus, acidic compartments and peroxisomes), they are not taken into consideration here and the interested reader is referred to a recent review (Zampese E. and Pizzo P., 2012).

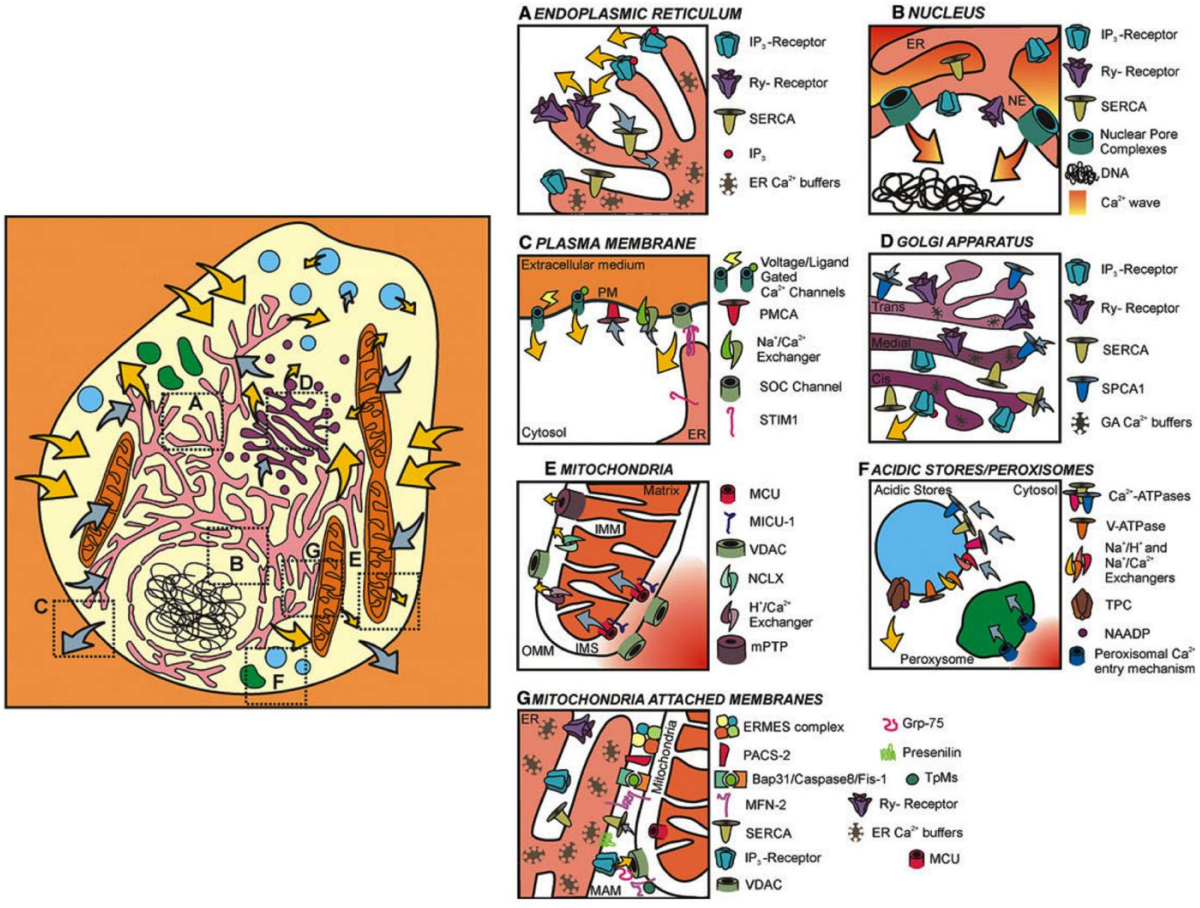

Fig.9: Ca^{2+} handling organelles and molecular toolkit. From Zampese E. and Pizzo P., 2012.

PLASMA MEMBRANE

The plasma membrane (PM) is the barrier that isolates the intracellular environment from the extracellular milieu, maintaining different features (such as ionic composition) between these two compartments. This allows PM to rapidly transmit signals from the extracellular environment to the cell, as ionic movements, thanks to a lot of different receptor and channels present on its surface (Rizzuto R. and Pozzan T., 2006). The ionic movements are driven by electrochemical gradients (maintained by the PM itself) and are allowed by the opening of specific channels. These channels could be distinguished on the basis of their ionic selectivity and the mechanism for their activation/opening (Berridge M.J. et al., 2003).

As far as Ca^{2+} is concerned, in excitable tissues, such as nervous system and heart, an important role is played by the Voltage Operated Ca^{2+} Channels (VOCCs), whose opening is regulated by membrane depolarization. They are classified in different subtypes, depending on their voltage and inhibitors sensitivity. For example, the N- and P/Q-subtypes are present in synapses and control the Ca^{2+} dependent release of neurotransmitters, while the L-type are present in dendrites and could mediate a Ca^{2+}-dependent gene transcription (Berridge M.J. et al., 2003).

Receptor Operated Ca^{2+} channels (ROCCs) are gated by the binding of an extracellular ligand to the same polypeptide forming the channel. This binding opens the channel allowing Ca^{2+} to enter into the cell (Clapham D.E., 2007). Among them, NMDAr and AMPAr are activated by their physiological ligand glutamate and play a fundamental role in neurons, where, depending from their specific sub-cellular localization (*i.e.*, in the soma or at synapses) and the amount of Ca^{2+} that they allow to enter, could generate different or even opposite signals, such as LTD or LTP (Wojda U. et al., 2008).

Extracellular ligands do not bind only to ROCCs, but also to other kind of receptors, like Receptor-Tyrosin-Kinases (RTKs) and G-protein-coupled Receptors (GPCRs). RTKs initiate a phosphorylation cascade inside the cells upon their dimerization and self-phosphorylation. On the other hand, GPCRs activate trimeric G-proteins to which they are functionally coupled, that in turn can activate Phospolipase-C β (PLCβ): once activated, this enzyme cleaves phosphatidylinositol-4,5-biphosphate (PIP2) present in the PM producing the second messengers inositol-1,4,5-triphosphate (IP3) and diacylglicerol (DAG). IP3 is the main agonist of a receptor (IP3R) expressed on the membrane of intracellular Ca^{2+} stores and induces its opening with a massive release of Ca^{2+} (see the ER section). Moreover, different

mechanisms than GPCRs can activate other isoforms of PLC and lead to the production of IP3 (Berridge M.J., 2003).

Store Operated Ca^{2+} channels (SOCCs) are regulated by depletion of intracellular Ca^{2+} stores and generate the so called Capacitative Ca^{2+} Entry (CCE). The channel is formed by the protein Orai1, present in the PM, while STIM1 is an ER membrane protein that senses ER [Ca^{2+}] through an EF-hand domain. Upon ER Ca^{2+} depletion, STIM1 oligomerizes and forms clusters/punctae close to the PM, contacting and activating Orai1 (also called CRAC channels) by its oligomerization (Fig.10) (Wang Y. et al., 2010).

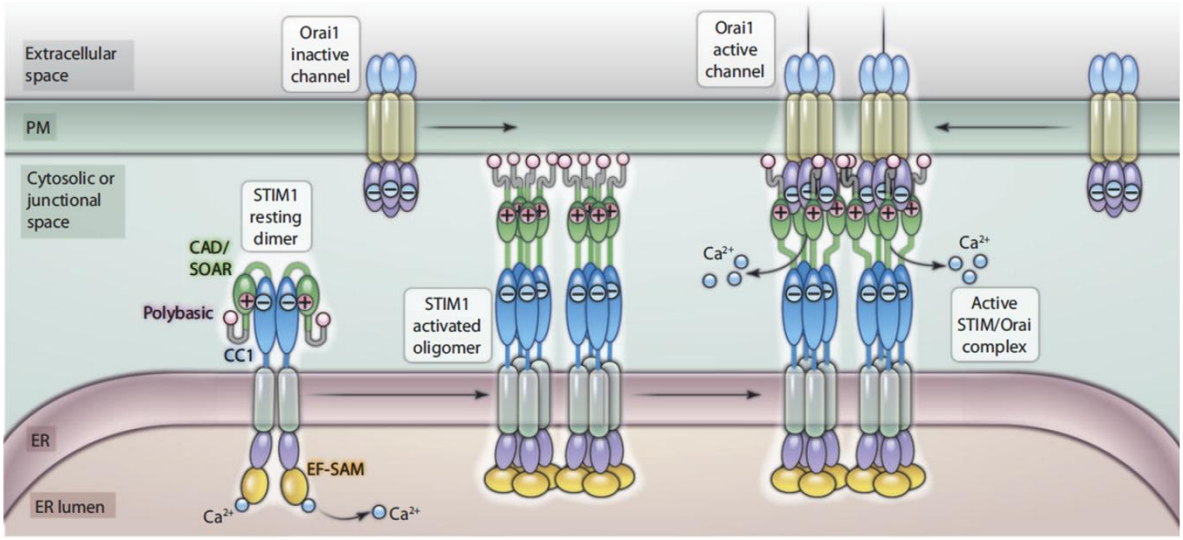

Fig.10: Representation of CCE activation upon Ca^{2+} store depletion. From Yang Y. et al., 2010.

On the other hand, in PM there are also proteins capable of extruding Ca^{2+} from the cytosol to the extracellular compartment. In particular, the PM Ca^{2+} ATPase (PMCA) can export 1 Ca^{2+} with the hydrolysis of 1 ATP molecule and is essential in maintaining low cytosolic [Ca^{2+}] (Strehler E.E. et al., 2007), while the Na^{+}/Ca^{2+} exchanger is able to export Ca^{2+} and import Na^{+} with a ratio 1 : 3, respectively. Upon membrane depolarization, this exchanger can work in a reverse mode (Blaustein M.P. and Lederer W.J., 2009).

ENDOPLASMIC RETICULUM

The endoplasmic reticulum (ER) is an organelle diffuse in the whole cytoplasm, composed of membrane sheets that enclose the nucleus and a network of tubules. The ER is sub-divided into three major compartments: the smooth ER, the rough ER (with bound ribosomes on its surface) and the nuclear envelope. A specialized version of ER is the sarcoplasmic reticulum (SR), found in the striated muscle cells.

In addition to its fundamental role in protein synthesis/folding/modifications/transport and lipid synthesis, the ER represents also the main intracellular Ca^{2+} store and plays a major role in cell Ca^{2+} homeostasis and signalling (for a recent review, see Zampese E. and Pizzo P., 2012): it contains ATP driven pumps for Ca^{2+} uptake (the so-called SERCAs), Ca^{2+} binding proteins for Ca^{2+} storage within the lumen, and channels for Ca^{2+} release (the ubiquitous IP_3 receptors, IP_3Rs, and, in many cells, also the ryanodine receptors, RyRs) (Fig.9). Some of these molecular components are non randomly distributed within ER membranes, concurring to a sort of heterogeneity in Ca^{2+} storage within different ER sub-compartments.

The free [Ca^{2+}] into the ER lumen (without considering the Ca^{2+} bound to different Ca^{2+} binding proteins) depends on the cell type, but is usually between 300 and 800 μM and is determined by an equilibrium between the ER Ca^{2+} release/leak, the ER Ca^{2+} uptake and its buffering capacity (Zampese E. and Pizzo P., 2012).

Ca^{2+} is accumulated in the ER through the Sarco/Endoplasmatic Ca^{2+}-ATPase (SERCA), a 110 kDa enzyme that moves 2 Ca^{2+} ions from the cytosol into the ER lumen against its chemical gradient by hydrolysis of 1 ATP molecule. In mammals, SERCA is coded by three different genes and alternative splicing events further increase the complexity of its expression pattern, that depends from the cell type and the development stage. SERCA2b is expressed ubiquitously and is considered the housekeeping variant. SERCA is a single polypeptide with 10 TM domains and a large cytosolic domain (Toyoshima C., 2009). Different proteins are able to modulate its activity and different drugs block it (Zampese E. and Pizzo P., 2012). Among the latter, thapsigargin is an irreversible blocker, while cyclopiazonic acid (CPA) is reversible.

The two Ca^{2+}-releasing channels within the ER membranes are inositol-1,4,5-triphosphate Receptors (IP3Rs) and Ryanodine Receptors (RyRs).

IP3Rs are encoded by three different genes, with the 3 isoforms that are differently expressed depending from the cell type, but that have also an overlapping pattern of expression, since they are thought to mediate different type of signaling. The IP3R is a protein of 260 kDa, with 6 TM domains, that oligomerizes into homo- or hetero-tetramers. It is a ligand-gated ion channels controlled by the second messenger IP_3, generated by enzymes of the PLC family, that include distinct isoforms differing in their activation mechanism (Foskett J.K. et al., 2007). The cytosolic N-terminal contains the IP3 binding domain: once

bound, IP3 gates the channel open. Different proteins have been reported to interact with and modulate IP3Rs activity (for a review, Zampese E. and Pizzo P., 2012), although one of the most important regulators of its activity is Ca^{2+} itself. The effect of Ca^{2+} on IP3R regulation is biphasic, since a modest increase in $[Ca^{2+}]_c$ favours its opening mediated by IP3, while a stronger increase inhibits it (Foskett J. K. et al., 2007). This contributes to the so called Ca^{2+}-induced Ca^{2+} release (CICR, see below in the RyR paragraph, since it is more important for RyR opening), a phenomenon capable of coordinating single elementary events (such as the opening of a single or few channels) transforming them into more complex events (such as the propagation of a Ca^{2+} wave), by recruiting neighbouring channels.

RyRs owe their name to the plant alkaloid ryanodine, that binds to the channel with high specificity and works as an antagonist. In mammals three different genes code for RyR1 (predominantly expressed in skeletal muscle), RyR2 (expressed mainly in the heart, but also in Purkinje cells and in cortical neurons) and RyR3 (ubiquitously expressed at low levels). RyR is a 550 kDa protein that assembles into homo-tetramer forming the largest known ion channel. The large cytosolic N-terminal domain is the site for interaction with a variety of proteins that has been reported to modulate its activity (for a review, see Zampese E. and Pizzo P., 2012). While in skeletal muscle RyR1 opening is primarily (or exclusively) due to the electromechanical coupling with dihydropyridine receptor (DHPR), RyR2 and RyR3 are predominantly opened by CICR: in this case, the opening of RyRs is due to the local Ca^{2+} increase occurring in the proximity of PM Ca^{2+} channels, as initially demonstrated for cardiac muscle cells (Fill M. and Copello J.A., 2002). CICR can be also induced by Ca^{2+} release from neighbouring ER channels, such as IP_3Rs or other RyRs, in a regenerative wave.

A basal Ca^{2+} leak from the ER contribute to determine the steady state $[Ca^{2+}]_{ER}$. However, despite it physiological relevance, the mechanism of ER Ca^{2+} leak still remains elusive. Several players have been proposed to take part in this process, including the ribosomal-translocon complex, channels of the transient receptor potential (TRP) family-like, such as polycystin-2 (TRPP2), presenilins (PSs), members of anti-apoptotic Bcl-2 families, hemichannel-forming proteins such as pannexins (Zampese E. And Pizzo P., 2012). Also RyRs and IP_3Rs are known to undergo spontaneous activity, maybe contributing to the basal ER Ca^{2+} leak.

Finally, in the ER lumen different proteins bind Ca^{2+}, acting as Ca^{2+} buffers or chaperones. Among them, Calreticulin (CRT) is responsible for the binding of almost half of the Ca^{2+} present in the ER (Michalak, M. et al., 2009). Calsequestrin (CSQ) is the main Ca^{2+}

buffering protein in the SR, Calnexin shares homology with CRT but is membrane bound, while GRP78 (Bip) and GRP94 are ER chaperons also acting as a buffer (Zampese E. and Pizzo P., 2012). These proteins allow to store large amounts of Ca^{2+} into the ER, but also its prompt release upon the opening of releasing channels, since they are characterized by a large number of Ca^{2+} binding sites with relatively low affinity, and ER free Ca^{2+} is in continuous equilibrium with protein-bound ion. Upon release into the cytosol and consequent store depletion, the SERCA activity and the activation of CCE (see above) ensure a rapid reuptake of Ca^{2+} into the ER, reestablishing a new equilibrium.

GOLGI APPARATUS

The Golgi apparatus (GA) is an organelle with a fundamental role in protein post-translational modifications and sorting. It is sub-divided in three different compartments with distinct functions (and distinct enzymatic/chaperone activities): the cis-, the medial- and the trans-Golgi, whose dynamic architecture depends from the balance of anterograde and retrograde vesicles trafficking through the GA. In addition, the GA plays a key role as an intracellular Ca^{2+} store, as originally demonstrated using the whole Golgi targeted aequorin Ca^{2+} probe (Pinton P. et al., 1998). GA contains all the essential components of a Ca^{2+}-storage organelle: pumps for Ca^{2+} uptake, channels for Ca^{2+} release, and Ca^{2+} binding proteins for Ca^{2+} storage (recently reviewed in Zampese E. and Pizzo P., 2012). In addition to SERCA, GA expresses another ATP-dependent Ca^{2+} pump, the Secretory Pathway Ca^{2+} ATPase 1 (SPCA1). The distribution of the two pumps within the GA is heterogeneous (Fig.9), with the former present in the cis- and medial-GA and the latter in the trans- and medial GA, as recently demonstrated in our lab (Lissandron V. et al., 2010; Pizzo P. et al., 2011; Wong A.K. et al., 2013). Similarly, the IP3R is present in the cis- and, to a lower extent, in the medial Golgi, but not in the trans-Golgi, thus rendering this latter compartment insensitive to an IP3 mediated stimulation. On the contrary, RyRs are distributed throughout the whole GA, making also the trans-Golgi an importat, dynamic Ca^{2+} store that could contribute to Ca^{2+} release into the cytosol, at least in those tissues in which RyRs are abundantly expressed (such as heart) (Lissandron V. et al., 2010; Pizzo P. et al., 2011; Wong A.K. et al., 2013).

MITOCHONDRIA

The ability of mitochondria to take up Ca^{2+} was firstly documented more than 50 years ago (De Luca H. F. and Engstrom G.W. , 1961; Vasington F. D. and Murphy J. V., 1962;

Lehninger A. L. et al., 1963). These seminal studies revealed that isolated mitochondria can rapidly take up from the external medium massive amounts of Ca^{2+} and buffer them in their matrix.

After few years, the chemiosmotic theory (Mitchell P. and Moyle J., 1967) provides the thermodynamic basis for this accumulation. Indeed, in respiring mitochondria supplied with oxygen and carbon source, the proton pumping by the respiratory chain complexes from the matrix to the inter-membrane space generates an electrochemical gradient ($\Delta\Psi$) across the inner mitochondrial membrane (IMM), which is negative inside the matrix (-180 mV). This gradient is the driving force that permits the accumulation of cations into the matrix.

Although the outer mitochondrial membrane (OMM) is known to be largely permeable to small solutes (< 5 KDa) and ions (also through the voltage-dependent anion channel, VDAC, which over-expression favors Ca^{2+} accumulation into mitochondria (Rapizzi E., et al., 2002)), thus representing not a limiting step for mitochondrial Ca^{2+} uptake, the transfer of Ca^{2+} across the highly ions-impermeable IMM requires transport mechanisms, whose activity was characterized in the 70s (Bragadin M. et al., 1979). The high-capacity mechanism was defined "mitochondrial Ca^{2+} uniporter" (MCU) and was classically defined by its dependence on $\Delta\Psi$, sensitivity to ruthenium red (that display an inhibitory action), and activity when extra-mitochondrial [Ca^{2+}] is in the micromolar range. The molecular identity of the underlying proteins remained however unknown until recently (see below).

Moreover, mitochondrial Ca^{2+} accumulation does not proceed until an electrochemical equilibrium is reached, that on the basis of the Nernst equation is around 1 M for a $\Delta\Psi$ of -180 mV and for typical cytosolic [Ca^{2+}], a scenario not compatible with the normal cell physiology. This accumulation is limited by both the low apparent affinity for Ca^{2+} of the MCU (for a review see Carafoli E., 2003) and by the existence of antiporter mechanisms that export Ca^{2+} from the matrix. The antiporters exchange Ca^{2+} with Na^{+} (especially in excitable tissues, such as heart and brain), or with H^{+} (especially in non excitable tissues, like liver) (Nicholls D.G. & Crompton M., 1980) and their molecular identity has been discovered only recently (see below) (Fig.9 and 11).

Once in the matrix, it seems that Ca^{2+} is buffered by phosphate group P_i, with the formation of insoluble $xCa2+\text{-}xPO_4^{x-}$ $\text{-}xOH^{-}$ complexes that precipitate (Nicholls D.G. and Chalmers S., 2004; for a review Szabadkai G. and Duchen M. R., 2008).

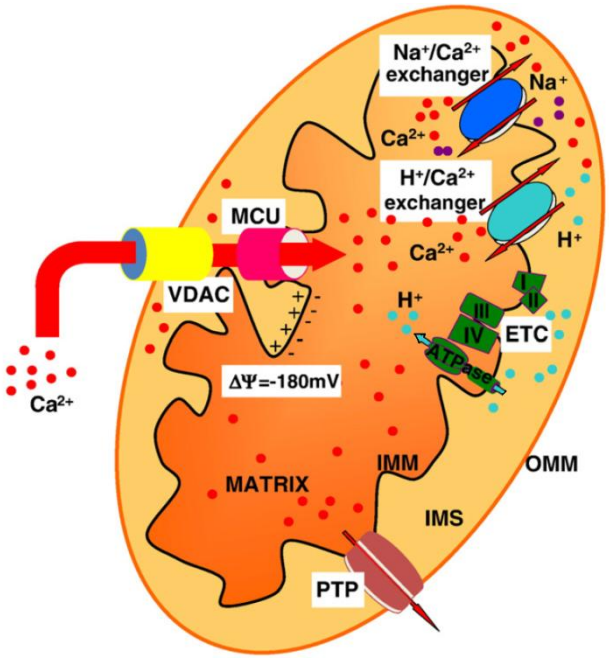

Fig.11: Schematic representation of the main mitochondrial Ca^{2+}-handling toolkit. From Celsi F. et al., 2009.

Below, a list of the main proteins that have been demonstrated to take part in the mitochondrial uptake and extrusion mechanisms is presented.

MCU

Although the molecular identity of MCU has been elucidated only few years ago, the idea that mitochondria exert an important role in the maintenance of cellular Ca^{2+} homeostasis, by rapidly changing their [Ca^{2+}], was widely accepted since the 70s, when seminal studies functionally characterized mitochondrial Ca^{2+} uptake. Those studies revealed however a low apparent affinity of MCU for Ca^{2+} (K_D around 20 μM). When, in the 80s, it was firstly discovered that IP3, generated upon stimulation of PM receptors coupled to PLC, is able to mobilize Ca^{2+} from a "non-mitochondrial intracellular store" (the ER) (Streb H. et al., 1983) and, with the development of fluorescent indicators, it was allowed to precisely measure the cytosolic [Ca^{2+}], it became clear that under physiological oscillation of [Ca^{2+}]$_c$ (ranging from 100nM, in basal condition, to peaks of 1-3μM, after cell stimulation) MCU does not permit significant Ca^{2+} accumulation into mitochondrial matrix (for a review see Patron M. et al., 2013). Thus, a remarkable Ca^{2+} uptake into the organelle was predicted to occur only under conditions of substantial Ca^{2+} overload, and the initial idea of a key role of mitochondria in cellular Ca^{2+} homeostasis gradually disappeared.

The development of genetically encoded Ca^{2+} probes targeted to mitochondrial matrix (firstly the photoprobe aequorin (Rizzuto R. et al., 1992), and then other GFP-based fluorescent probes (Rudolf R. et al., 2003)) clearly demonstrated that this is not the case, since upon cell stimulation with an agonist, mitochondria take up Ca^{2+} with a speed and an amplitude that largely exceed those expected on the basis of MCU low affinity. Not only, but the rise in $[Ca^{2+}]_m$ closely follows that in $[Ca^{2+}]_c$. This apparent paradox was solved through the demonstration that mitochondria are located in very close proximity to the channels that elicit the release of Ca^{2+} from the ER (Rizzuto R. et al., 1998; Csordas G. et al., 1999) or the entry from the plasma membrane (David G. et al., 1998). Thus, transient microdomains of high $[Ca^{2+}]$ formed near the mouth of these channels (see below for the microdomain theory) allow to overcome the low affinity of the MCU, with a prompt Ca^{2+} accumulation into the matrix. This discovery represent "the resurrection of mitochondria" as key players in cellular Ca^{2+} homeostasis (Patron M. et al., 2013).

The first studies investigating the molecular nature of MCU began in the 70s (for a review see Marchi S. and Pinton P., 2013), when a soluble Ca^{2+}-binding glycoprotein was isolated from rat liver mitochondria (Sottocasa G. et al., 1972). This protein was able to induce a Ca^{2+} current after reconstitution in lipid bilayers. Moreover, this Ca^{2+} import was blocked by both ruthenium red (a well known MCU inhibitor) and by antibodies directed against this protein (Panfili E. et al., 1976). Later, proteoliposomes containing mitochondrial proteins with MW > 35kDa were described to take up Ca^{2+} in a ruthenium red-sensitive way (Zazueta C. et al., 1991), and a 40kDa protein forming Ca^{2+}-conducting channels in lipid membranes was isolated from heart mitochondria (Saris N.E. et al., 1993).

Finally, after 5 decades of studies, in 2011 two independent groups used a novel *in silico* approach to discover the MCU molecule by analyzing, for the known biological properties of the MCU, the so called "MitoCarta", a mass spectrometry-based compendium of 1098 proteins from 14 different mouse tissues with validated mitochondrial localization (Pagliarini D.J. et al., 2008). These groups identified CCDC109A as the channel-forming subunit of MCU (Baughman J.M. et al, 2011; De Stefani et al., 2011). The parameters used to screen the MitoCarta were, in the case of the Baughman group, a phylogenetic profile with common evolutionary patterns to the previously identified protein MICU1 (see below) and, in the case of the other (De Stefani et al., 2011), a set of known MCU properties.

CCDC109A/MCU displays all the typical biological characteristics previously established for the MCU (for reviews, see Raffaello A. et al., 2012; Patron M. et al., 2013; Marchi S. and Pinton P., 2013):

a) The reconstitution of CCDC109A into a planar lipid bilayer generates a Ca^{2+} current with properties similar to those previously reported for MCU;

b) This activity was completely inhibited by the addition of ruthenium red (and Gd^{3+}, another known MCU inhibitor);

c) MCU is a protein of 40 kDa that loses its mitochondrial targeting sequence during import, resulting in a 35 kDa IMM protein (very similar to the glycoproteins with MCU-like activity isolated in the 90s, see above);

d) MCU has two trans-membrane domains (the minimal number required for all ion channels), highly conserved among different species;

e) MCU is ubiquitously expressed in mammals, but is not present in *S. cerevisiae* (as expected, since *S. cerevisiae* does not show an MCU-like Ca^{2+} uptake activity);

f) MCU down-regulation strongly inhibits mitochondrial Ca^{2+} uptake both in intact and permeabilized cells, without changing other features of the mitochondria, such as $\Delta\Psi$ or morphology. On the contrary, MCU over-expression enhances mitochondrial Ca^{2+} uptake and, of note, cause a reduction in cytosolic Ca^{2+} rises upon cell activation due to an enhanced mitochondrial buffering capacity.

The topology of the channel was initially matter of debate, since the two groups obtained opposite results. However, it is now clear that both the N- and the C-termini of the protein face the matrix and the small linker (9aa, DIME domain) between the two TM domains spans in the inner mitochondrial space (IMS; Martell J.D. et al., 2012). The mutation of two negatively charged aa into the DIME motif (D261/E264 in the human MCU sequence) abolishes MCU activity (Baughman J.M. et al, 2011; De Stefani et al., 2011), and the mutation S259A eliminate the sensitivity to ruthenium red (Fig.12).

MCU is part of a complex that migrates in blue native PAGE at ~480kDa (Baughman J.M. et al, 2011). Indeed, the existence of only two TM domains suggests that a functional channel could be formed by oligomers of MCU, and the computationally predicted quaternary structure indicates a tetramer as the most likely (Raffaello A. et al., 2013). Of note, the over-expression of the above mentioned D261/E264 mutant form of MCU results in a decrease mitochondrial Ca^{2+} uptake (De Stefani et al., 2011), strongly suggesting a dominant negative effect toward the endogenous wt MCU and, thus, that they are both

inserted into a higher molecular weight complex. Recently, the computational model of an oligomer has been confirmed by co-immunoprecipitation of differently tagged MCU monomers, FRET analysis and immunoblotting of *in vitro* expressed MCU (Raffaello A. et al., 2013).

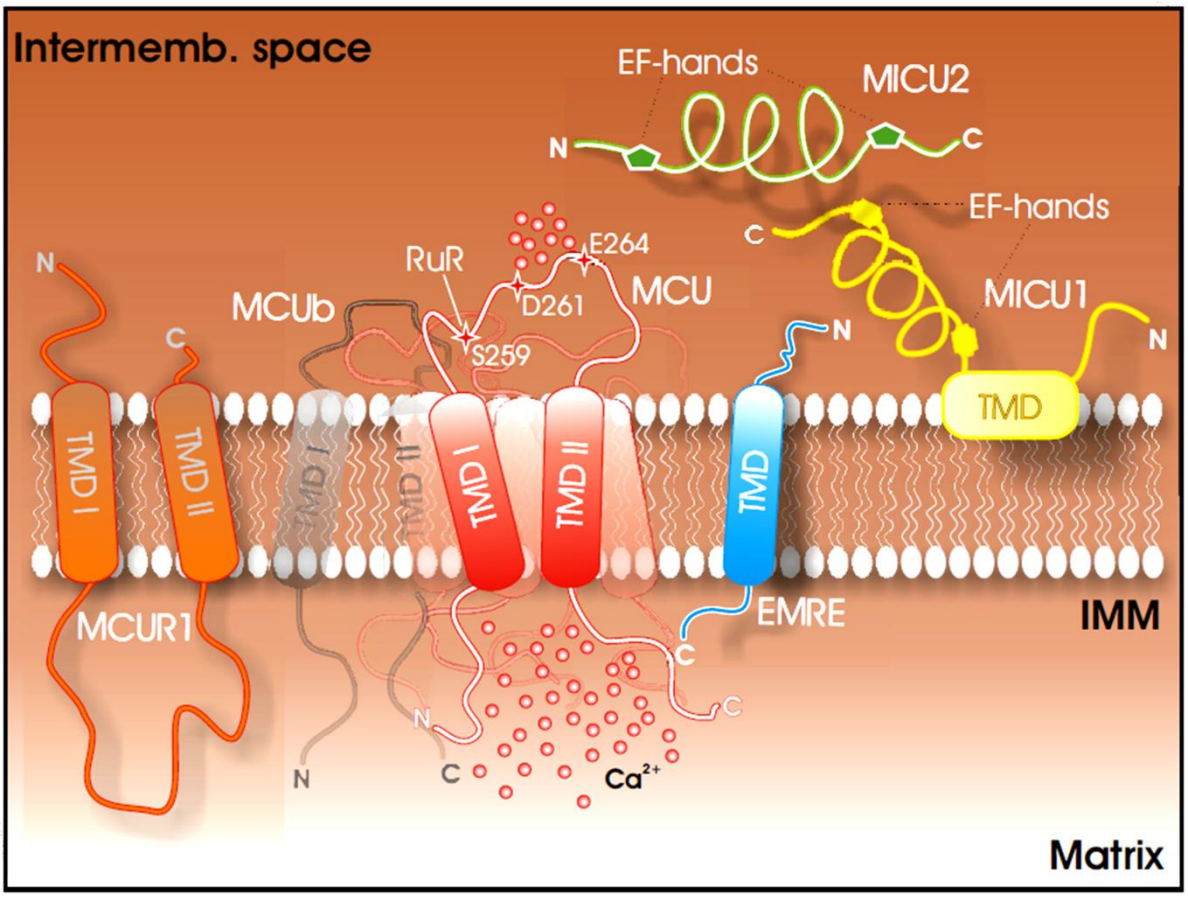

Fig.12: Representation of the different components of the MCU complex so far identified, with their relative topology. From Marchi S. and Pinton P., 2013.

The screening of putative MCU-targeting miRNA revealed that miR-25 (up-regulated in different human cancers) modulates mitochondrial Ca^{2+} uptake through the specific down-regulation of MCU (leaving other mitochondrial parameters and cytosolic Ca^{2+} signals unaffected), conferring resistance to Ca^{2+}-dependent apoptotic stimuli through a reduced mitochondrial Ca^{2+} content (Marchi S. et al., 2013). On this line, the over-expression of MCU was originally associated to an increase sensitivity to Ca^{2+}-dependent apoptotic stimuli, confirming that increased mitochondrial Ca^{2+} loading can predispose to cell death (De Stefani D. et al., 2011).

In a recent paper, exogenously expressed MCU has been demonstrated to increase mitochondrial Ca^{2+} levels following NMDA receptor activation in cortical and hippocampal

mouse neurons, leading to increased mitochondrial membrane depolarization and excitotoxic cell death, without changing the NMDA-evoked whole-cell currents (Qiu J. et al., 2013). The contrary has been obtained by silencing endogenous MCU. Moreover, it has been also demonstrated that synaptic activity transcriptionally represses MCU, via a mechanism involving the nuclear Ca^{2+} and CaM kinase-mediated induction of Npas4, resulting in a protective effect from excitotoxic death through inhibition of NMDA receptor-induced mitochondrial Ca^{2+} uptake.

The ability of mitochondria to shape whole-cell Ca^{2+} signals has been demonstrated in different cell types, but it is still matter of debate in heart cells. This is due to the high speed of systolic Ca^{2+} transients, that could limit the capacity of mitochondria to take up significant amounts of Ca^{2+}. So far, the involvement of the organelles on a beat-to-beat basis remains elusive. However, a recent paper reported that in rat neonatal cardiomyocytes, during spontaneous Ca^{2+} pacing, a large number of Ca^{2+} hot spots (high [Ca^{2+}] microdomains) are generated on OMM surface (Drago I. et al., 2012). The over-expression or down-regulation of MCU reduces or increases the cytosolic Ca^{2+} peaks, due to increased or decreased mitochondrial Ca^{2+} uptake, respectively. Accordingly, the extent of contraction is reduced by over-expression of MCU and augmented by its silencing. Thus, the authors conclude that mitochondria significantly contribute to buffering the amplitude of systolic Ca^{2+} rises, at least in neonatal cardiac myocytes. Further investigations are necessary to clarify whether such a kind of modulation is present also in adult cardiomyocytes, where SR-mitochondria interactions seems to be more ordered and tighter than in neonatal cells.

The characterization of a MCU-KO mouse model produced, however, unexpected results (Pan X. et al., 2013). The authors confirm, as expected, that mitochondria derived from MCU KO mice have no apparent capacity to rapidly take up Ca^{2+}. However, despite the fact that MCU KO mice are slightly smaller, they are surprisingly alive, without evident basal metabolism impairments. They only display alterations in phosphorylation and pyruvate dehydrogenase (PDH) activities in skeletal muscle (consistently with the role of the Ca^{2+}-sensitive phosphatase PDP1 in the regulation of PDH phosphorylation and the observed lower levels of mitochondrial matrix Ca^{2+} in this tissue), with marked impairment in their ability to perform strenuous works. The skeletal muscle phenotype is consistent with a particularly important role of the MCU in this tissue, as suggested by its particularly high expression level (see MCUb section).

Moreover, mitochondria from MCU KO mice lack evidence for Ca^{2+}-induced permeability transition pore (PTP) opening, but surprisingly this defect does not seem to protect MCU KO cells and tissues from cell death. Furthermore, whereas, as expected, the PTP inhibitor Cyclosporin A (CsA) provided significant protection against ischemia-reperfusion injury to WT hearts, this agent had no demonstrable effect on MCU KO hearts. Thus, in the absence of MCU, alternative PTP- or Ca^{2+}-independent cell death mechanisms could emerge and become predominant.

It must be underlined that the authors found a significant reduction, but not a complete absence, of mitochondrial matrix Ca^{2+} in mice lacking MCU, suggesting that alternative Ca^{2+} players (that do not reside inside the uniporter complex) may exist and these slower and presumably low capacitance mechanisms might allow for some physiological adaptation over time, ensuring a slow but continuous Ca^{2+} influx into the matrix. Further studies are needed to better understand the physio-pathological implications of the lack of Ca^{2+} entry into the mitochondrial matrix, and the specific contribution of MCU to this feature .

MCUb

CCDC109B (MCUb) is a paralog of CCDC109A/MCU that encodes a 33 kDa protein, with 50% sequence identity to MCU. Protein topology and structure is very similar to that of MCU, with two TM domains and both the N- and C-termini spanning into the matrix (Fig.12). Compared to MCU, however, sequence differences in aa residues predicted to be critical for ion permeation (in particular two residues in the pore forming region), impede MCUb to display channel activity (*i.e.*, Ca^{2+} current) in reconstituted planar lipid bilayer (Raffaello A. et al., 2013). Moreover, when co-expressed with MCU it abolishes the Ca^{2+} channel activity of the endogenous protein and, in intact cells, its over-expression reduces mitochondrial Ca^{2+} uptake, indicating that it interferes with the activity of the endogenous channel.

MCUb has been demonstrated to directly interact with MCU by co-immunoprecipitation and FRET analysis, thus supporting the idea that it may be incorporated into the MCU oligomer and act as an endogenous dominant negative subunit within the channel (Raffaello A. et al., 2013).

Interestingly, MCUb expression levels are in general lower than those of MCU and the expression profiles of the two proteins in different tissues do not correlate. Thus, as stated by the authors, "*the MCU/MCUb ratio appears to widely differ in the various tissues, possibly*

providing a molecular mechanism for tuning the efficiency of mitochondrial Ca^{2+} *uptake"* (Raffaello A. et al., 2013).

On this line, the MCU/MCUb ratio is particularly high in the skeletal muscle (at least compared to heart) and a recent paper reported a Ca^{2+} influx in skeletal muscle mitoplasts 28-fold higher than that found in cardiac preparations (Fieni F. et al., 2012).

MICU1

The paper that firstly described the discovery of the Mitochondrial Calcium Uptake 1 (MICU1) (Perocchi F. et al., 2010) can be considered the seminal work that has opened the way to the identification of MCU. Indeed, MICU1 was the first component of the MCU complex that has been identified by screening the MitoCarta, searching for proteins directly involved in mitochondrial Ca^{2+} entry.

MICU1 is a 54 kDa protein with a single IMM-associated domain and two highly conserved EF-hand domains (Fig.12). It was initially proposed to be a positive regulator of mitochondrial Ca^{2+} uptake, since its down-regulation reduces this pathway in a way that depends on the presence of the EF-domains (Perocchi F. et al., 2010), without changing cell respiration or mitochondrial membrane potential. MICU1 was demonstrated to physically interact with MCU (Baughman J.M. et al, 2011; Mallilankaram K. et al., 2012).

However, the initially proposed role of MICU1 is different from the currently understood role. In particular, it has been proposed to work as a gatekeeper for MCU (Mallilankaram K. et al., 2012), with the knock-down not significantly changing mitochondrial Ca^{2+} uptake upon cell stimulation, but strongly increasing mitochondrial basal Ca^{2+} content during resting conditions. Thus, MICU1 limited MCU activity when $[Ca^{2+}]_c$ is low (< 3μM), preventing mitochondrial ROS generation and cell stress susceptibility due to exaggerate mitochondrial Ca^{2+} accumulation.

Few months ago another paper however reassessed its role (Csordas G. et al., 2013). First of all, this paper highlighted the correct topology of MICU1, originally proposed to have a TM domain passing through the IMM (Perocchi F. et al., 2010): MICU1 seems to have only an association with the IMM, without traversing it, facing the IMS rather than the matrix. This is important, because MICU1 has been proposed to control MCU activity in a Ca^{2+}-dependent way, by sensing Ca^{2+} through its EF-hand domains (Perocchi F. et al., 2010; Mallilankaram K. et al., 2012). If the topology described by Perocchi presumed that MICU1

senses mitochondrial matrix [Ca^{2+}], that described by Csordas suggests a molecular response to changes in $[Ca^{2+}]_c$. However, it must be pointed out that Csordas's group describes an EF hand-independent mechanism of MICU1 activation in order to stabilize the closed state of the MCU complex. Moreover, differently from Mallilankaram et al., Csordas shows a Ca^{2+} cooperative activation of MCU by MICU1, in particular at high $[Ca^{2+}]_c$. In their hands, the basal $[Ca^{2+}]_m$ is unaltered and the mitochondrial IP3-dependent Ca^{2+} uptake is severely impaired in MICU1 knock-down cells, similarly to those found by Perocchi et al. The different experimental conditions used by these three groups and the different methodologies used to measure Ca^{2+} could partially explain these discrepancies (for a review see Marchi S. and Pinton P., 2013).

Anyway, it appears clear that MICU1 regulates the activity of the MCU complex in a specific range of [Ca^{2+}], probably stabilizing its closed state at low $[Ca^{2+}]_c$, in a way that could depend on Ca^{2+} binding to the MICU1- EF- hand domains. Further investigations will be required to exactly understand the mechanism and the extent of this regulation.

MICU2/3

MICU2 and MICU3 are paralogs of MICU1 and have 25% sequence identity with it. Although both proteins have an N-terminal targeting sequence consistent with mitochondrial localization, MICU3 has not been included in MitoCarta, since it has not a strong mitochondrial localization. Thus, only MICU2 has been so far functionally characterized (Plovanich M. et al., 2013). MICU2 is predominantly expressed in visceral organs, whereas MICU3 is almost exclusively found in neural tissues and skeletal muscle.

Similarly to MICU1, MICU2 possesses two highly conserved EF-hand domains and seems to localize in the IMS (Fig.12). *In vivo* silencing of MICU2 in mouse liver results in a reduced mitochondrial Ca^{2+} uptake upon Ca^{2+} additions, without changing mitochondrial respiration or $\Delta\Psi$, with an effect similar (and additive) to that observed silencing MICU1.

MICU1, MICU2 and MCU physically interact and reside within a complex that migrates at around 480 kDa in Blue Native PAGE. The silencing of MICU1 or MICU2, or of both proteins, shifts this complex to 350 kDa: the three proteins seem to stabilize one each other into the complex, and the down-regulation of one of them induces a destabilization of the others (Plovanich M. et al., 2013). This cross-stabilization seems to be tissue-specific.

Of note, in MICU1-silenced HeLa cells the over-expression of MICU2 restores the wt phenotype rescuing mitochondrial Ca^{2+} uptake, increasing/stabilizing MICU1 protein level. Further studies will be required to elucidate whether the role of MICU2 is redundant or complementary to MICU1, and to clarify the role played by MICU3, at least in those tissues (CNS and skeletal muscle) where it is highly expressed.

Since the levels of expression of these proteins seems to be in some way inter-dependent (De Stefani D. and Patron M. personal communication), and the genetic manipulation of one of them could seriously complicate the interpretation of any data, it will be necessary to use null genetic background models, in which the activity of one paralog can be rigorously assessed in the absence of the others, to exactly solve the puzzle.

MCUR1

Mitochondrial Calcium Uniporter Regulator 1 (MCUR1) is a 40 kDa protein, that was identified by a RNAi screening of 45 human IMM proteins, in order to identify molecules important for mitochondrial Ca^{2+} uptake (Mallilankaram K. et al., 2012b).

MCUR1 has two TM domains, with both the N- and C-termini facing the IMS and a large coiled coil domain spanning into the matrix (Fig.12).

MCUR1 down-regulation results in a strongly decreased $[Ca^{2+}]_m$, both upon cell stimulation or at resting, with a consequent impairment in oxidative phosporilation, an increased AMP/ATP ratio and the activation of an AMP-kinase-dependent pro-survival autophagy (Mallilankaram K. et al., 2012b).

MCUR1 co-immunoprecipitates with MCU but not with MICU1, thus suggesting that MCU exists in a complex with both MICU1 and MCUR1, but not simultaneously. Notably, a recently published paper (Sancak Y. et al., 2013), employing quantitative mass spectrometry of the affinity-purified MCU complex (uniplex), recovered MICU1, MICU2, MCU, its paralog MCUb and an essential MCU regulator (EMRE, see below), but not MCUR1, thus suggesting that this latter protein is not stably associated to the MCU complex and has a role that is not yet completely understood.

However, MCUR1 overexpression enhances mitochondrial Ca^{2+} uptake in histamine-stimulated HeLa cells, but this increase is blunted by MCU knock-down. On the other hand, MCU over-expression increase $[Ca^{2+}]_m$, but not in MCUR1 silenced cells. Of note, MCU levels are increased in MCUR1 knock-down HeLa cells (Mallilankaram K. et al., 2012b). All

these results strongly suggest that both MCU and MCUR1 are required for an efficient mitochondrial Ca^{2+} entry, and that a deep relationship exists between these two proteins, despite the fact that MCUR1 is not stably associated to the MCU complex.

EMRE

Using a quantitative mass spectrometry-based approach of the affinity purified MCU complex, the authors of a recent paper reported the discovery of EMRE (Essential MCU Regulator), a component of the uniporter "uniplex" (Sancak Y. et al., 2013). EMRE is a metazoan-specific 10 kDa IMM protein with a single TM domain (Fig.12).

EMRE silencing severely impaired mitochondrial Ca^{2+} uptake and MCU over-expression in EMRE knockdown cells is unable to rescue this parameter. Loss of MCU decreases EMRE (and MCUb) abundance in a post-translational way, thus confirming a strict inter-dependence between these proteins.

Loss of EMRE or MICU1 reduces the size of the MCU complex from 480 kDa to 300 kDa in Blue Native PAGE. In EMRE KO cells, MICU1/2 do not co-immunoprecipitate with MCU (but MCUb does). On the contrary, the absence of MICU1 does not impair MCU/EMRE interaction, suggesting that EMRE could work like an essential bridge, that links MICU1/2 Ca^{2+} sensing activity in the IMS to the MCU oligomers channel activity in the IMM.

OTHERS PROTEINS DIFFERENTIALLY INVOLVED IN MITOCHONDRIA Ca^{2+} UPTAKE

Different proteins have been reported to be involved in the mechanism of mitochondrial Ca^{2+} uptake, although several data are controversial and still to confirm (for a review see Pizzo P. et al., 2012).

For example, by immune-electron-microscopy RyR1 has been found in IMM of heart mitochondria and it was suggested to work in reverse mode, mediating mitochondrial Ca^{2+} uptake (Beutner G. et al., 2001). Excluding the possibility of a contamination from the SR, since cardiac cells express RyR2 (and not RyR1), this conclusion needs further investigations. In particular, it is not clear how mitochondria isolated from different tissues that do not express RyR1 show an efficient mitochondrial Ca^{2+} uptake as that observed in cardiac organelles. The possibility that RyR1 is directly involved in mitochondrial Ca^{2+} uptake appears thus unlikely.

In another paper, it has been reported that the down-regulation or the over-expression of the uncoupling proteins 2 and 3 (UCP2/3) reduces or increases the accumulation of Ca^{2+} into mitochondria (Trenker M. et al., 2007). The same group reported also that UCP2 and 3 are able to modulate the activity of the uniporter, and thus mitochondrial Ca^{2+} uptake, only when cytosolic Ca^{2+} rises because released from the ER (Waldeck-Weiermair M. et al., 2010). A direct role of UCP2/3 on mitochondrial Ca^{2+} uptake, however, has not been confirmed by others. In particular, mitochondria isolated from UCP2 KO and UCP3 KO mice take up Ca^{2+} normally (Brookes P.S. et al., 2008). Moreover, UCP3 has been reported to inhibit SERCA activity by decreasing the ability of mitochondria to produce ATP (De Marchi U. et al., 2011). Thus, UCP2/3 effects on mitochondrial Ca^{2+} uptake, if any, could be explained by a general cellular metabolic alteration.

In 2009, the previously believed component of the PM H^+/K^+ exchanger Letm1 was proposed to be a mitochondrial H^+/Ca^{2+} electrogenic antiport with high Ca^{2+} affinity, distict from the low affinity MCU (Jiang D. et al., 2009). Purified Letm1 reconstituted into liposomes was able to mediate a Rutenium Red sensitive mitochondrial Ca^{2+} uptake. Other groups, however, challenged this idea, showing compelling evidence that Letm1 is probably a H^+/K^+ antiporter, since in MEFs the Letm1 KO phenotype could be rescued by nigericin, a bona fide H^+/K^+ ionophore (Fig.13) (for a review see Nowikovsky K. et al., 2012). For these reasons, the Letm1 role in mitochondria Ca^{2+} uptake is still matter of debate. Anyway, the recent RNAi screening that permitted the identification of MCUR1 (Mallilankaram K. et al., 2012b) confirmed a role for Letm1 in mitochondrial Ca^{2+} handling, since its silencing induces a decreased Ca^{2+} uptake into the organelles. Further investigations will be required to better clarify this issue.

NCLX

Immediately after the afore mentioned seminal studies in the 60s revealing the capacity of mitochondria to take up massive amount of Ca^{2+}, it was soon realized that this uptake must be balanced by a subsequent Ca^{2+} release.

The suggestion that a mitochondrial Na^+/Ca^{2+} exchanger (NCX) could exist was initially based on the observation that, in isolated mitochondria, upon addition of Na^+ to the external solution, a release of Ca^{2+} is activated (Carafoli E., 1974; Crompton M. et al., 1977; Crompton M. et al., 1978. For reviews see Boyman L. et al., 2013; Palty R. and Sekler I., 2012). Among the other tested cations, only Li^+ was found to be also effective on the

activation of this Ca^{2+} efflux and the amount of the released Ca^{2+} was found to be dependent on [Na^{+}]. This release was however not inhibited by Ruthenium Red, thus suggesting that it is mediated by a mechanism distinct from the one responsible for the uptake. Moreover, the direction and the amplitude of ion movements were strictly dependent on the relative [Na^{+}] and [Ca^{2+}] in the extra-mitochondrial (*i.e.*, the cytosol in a cellular context) and matrix environment (this mean that it could work also in a reverse mode, extruding Na^{+} and taking up Ca^{2+}, although the physiological relevance of this pathway remains to be proved).

This NCX was observed to be particularly effective in excitable tissues, such as heart, brain and skeletal muscle, while in other non excitable tissues like liver, although this activity is present and physiologically relevant, the H^{+}/Ca^{2+} exchanger seems to be more prominent.

Similarly to what happened for MCU, although the properties of this exchanger were known for decades, the molecular identification of the mitochondrial NCX was still lacking till 2010. In 1992, a ~110-kDa polypeptide was purified from bovine heart mitochondria and, when reconstituted in liposomes, catalyzed a Na^{+}/Ca^{2+} and Na^{+}/Li^{+} exchange (NCLX) (Li W. et al., 1992). In 2010, Sekler and co-workers demonstrated that the NCLX (until then considered an isoform of the PM Na^{+}/Ca^{2+} exchanger family) fulfils the criteria to be the elusive mitochondrial Na^{+}/Ca^{2+}antiport (Fig.13) (Palty R. et al., 2010).

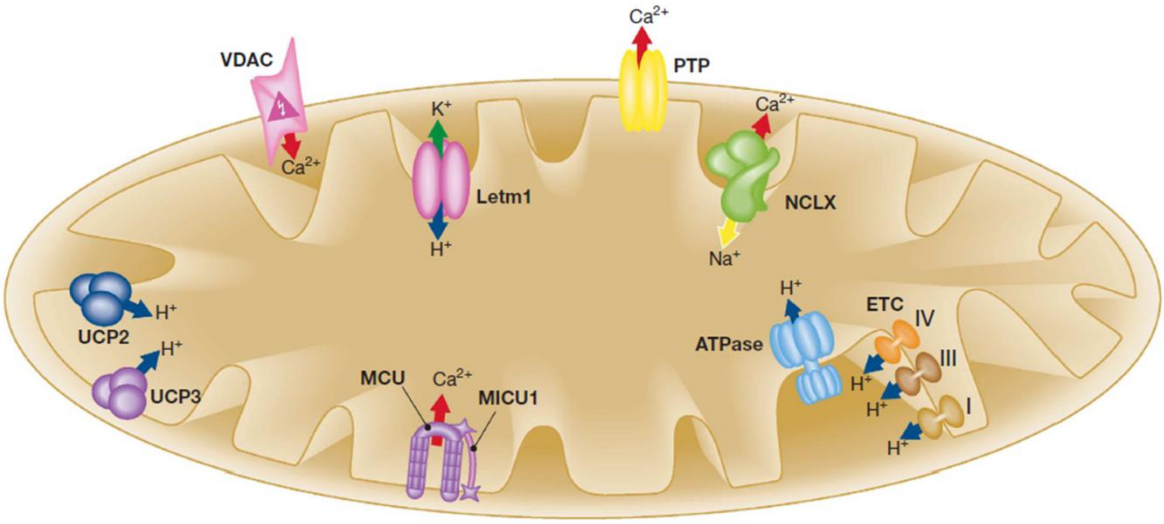

Fig.13: Schematic representation of the main mitochondrial Ca^{2+}, Na^{+} and H^{+} handling machineries. From Drago I. et al., 2011.

The same group has previously isolated NCLX thinking, however, that it was a novel PM Na^{+}/Ca^{2+} exchanger (Palty R. et al., 2004); the final discovery has originated from a

fortuitous manifestation, *i.e.*, the partial mis-targeting of the over-expressed NCLX to PM. Indeed, they found that this mis-targeted protein was able not only to exchange Na+/Ca2+, but is also to mediate an efficient Li^+/Ca^{2+} exchange, a unique feature of the unidentified mitochondrial NCLX, not shared with members of the PM-NCX family. They also demonstrates that (for a review see also Drago I et al., 2011):

a) NCLX appears as a 50 kDa monomer, an additional 70 kDa monomer and forms also a 100 kDa dimer, a size similar to that of the 110 kDa polypeptide previously isolated from heart mitochondria and displaying NCLX activity (Li W. et al., 1992);

b) endogenous NCLX is present in the IMM;

c) NCLX is sensitive to the well known mitochondrial NCX inhibitor CGP-37157;

d) knock down of NCLX drastically reduces the Na^+-dependent Ca^{2+} efflux in isolated mitochondria;

e) a catalytically inactive mutant of NCLX blocks the Na^+/Ca^{2+} exchange in isolated mitochondria from transfected cells, thus acting as a dominant negative and suggesting that the protein works as an oligomer;

f) the PM mis-targeted NCLX appears to mediate an electrogenic transport of 3(4) Na^+ ions per Ca^{2+} transported.

The stoichiometry of the NCLX-mediated exchange is still matter of debate, although compelling evidence suggest a 3 Na^+/1 Ca^{2+} ratio, thus being electrogenic and exploiting a still poorly characterized Na^+/H^+ exchanger to remove Na^+ entered into the matrix (at the expense of some $\Delta\Psi$).

OTHERS EFFLUX PROTEINS

In different non excitable tissues (especially in liver) most of the mitochondrial Ca^{2+} efflux depends on a H^+/Ca^{2+} antiporter (Fig.11). Despite the fact that a polypeptide of 55 and 66 kDa with exchange activity has been purified by affinity chromatography years ago (Villa A. et al., 1998), a complete characterization of this antiporter is far from being obtained. Importantly, although some evidence that it could be modulated by membrane potential has been provided (Bernardi P. and Azzone G.F., 1983), it is still unclear whether this exchanger is electroneutral or electrogenic (*i.e.*, 2 H^+ or 3 H^+/1 Ca^{2+}).

Finally, it has been proposed that Ca^{2+} could efflux from mitochondria through the large-size permeability transition pore (mPTP; for a review see Bernardi P., 1999). Notably, PTP can undergo transient openings (flickerings), both in isolated mitochondria and in intact cells, thus permitting Ca^{2+} release from mitochondria when the [Ca^{2+}] into the matrix is higher than in the external medium. This phenomenon contributes to organelle Ca^{2+} homeostasis, acting as a rapid, pro-survival Ca^{2+}-induced Ca^{2+} release mechanism without causing catastrophic and irreversible PT (for a review see Rasola A. and Bernardi P., 2011). The molecular nature of PTP is not completely clear. A recent paper, however, provided compelling evidence that dimers of the F0F1 ATP synthase form a channel with features identical to those of the mitochondrial megachannel (MMC), the electrophysiological equivalent of the PTP (Giorgio V. et al., 2013).

ROLE AND SIGNIFICANCE OF MITOCHONDRIAL Ca^{2+} UPTAKE

The functional role of mitochondrial Ca^{2+} uptake is multifaceted. Three are the main functions that have been reported: ATP synthesis, cell death activation and buffering/shaping of cytosolic Ca^{2+} rises.

As far as ATP synthesis is concerned, a general consensus exists on the stimulatory role of mitochondrial Ca^{2+} uptake on the activity of three key enzymes of the Krebs cycle, *i.e.*, pyruvate dehydrogenase (PDH), isocitrate dehydrogenase (ICDH) and α-ketoglutarate dehydrogenase (OGDH). All three enzymes increase their V_{max} upon Ca^{2+} binding, although through different mechanisms (Denton R.M., 2009). Activation of the dehydrogenases results in stimulation of electron flow in the respiratory chain and, as a consequence, increased ATP synthesis. Indeed, rises in mitochondrial Ca^{2+} have been observed to induce cytoplasmic and intra-mitochondrial ATP increases in different cell models (Fig.14) (see the review attached at the end of this manuscript, Pizzo P. et al., 2012). Moreover, Ca^{2+} modulates several IMM-located carriers for ions and metabolites (Del Arco A. et al., 2000). Recently, Foskett group reports that in normal conditions, a constitutive IP3-mediated Ca^{2+} release from the ER occurs and this Ca^{2+} is taken up by mitochondria, a phenomenon that is required to inhibit pro-survival mitophagy, promote efficient mitochondrial respiration and maintain cellular bioenergetics (Cardenas C. et al., 2010).

A particular relationship exists between ATP synthesis and control of mitochondrial motility by Ca^{2+}. It is well established that micromolar $[Ca^{2+}]_c$ stops mitochondria movements (through Ca^{2+} binding to the EF-hand domains of Miro1, a protein involved in

mitochondrial movement; MacAskill A.F. and Kittler J.T., 2010) and traps them in the neighborhood of active high [Ca^{2+}] sites. This allows an higher mitochondrial Ca^{2+} uptake and an increased ATP production at sites that are generally high energy demanding, such as those in close apposition to ER or the synapses in neurons (MacAskill A.F. and Kittler J.T., 2010; Chang K.T. et al., 2011; Yi M. et al., 2004). Here, the ATP released from mitochondria regulates the activity of various proteins, *in primis,* the SERCA and the IP3R, thus also locally shaping the cytosolic Ca^{2+} signal and establishing a bi-directional relationship between Ca^{2+} release from the ER and ATP production.

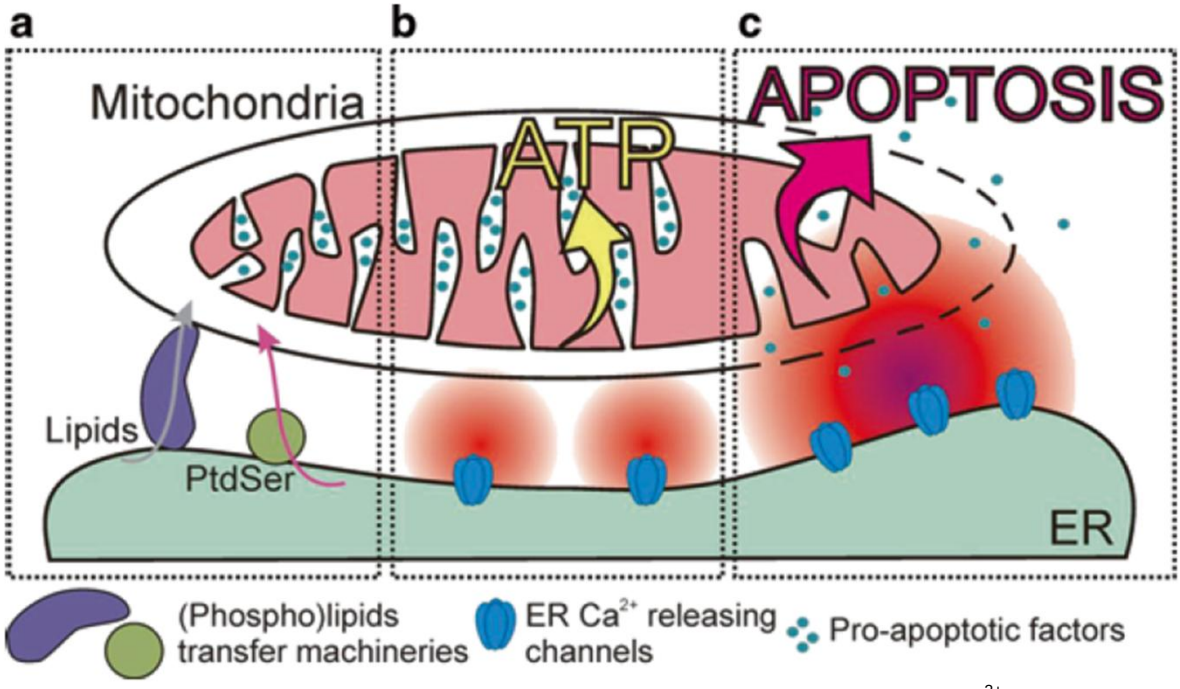

Fig.14: Under physiological conditions, ER and mitochondria exchange lipids (a) and Ca^{2+} (b). A controlled mitochondrial Ca^{2+} uptake (b) promotes ATP production, but its excessive uptake can induce apoptosis (c). From Filadi R. et al., 2012 (see attachments).

On the same line, recent works have revealed how, during ER stress, cells can modulate Ca^{2+} transfer between ER and mitochondria, in order to handle this particular condition of emergency. In particular, during early phases of ER stress the reticular and mitochondrial networks are redistributed towards the perinuclear area, with an increase in their physical connection that results in a higher mitochondrial Ca^{2+} uptake, a more efficient respiration and a rise in ATP production (Bravo R. et al, 2011). This stimulation of mitochondrial metabolism seems to be a cell attempt to adapt to ER stress conditions, by enhancing their bioenergetics in order to supply the increased energy demand. Similarly, Sigma-1 receptor (Sig-1R) is a MAMs resident ligand-operated receptor chaperone, which under normal/physiological conditions is associated with BiP in a dormant state. This association is

Ca^{2+} dependent and, upon ER stress associated to a decrease in ER [Ca^{2+}], Sig-1R dissociates from Bip, binds IP3R-3 and attenuates its degradation, thus promoting a Ca^{2+} transfer to mitochondria sufficient for metabolic activities and allowing cell survival (Hayashi T. and Su T.P., 2007).

On the other hand, it is well established that mitochondrial Ca^{2+} overload could result in cell death (for a review, see Pinton P. et al., 2008). Excessive Ca^{2+} uptake collapses the proton gradient between the two sides of IMM, thus causing bioenergetic impairment and cell death by necrosis. However, mitochondrial Ca^{2+} can also induce cell death by apoptosis in a more fine way, sensitizing cells to apoptotic stimuli (Fig.14). In particular, physiological oscillations in mitochondrial [Ca^{2+}] do not induce mitochondrial PTP opening *per se*, but when concomitant with pro-apoptotic stimuli, like ceramide, mitochondrial Ca^{2+} rises favour PTP opening by binding to cyclophilin D, inducing the release of pro-apoptotic factors in the cytosol (such as cytocrome-c) and the activation of the apoptotic cascade (for a review, see Rasola A. and Bernardi P., 2011). Moreover, VDAC1 has been reported to selectively transfers apoptotic Ca^{2+} signals to mitochondria, forming a physical interaction via Grp75 with IP3Rs (expecially IP3R-3) (De Stefani D. et al., 2012). This interaction is not static, but is enhanced by apoptotic stimuli. Furthermore, the mitochondrial fission protein Fis1 has been demonstrated to convey an apoptotic signal from the mitochondria to the ER, by interacting with Bap31 at the ER and facilitating its cleavage into the pro-apoptotic p20Bap31, an event associated with Ca^{2+} release from the ER and activation of mitochondria for apoptosis (Iwasawa R. et al., 2011).

Finally, considering their buffering function, it is reported that mitochondria are able to actively buffer and shape both local and bulk cytosolic Ca^{2+} rises. In the first case, the sites are those in close contact with ER or plasma membrane, where Ca^{2+} microdomains are created near the mouth of Ca^{2+} channels. While the ability of mitochondria to promptly detect Ca^{2+} microdomains close to the ER is widely demonstrated, their action close to the PM is more controversial. In particular, it seems that mitochondria are able to buffer Ca^{2+} influx through VOCCs, but not that through Orai1 when CCE is activated. On the other hand, in the case of bulk cytosol, mitochondria modulate the amplitude and the extension of Ca^{2+} rises. On this line, MCU over-expression or knock-down respectively decreases or increases cytosolic Ca^{2+} peaks upon release from ER, accordingly to augmented or diminished Ca^{2+} uptake by mitochondria (see also MCU paragraph). All these aspects are extensively reviewed in the attached review (Pizzo P. et al., 2012).

ER-MITOCHONDRIA CONNECTIONS

The first evidence of the existence of close contacts between ER membranes and the OMM date back to the 1960s (Fig.15) (Robertson J.D., 1960; Ruby J.R. et al., 1969; Morré D.J. et al., 1971), but the multifaceted significance of these appositions has started to be elucidated only more recently. In particular, the specific sub-domains of ER membranes that interact with the OMM were defined MAMs (Mitochondria-Associated Membranes) by Jean Vance in 1990, when she firstly discovered that these tight associations were essential for lipid synthesis and exchange between the two organelles (Vance J., 1990). In particular, an ER fraction that is attached to mitochondria can be biochemically isolated (mitochondria-associated membrane (MAM) fraction, enriched in enzymes that are involved in lipid synthesis, including phosphatidylserine (PS) synthase; Stone S. J. and Vance J. E., 2000).

Very soon it became clear that the ER/mitochondria tethering is essential also for the Ca^{2+} cross-talk between the two organelles. Indeed, despite the Ca^{2+} low affinity of MCU, Ca^{2+} is promptly taken up by mitochondria upon release from the ER, thanks to the existence of close contacts (enriched in IP3Rs and RyRs) between the two organelles. At this level, cytosolic microdomains of high [Ca^{2+}], "Ca^{2+} hot spots", can be generated (Rizzuto R. et al, 1993; Rizzuto R. et al., 1998; Csordas G. et al, 1999; Rizzuto R. and Pozzan T., 2006) and efficiently detected (Fig.16). This hypothesis was supported by a variety of indirect evidence that culminated with the possibility to directly visualize, in living cells, the close proximity of mitochondria to ER membranes (Rizzuto R. et al., 1999; Rizzuto R. and Pozzan T., 2006). The idea that high cytosolic Ca^{2+} microdomains, very close to mitochondria, are required to allow significant organelle Ca^{2+} uptake was finally proved by FRET-based Ca^{2+} probes specifically targeted to the cytosolic side of the OMM. With this approach, it was possible to show that upon cell stimulation and Ca^{2+} release from the ER, mitochondria are indeed exposed to local [Ca^{2+}] higher than those of the bulk cytosol (10-30μM vs 1-3μM, respectively) (Giacomello M. et al., 2010; Csordas G. et al., 2010).

Regions of close contact between the ER and mitochondrial membranes, in which the two membranes are closely apposed but do not fuse, thus keeping organelle identity, can be observed by electron and fluorescence microscopy in animal cells and yeast (Fig.15). The distance between the ER and mitochondria in these regions have been measured to be 10–30 nm. This distance is close enough to suggest that the two organelles are tethered together by proteins located on the apposing membranes. Moreover, ribosomes are excluded from the ER membrane at this level, thus further indicating that contact sites form at specialized ER

domains (for a review, see Rowland, A.A. and Voeltz, G.K., 2012). The presence of trypsin-sensitive proteinaceous tethers between the two membranes is now well established (Fig.15) (Csordas G. et al., 2006) and the list of proteins with structural and signaling functions at the ER/mitochondria interfaces is constantly increasing, revealing a previously unexpected complexity (for recent reviews the reader is reffered to the attached chapter Filadi R. et al., 2012; and to Giorgi C. et al., 2009; Hayashi T. et al., 2009; Raturi A. and Simmen T., 2013).

In yeast, the ERMES complex (ER-mitochondria encounter structure) is a complex of at least four proteins (Mdm10/ Mdm34, which are integral OMM proteins, Mmm1, an integral ER protein and the cytosolic Mdm12) whose assemblying favours lipid/metabolite exchange and zippers ER to mitochondria (Kornmann B. et al., 2009).

To date, the best characterized ER-mitochondria tether in mammals is Mitofusin-2 (Mfn2). Mfn2 is an OMM protein, but a fraction resides also in the ER, particularly at the level of MAMs (de Brito O.M. and Scorrano L., 2008). ER resident Mfn2 has been proposed to engage homo- or hetero-typic interactions with respectively Mfn2 or its homologous Mfn1 on OMM, thus mediating a physical tethering between the two organelles that has been shown to affect their Ca^{2+} shuttling (de Brito O.M. and Scorrano L., 2008). The presence however of residual ER-mitochondria apposition in Mfn2 KO MEFs suggests that additional tethers should exist.

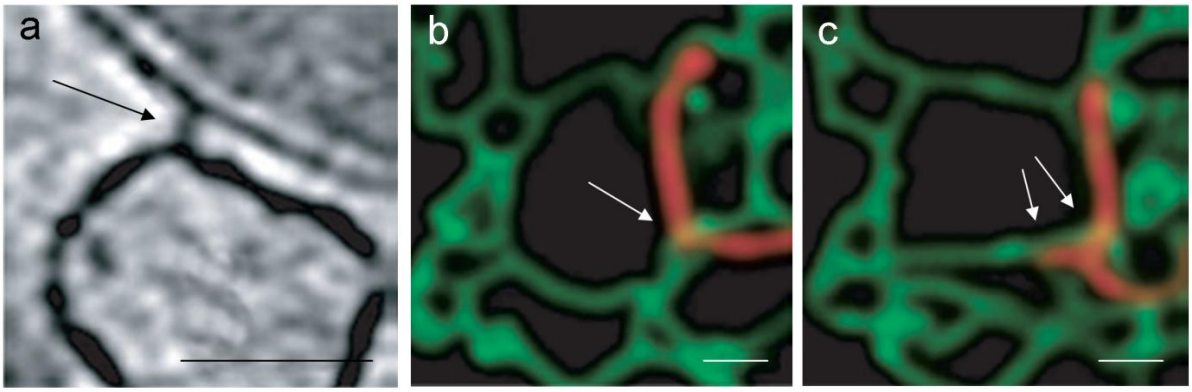

Fig.15: a) EM tomograph of a rat liver cell: the image reveals electron-dense 'tethers' between the ER and mitochondrial membranes (marked by an arrow). Bar = 50nm. b) and c) Arrows indicate ER and mitochondria movements from 0 to 30 seconds. As the mitochondria moves, the ER moves with it. Bars = 1μm. From Rowland A.A. and Voeltz G.K., 2012.

Of note, both PS1 and PS2 have been found to be highly enriched in MAMs (Area-Gomez E. et al., 2009). However, we recently demonstrated that only PS2, and not PS1, favours ER-mitochondria tethering and Ca^{2+} tranfer, with its FAD mutants particularly effective in this

novel function (Zampese E. et al., 2011; Kipanyula M.J. et al., 2012). An increased ER-mitochondria tethering has been also showed in cells expressing FAD PS1 and APP mutations (and even in fibroblasts from sporadic AD patients), although the mechanism of this common effect is unclear (Area-Gomez E. et al., 2012).

The role played by PS2 in ER-mitochondria juxtaposition and the molecular mechanism involved is the issue investigated and presented in this thesis (see Results).

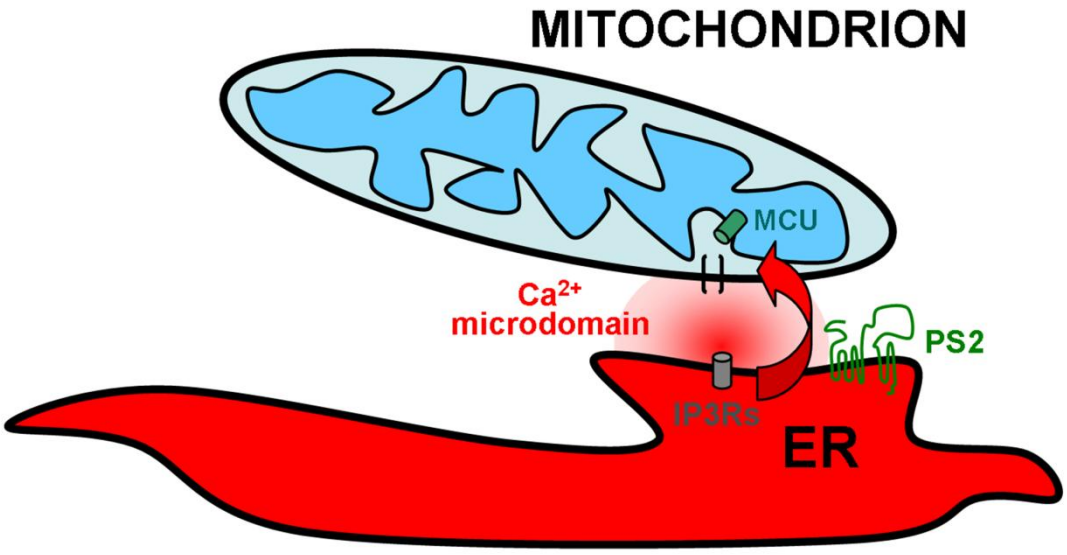

Fig.16: Schematic representation of a high [Ca^{2+}] microdomain in a region of close contact between ER and mitochondria.

Contact sites can have different structural features, ranging from discrete, punctate regions to more extensive ones, where ER membranes circumscribe almost completely around a mitochondrion. The contacts, although dynamic, appear to be relatively stable structures, because the two organelles stay tethered to each other even if they move along the cytoskeleton, thus suggesting that their maintenance is important (Fig.15) (Rowland, A.A. and Voeltz, G.K., 2012).

To date, the best characterized functions of the intimate liaison between ER and mitochondria are the exchange of lipids and the transfer of Ca^{2+}. Among others, it has also been proposed that the ER/mitochondria axis is important for mitochondrial morphology/biogenesis (in particular their fission) (Korobova F. et al., 2013; Friedman J.R. et al., 2011), autophagosome formation (Hamasaki M. et al., 2013), mitochondrial inheritance (Rowland, A.A. and Voeltz, G.K., 2012) and mitochondrial quality control

(Westermann B., 2010). The issue is complex and for more details the reader is referred to a couple of excellent recent reviews (Raturi A. and Simmen T., 2013; Rowland, A.A. and Voeltz, G.K., 2012) and to the attached chapter at the end of this manuscript (Filadi R. et al., 2012), where additional references to other studies are described.

Ca^{2+} MEASUREMENTS IN LIVING CELLS

An adequate measurement of Ca^{2+} dynamics in living cells requires tools with sufficient sensitivity and spatial/temporal accuracy. Indeed, [Ca^{2+}] inside the cell can change quickly, depending from the state of the cell (resting/stimulated) and the specific sub-cellular compartment analyzed. Chemical and protein-based Ca^{2+} indicators are commonly used.

Chemical probes are fluorescent compounds that can be loaded in living cell and used for measurements, such as Fura-2, Fluo-3, Indo-2; these indicators, originally devised by R.Y. Tsien (Tsien R.Y., 1980), are based on the EGTA Ca^{2+}-chelator structure. The structural changes induced by Ca^{2+} binding lead to a change in the spectral emission and/or excitation properties of the probe, thus allowing an estimation of [Ca^{2+}] variations. The chemical indicators now available allow intracellular Ca^{2+} detection over a large range of concentration (<50 nM to >50 μM). High affinity indicators can be used to quantify Ca^{2+} levels in the cytosol while lower affinity indicators can be optimized for measuring Ca^{2+} within sub-cellular compartments with higher concentrations (for a review, see Paredes R.M. et al., 2008). Indicators can be classified into either single wavelength or ratiometric dyes. Both classes require specific excitation and detection equipments, depending on their spectral properties. Single wavelength indicators are generally brighter and could facilitate Ca^{2+} detection when more than one fluorophore is used. Ratiometric dyes can be calibrated very precisely and minimize the most common problems associated with synthetic indicators, including different dye loading, photobleaching, leakage and changes in cell volume (Paredes R.M. et al., 2008).

Protein-based Ca^{2+} probes include aequorin and GFP-based dyes. Aequorin (Aeq) is a 22 kDa Ca^{2+}-sensitive photoprotein, with an hydrophobic core that binds the prostetic group coelenterazine. It has three Ca^{2+} binding sites: upon Ca^{2+} binding, the covalent link between the prosthetic group and the apoprotein is quickly broken with the emission of one photon, as an irreversible reaction; importantly, the rate of photon emission depends on the [Ca^{2+}], thus allowing the conversion of the amount of emitted light into [Ca^{2+}] through a specific algorithm, that take into consideration the different experimental conditions (Brini M. et al.,

1995). Aeq (wt) is normally expressed in the cytosol and allow to measure [Ca^{2+}] in the range 0.5-10 μM. The addition of targeting sequences for specific intracellular localization, together with mutations within its aa sequence to decrease the affinity for Ca^{2+} (mut Aeq), allowed the measurements of [Ca^{2+}] in intracellular organelles where the [Ca^{2+}] is high, such as the ER, the Golgi apparatus and mitochondria (for a review, see Brini M., 2008). Moreover, the combination with modified prosthetic groups (coelenterazine N) or the substitution of Ca^{2+} with the surrogate Sr^{2+}, as detected cation, further increase the dynamic range of Aeq. Among several advantages in the use of Aeq, there are a low Ca^{2+} buffering effect, a low pH sensitivity, a high signal/noise ratio, a relatively cheap/simple equipment and, in the case of co-transfection, the possibility to limit the analysis only to cells expressing the protein of interest (Brini M. et al., 2008). Among the disadvantages, however, the need of transfect the cells to analyze (or the use of stably expressing clones), the need of reconstitute the protein with coelentarazine for at least 1h before the experiment, the low amount of light emitted by the photoprotein. This latter feature implicates that, by using Aeq-probes, it is quite difficult to obtain results at the single cell level, and thus it is mostly employed for cell population analysis (Brini M. et al., 2008).

On the other hand, several approaches to create GFP-based Ca^{2+} probes were conceived, all based on the Ca^{2+}-sensor CaM, because of its Ca^{2+} sensitivity and for its structural change upon binding to the cations. Indeed, the change in CaM conformation can be translated into a change in the spectral properties of the GFP(s) fluorescence, allowing the measurement of [Ca^{2+}] variations. Three different GFP-CaM-based probes are available: “pericams”, “camgaroo” and “cameleons” (Pozzan T. et al., 2003; Rudolf R. et al., 2003). Among the three, Cameleons are the most widely diffused. The first group of cameleons was based on two different GFPs, the Blue-shifted mutant Fluorescent Protein (BFP) and the Green Fluorescent Protein (GFP), linked by CaM and its binding peptide M13; upon Ca^{2+} binding, CaM rearranges and brings the two fluorophores in close proximity, thus increasing the fluorescence resonance energy transfer (FRET, see below) between them. As for Aeq-based probes, the possibility to selectively target the protein to specific organelles and to change the Ca^{2+}-affinity of the probe becames immediately clear. To overcome the major limitations of these first cameleons, in particular the pH sensitivity and the interference with endogenous CaM or CaM-binding proteins, the probes have been re-designed, substituting the BFP with a Cyan Fluorescent Protein (CFP) and the GFP with a modified Yellow Fluorescent Protein (YFP), the circularly permutated Venus, cpV, obtaining a lower sensitivity to intracellular environment, different Ca^{2+} affinity and a broader dynamic range (Palmer A.E. et al., 2006).

FRET is a non-radiative energy transfer between a donor and an acceptor cromophore, that occurs when the emission spectrum of the donor overlaps with the excitation spectrum of the acceptor and when the two molecules are close enough (2-7 nm, the more they are closer, the more FRET is efficient) and in an adequate relative orientation. Considering Cameleon probes, when FRET does not occur (low [Ca^{2+}]) CFP is excited at 440 nm and emits at 480 nm, while YFP is substantially unaffected; when [Ca^{2+}] rises, the conformational change of CaM brings closer CFP and YFP, so that excited CFP transfers its energy to YFP, that emits at 530 nm. Thus, a rise in [Ca^{2+}] can be observed both as an increase in YFP (530 nm) emission and as a decrease in CFP (480 nm) emission: the ratio between F530/F480 allows to magnify changes in [Ca^{2+}]. Cameleon FRET-based Ca^{2+} probes can be target to several organelles and efficiently used to monitor Ca^{2+} dynamics at the single cell level (Rudolf R. et al., 2003).

AD AND Ca^{2+}

In 1989, Khachaturia proposed that sustained alterations in Ca^{2+} homeostasis could be responsible for the neurophathological degeneration observed in AD. After few years, evidence started to accumulate in support of this hypothesis. An exaggerated IP3-mediated Ca^{2+} release from the ER was observed in fibroblasts from patients still asymptomatic but harboring PS-FAD mutations, thus indicating that alterations in Ca^{2+} homeostasis is an early event and not just a consequence of neurodegeneration (Ito E. et al., 1994; Etcheberrigaray R. et al., 1998). Numerous follow-up studies have confirmed the FAD-PS-mediated excessive ER Ca^{2+} release in other models, including neurons from FAD-PS1 transgenic mice (reviewed in LaFerla F.M., 2002; Honarnejad K. and Herms J., 2012). Interestingly, Ca^{2+} release from RyRs was also found to be potentiated as a consequence of the presence of FAD-PS, probably due to an upregulation of RyR expression (reviewed in Honarnejad K. and Herms J., 2012).

Thus, from these early studies the “calcium overload” hypothesis was proposed, arguing that the ER Ca^{2+} overload is the primary cause of excessive release from the ER, mitochondrial Ca^{2+} overload, altered kinase activities and, eventually cell death and neurodegeneration. In support of this hypothesis came the finding that wt PS holoprotein forms passive Ca^{2+} leak channels on planar lipid bilayers and FAD-PS mutants impaire this leak activity, thus leading to an increased ER Ca^{2+} content (Tu H.et al., 2006).

More recent data (obtained among others also by our groups), however, have challenged the "Ca^{2+} overload" hypothesis (Brunello L. et al., 2009; Cheung K.H. et al., 2008). By directly monitoring the absolute ion content within the ER, these groups found that the expression of FAD-PS mutations lead to an unchanged or even attenuated ER Ca^{2+} level, especially when considering FAD-PS2 mutations (Zatti G. et al., 2004; Giacomello M. et al., 2005; Zatti G. et al., 2006; Brunello L. et al., 2009; McCombs J.E. et al., 2010; Shilling D. et al., 2012; Kipanyula M.J. et al., 2012). As far as the mechanism is concerned, our group found a reduction in SERCA activity and a slight increase in basal Ca^{2+} leakage through IP3Rs and RyRs upon PS2 over-expression (Brunello L. et al., 2009), with a reduced response to IP3-linked stimuli but an increase response to caffeine (a RyR activator) (Kipanyula M.J. et al., 2012); others proposed that the reduction in ER Ca^{2+} content in the presence of FAD-PS is due to a sensitization of IP3Rs to lower concentration of IP3, thus enhancing its gating. Inconsistent results have been obtained using PS-DKO MEF cells, describing either attenuated (Kasri N.N. et al., 2006) or amplified (Tu H. et al., 2006) Ca^{2+} release from the ER.

Physical interactions of PS with SERCA2b, IP3Rs and RyRs have been reported (reviewed in Honarnejad K. and Herms J., 2012), thus revealing the complex and multifaceted role of PS in modulation of Ca^{2+} homeostasis. Moreover, as far as CCE is concerned, different studies indicate that it is attenuated in presence of FAD-PS mutants (Yoo A.S. et al., 2000; Herms J. et al., 2003; Giacomello M. et al., 2005), although it is not completely clear if such a reduction is due to a direct effect of PS on CCE, it simply reflects changes in the ER Ca^{2+} content or is associated to an indirect effect mediated by the produced Aβ peptide.

mRNA levels of several genes involved in the mainteinance of Ca^{2+} homeostasis are altered in cerebral tissue from AD patients (Emilsson L. et al., 2006). Recently, a single nucleotide polymorphism in CALHM1 (a newly discovered Ca^{2+} channel) has been described to modulate the permeability of the channel to Ca^{2+}; CALHM1 polymorphism has been considered a risk factor for the development of sporadic AD (Dreses-Werringloer U. et al., 2008), although different recent studies argued against this conclusion (reviewed in Supnet C. and Bezprozvanny I., 2010).

Finally, a reciprocal inter-relation between Ca^{2+} homeostasis alterations and APP processing has emerged, with some studies associating an increased $[Ca^{2+}]_c$ with an increased Aβ production, although controversial results have been obtained (reviewed in LaFerla F.M.,

2002; Bojarski L. et al., 2008). Aβ has been proposed to form low conductance cationic channels in PM permeable to Ca^{2+}, and is reported to interfere with NMDA and AMPA receptors activity, affecting LTP (Haass, C. and Selkoe, D.J., 2007; Querfurth H.W. and LaFerla F.M, 2010). These data suggest the intriguing possibility that the "amyloid cascade" and the "Ca^{2+} hypothesis" are just the expression of a multifaceted but interconnected background at the basis of the AD pathogenesis. Fig.17 represents a scheme of the possible mechanisms that link Ca^{2+} homeostasis alteration to AD.

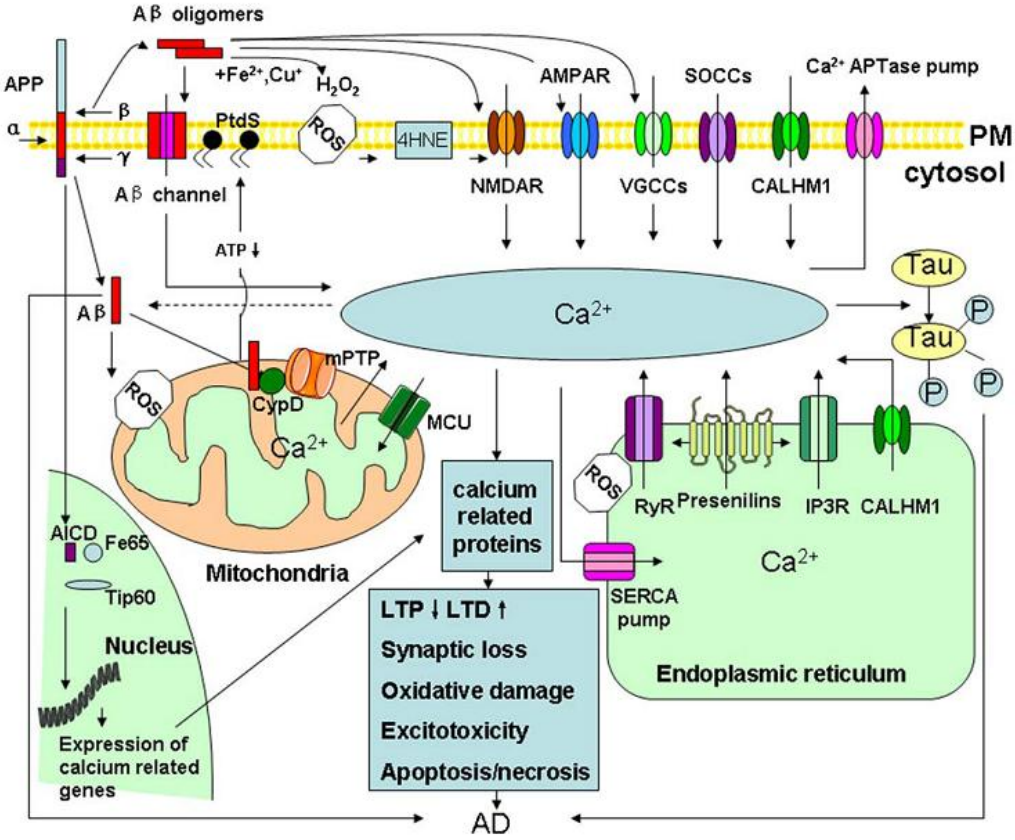

Fig.17: Scheme of the possible links between Ca^{2+} dynamic alterations and AD. From Yu J.T. et al., 2009.

2. RESULTS

PS2 needs Mfn2, but not Mfn1, to exert its effect on ER-mitochondria tethering

We have recently shown that PS2 (but not PS1) levels in ER membranes of different cell types modulate ER-mitochondria tethering and mitochondrial Ca^{2+} uptake upon ER Ca^{2+} release (Zampese E. et al., 2011; Kipanyula M.J. et al., 2012). Of major interest, the expression of FAD-linked PS2 mutants was particularly effective at increasing ER-mitochondria coupling. In order to unravel the mechanism of this PS2 effects, we investigated whether the PS2-dependent increased ER-mitochondria tethering requires the presence and/or the co-operation of the two homologue Mitofusins (Mfn1 and Mfn2), that so far are the only proteins that have been proposed to have a direct role in mediating mitochondria-ER juxtaposition in mammalian cells (de Brito O.M. and Scorrano L., 2008).

MEF cells wt or knock-out (KO) for Mfn2 were thus co-transfected with the FAD-PS2-T122R mutant (Fig.18c) together with a mitochondria-targeted RFP (mt-RFP) and an ER-targeted GFP (ER-GFP; Fig. 18a,b). This particular PS2 mutant form was chosen because it was one of the most effective at modulating Ca^{2+} homeostasis and ER-mitochondria tethering (Zampese E. et al., 2011). ER-mitochondria contacts were then analysed by confocal microscopy and a significant increase in the co-localization area (+17 ± 3% compared to control cells) was found only in wt cells (Fig. 18a), but not in Mfn2-KO MEFs (Fig. 18b).

Accordingly, since mitochondrial Ca^{2+} uptake largely depends on the formation of Ca^{2+} hot spots on the OMM in the regions of close apposition between ER and mitochondria (see Introduction), FAD-PS2-T122R over-expression induces an increase in mitochondrial $[Ca^{2+}]$ peaks value only in wt MEFs, but not in Mfn2-KO MEFs (Fig.18d,e,f). In particular, MEF cells, either wt or Mfn2-KO, co-expressing PS2-T122R and either cytosolic (cyt-Aeq) or mitochondria-targeted aequorin (mit-Aeq) as Ca^{2+} probes, were analysed for their Ca^{2+} responses: as previously shown (Zatti G. et al., 2006; Brunello L. et al., 2009), in response to stimulation with an IP3-generating agonist, PS2 expression in wt MEFs reduced the amplitude of both cytosolic ($[Ca^{2+}]c$, Fig. 18d inset) and mitochondrial Ca^{2+} ($[Ca^{2+}]m$, Fig. 18d) peaks compared to controls. However, as reported before (Zampese E. et al., 2011), when the amplitude of $[Ca^{2+}]c$ peaks of controls was reduced by a pre-depletion protocol (see Methods) to match that of the FAD-PS2 expressing cells, the $[Ca^{2+}]m$ peaks of the latter cells were substantially higher (Fig. 18d, red trace, and Fig. 18e, right). More relevant, in Mfn2-KO MEFs (Fig. 18f) the potentiated $[Ca^{2+}]m$ peak induced by FAD-PS2 expression

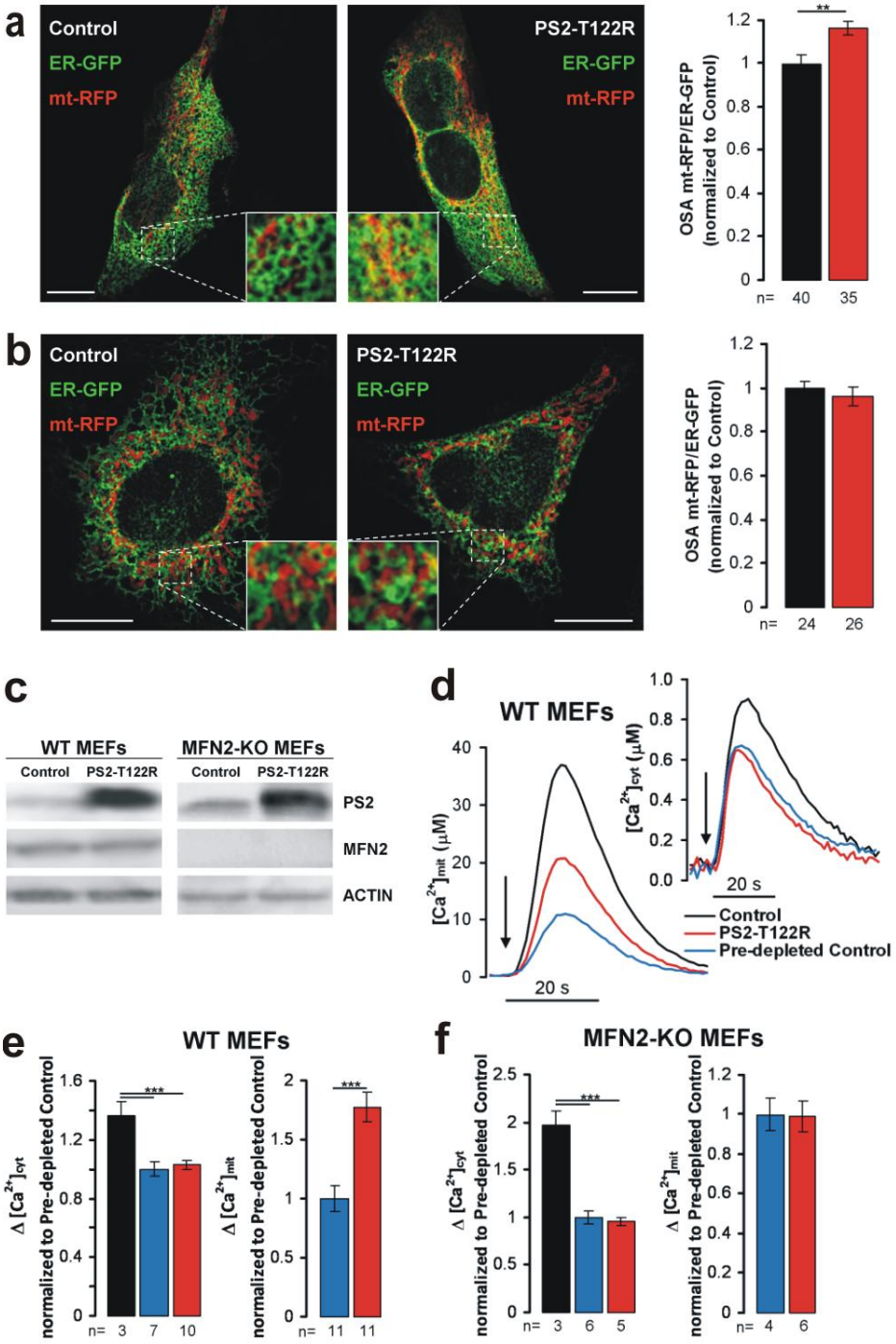

Fig.18: ER–mitochondria interactions in wt (a) and Mfn2-KO (b) MEFs upon expression of PS2-T122R, as revealed by confocal images of cells co-expressing mt-RFP and ER-GFP. Scale bar: 10 μm. Here and in the following figures, highlighted boxes show cellular zones at higher magnification to visualize better ER-mitochondria vicinity (yellow) in the different analyzed conditions. Overlapping signal area (OSA) quantification, calculated from entire single confocal images, is shown (right) for each condition. c) Western blot of wt and Mfn2-KO MEFs, transfected with the empty vector or with PS2-T122R. d), e), f) The same cells as in panel c were analysed for [Ca2+]c and [Ca2+]m changes by mit- and cyt-Aeq. Pre-depleted control cells were pre-incubated in a Ca^{2+}-free, EGTA-containing medium for a fixed period of time to reach a cytosolic Ca^{2+} release similar to that observed in PS2 over-expressing cells. d) Representative cytosolic (inset) and mitochondrial Ca^{2+} traces in control (black), pre-depleted control (blue) and PS2-T122R over-expressing (red) wt MEFs bathed in Ca^{2+}-free, EGTA-containing medium and challenged with ATP (200 μM). e),f) Bars represent mean $[Ca^{2+}]$c (left) and $[Ca^{2+}]$m (right) peaks upon stimulation in the different conditions, in wt (e) and Mfn2-KO (f) MEFs, respectively. In this and in following figures, each bar represent mean ± SEM; ***p < 0.001; **p < 0.01; *p < 0.05; n = number of independent experiments or number of cells (for microscopy images).

described above was not observed. On the contrary, the reduction of $[Ca^{2+}]c$ peaks caused by FAD-PS2 expression was observed in both wt and Mfn2-KO cells (-25 ± 2% and -51 ± 2%, respectively). Similar results were obtained when another FAD-PS2 mutant (N141I) was expressed in the same cell line (data not shown).

To further confirm that the increased mitochondrial Ca^{2+} uptake observed in PS2-T122R expressing wt MEFs, upon an IP3-induced ER Ca^{2+} release, is due to an increased physical interaction between ER and mitochondria, mitochondrial Ca^{2+} uptake was investigated in the same cells upon activation of Ca^{2+} influx through the plasma membrane (CCE, Fig. 19a,b) or by mobilization of ER Ca^{2+} with the Ca^{2+} ionophore ionomycin (Fig. 19c,d). In both cases, it is predicted that changes in ER-mitochondria proximity should not significantly affect Ca^{2+} uptake by mitochondria. Indeed, no difference in mitochondrial Ca^{2+} response of wt MEF cells over-expressing or not PS2-T122R was found with both protocols, confirming that the capacity and affinity of the machinery that controls mitochondrial Ca^{2+} uptake is not affected by PS2 expression.

To verify to what extent PS2-T122R expression is able to modify ER-mitochondria tethering, we carried out electron microscopy (EM) analysis of wt and Mfn2-KO MEF cells, expressing or not the FAD-linked protein, measuring close juxtapositions (< 13 nm) between the two organelles (Fig. 20a-d). While wt MEFs showed a significant increased in the number of close contacts between mitochondria and ER upon PS2-T122R expression, in Mfn2-KO cells the number of these interactions was not modified by the presence of the mutated protein (Fig. 20e,f). These results validate the confocal fluorescence analysis (Fig. 18a,b), as well as the functional ER-mitochondria Ca^{2+} coupling (Fig. 18d-f), and imply Mfn2 as a critical protein in the PS2-mediated modulation of ER-mitochondria tethering. Notably, when Mfn2-KO MEF cells were compared to wt MEFs, a decreased number of mitochondria profiles and an increased number of ER-mitochondria close contacts were observed, as reported by Cosson P. et al., 2012. We have no explanation for the increased number of contacts in these cells. We are trying to understand wether it could be in some way related to the changes in the number and morphology of mitochondria. Future investigations will be need to clarify this issue.

We have previously demonstrated that also endogenous wt PS2 plays a constitutive role in maintaining the proper distance between ER and mitochondria (Zampese E. et al., 2011). In Mfn2-KO MEFs the down-regulation of endogenous PS2 (Supplementary Fig. 21a), by specific siRNA (see Methods), was without effect on ER-mitochondria Ca^{2+} cross-talk (Fig.

21b), but it was instead effective in wt MEFs, inducing a decrease in ER-mitochondria functional coupling (Fig. 21c). This result indicates that also endogenous wt PS2 contributes to ER-mitochondrial tethering, but only in the co-presence of Mfn2. Indeed, when Mfn2 was re-expressed in Mfn2-KO MEFs (Fig. 21a), the effect of PS2 silencing on ER-mitochondria Ca^{2+} transfer was rescued (*i.e.*, a reduction in this parameter was observed; Fig. 21d).

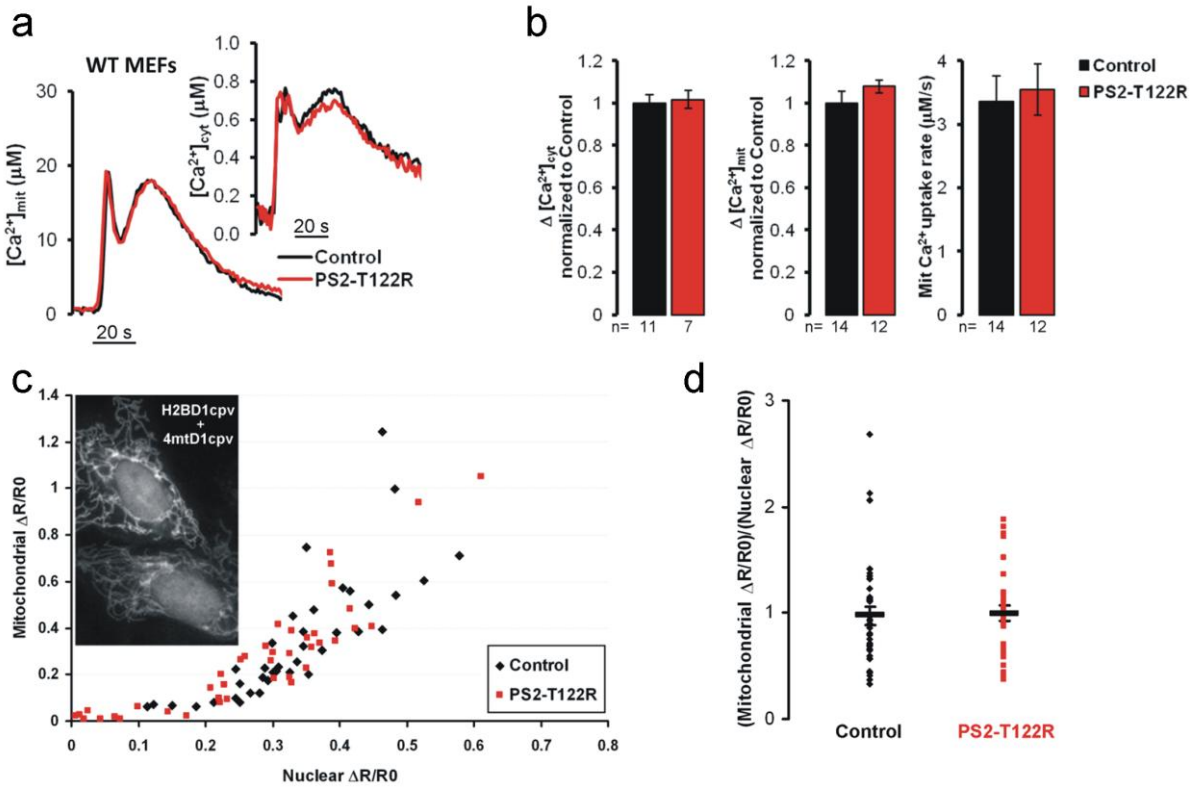

Fig.19: a) Representative cytosolic (inset) and mitochondrial Ca^{2+} traces in control (black) and PS2-T122R over-expressing (red) wt MEFs expressing also the specific Aeq probe. To induced CCE, CPA pre-treated cells (see Methods) were challenged with $CaCl_2$ (5 mM). b) Bars represent mean cytosolic and mitochondrial CCE peak values, as well as mitochondrial CCE rate values, of the data obtained in a. c) Mitochondrial ($[Ca^{2+}]_m$) and nuclear ($[Ca^{2+}]_n$) Ca^{2+} peak values (expressed as $\Delta R/R_0$) induced by ionomycin (1 μM) addition in single wt MEFs, expressing or not PS2-T122R, as revealed by specific cameleon Ca^{2+} probes (4mtD1cpv and H2BD1cpv, respectively). The increase in $[Ca^{2+}]_m$ (mitochondrial $\Delta R/R_0$) is plotted as a function of the corresponding increase in $[Ca^{2+}]_n$ (nuclear $\Delta R/R_0$) in the same cell. Each symbol represents one cell. d) Ratio between $[Ca^{2+}]_m$ and $[Ca^{2+}]_n$ peak values, measured as described in panel c for nuclear $\Delta R/R_0 > 0.2$, in controls and PS2-T122R expressing cells. The mean ratio value is not significantly different in the two conditions (n = 35 and n = 31 for control and PS2-T122R expressing cells, respectively).

To exclude the possibility that, in Mfn2-KO MEFs, PS2-T122R has not effect on ER-mitochondria tethering because of specific clonal features, we used the same experimental approach in MEFs KO for both Mfn1 and Mfn2 (Mfn-DKO; Fig. 22a). When PS2-T122R was expressed in these cells, ATP-induced $[Ca^{2+}]$c rises were reduced but, compared to pre-depleted controls, $[Ca^{2+}]$m peaks were not increased (Fig. 22b). Similarly, no increase in ER-mitochondria connection was observed in these cells upon PS2-T122R expression (Fig. 22c).

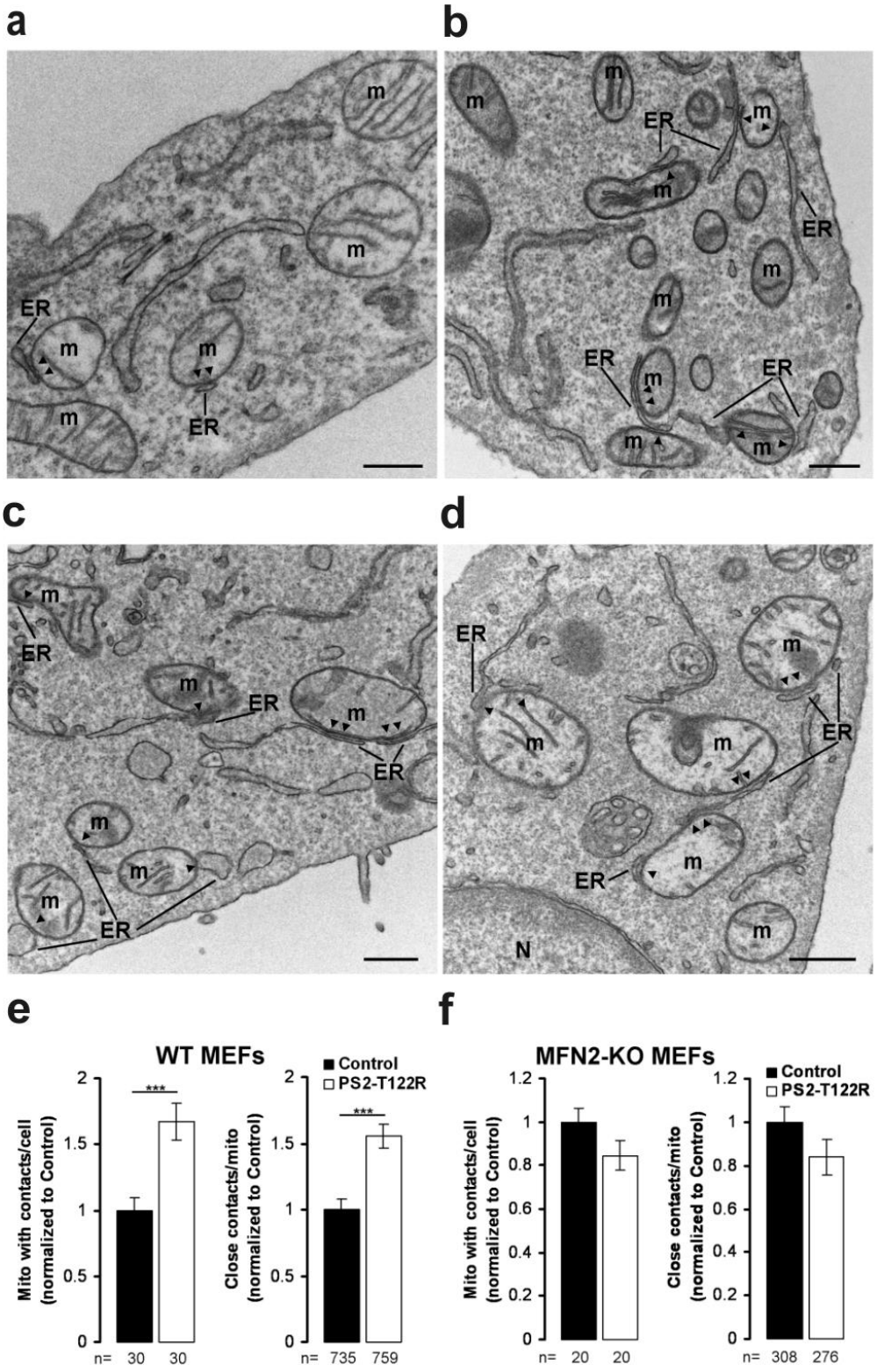

Fig.20: a-d) EM images of wt a), b) and Mfn2-KO c), d) MEFs, transiently expressing b), d), or not a), c), PS2-T122R. a), b) Several close (< 13 nm) appositions are visible between ER cisternae and mitochondria (m) in wt MEFs a) and, more frequently, in PS2-T122R expressing wt MEFs (b). The black arrowheads designate the zones of close contact between ER and mitochondria. Scale bar, 0.5 μm. c), d) In Mfn2-KO MEFs, upon PS2-T122R expression, no increase in the number of close appositions was observed. In these cells the ER membranes appear swollen. N, nucleus. Scale bar, 0.5 μm. e), f) Bars represent the average percentage of mitochondria with close contacts/cell (normalized to control; left) and the average number of close contacts/mitochondrion (normalized to control; right) observed in wt e) and Mfn2-KO f) MEFs transiently expressing, or not, PS2-T122R (n = number of cells or mitochondria in three independent experiments).

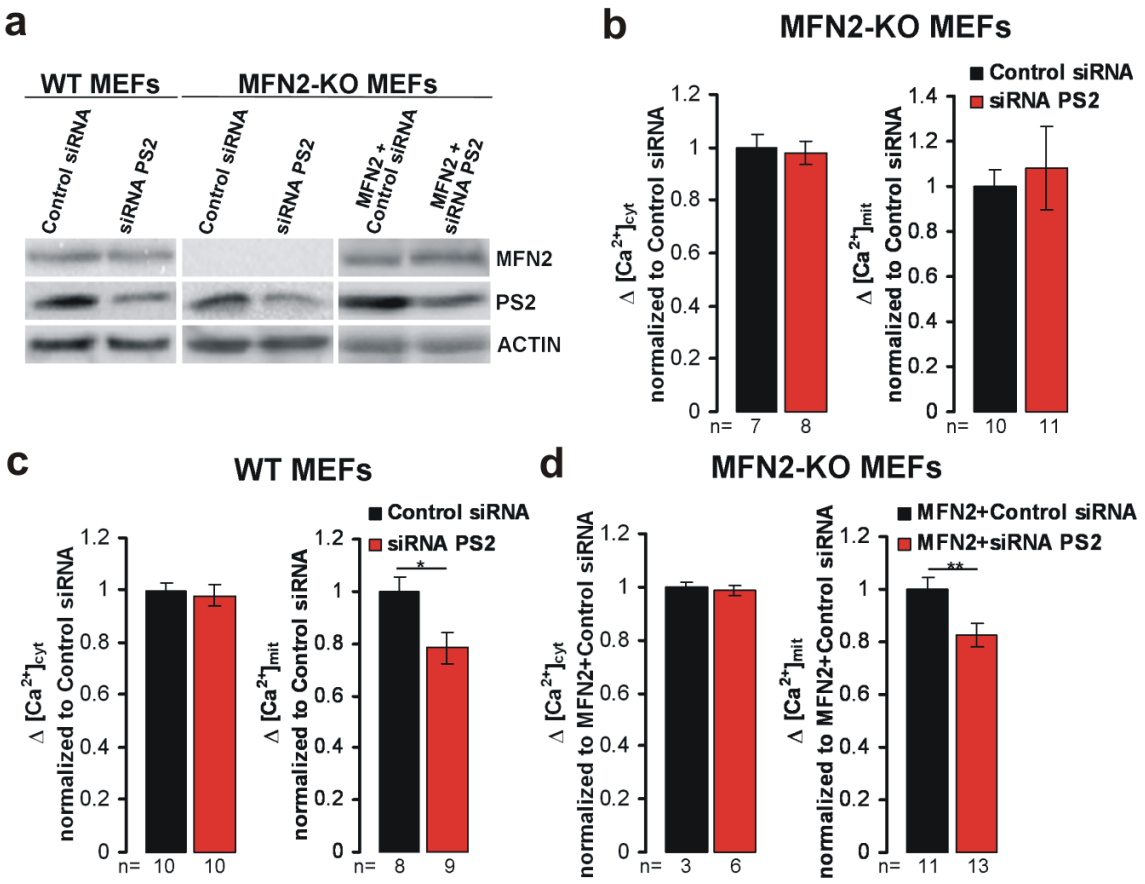

Fig.21: a) Western blot of wt and Mfn2-KO MEFs, transfected with scramble or PS2 specific siRNA (20 nM), alone or together with the cDNA of Mfn2. b-d) Cells as in panel a were analysed for $[Ca^{2+}]_c$ and $[Ca^{2+}]_m$ changes by mit-Aeq and cyt-Aeq. Bars represent mean $[Ca^{2+}]_c$ (left) and $[Ca^{2+}]_m$ (right) peaks upon cell stimulation in Ca^{2+}-free, EGTA-containing medium with ATP (200 μM), in wt c) and Mfn2-KO MEFs with d) or without b) Mfn2 re-expression, respectively.

Most importantly, in Mfn-DKO cells the effect of PS2-T122R on ER-mitochondria tethering was rescued by Mfn2 re-expression: the FAD-PS2 mutant induced a strong increase in $[Ca^{2+}]$m peaks, compared to pre-depleted Mfn-DKO MEFs re-expressing only Mfn2 (Fig. 22d). As predicted, the area of ER-mitochondria interaction (Fig. 22e) was significantly higher upon Mfn2 re-expression alone, and further increased upon Mfn2 and FAD-PS2 co-expression (Fig. 22c).

Taken together, these results suggest that PS2 needs Mfn2 to exert its modulation on ER-mitochondria coupling and that Mfn1 is instead dispensable: indeed, Mfn1-KO MEFs expressing PS2-T122R showed a remarkable increase in $[Ca^{2+}]$m peaks compared to pre-depleted controls (Fig. 23a). Of note, the lack of PS2 effect seen in Mfn2-KO MEFs (Fig. 18b,f) was not due to the mitochondrial morphological alterations induced by Mfn2 ablation,

since a similar, and even stronger, organelle fragmentation is evident also in MEFs lacking Mfn1 (Fig. 23b).

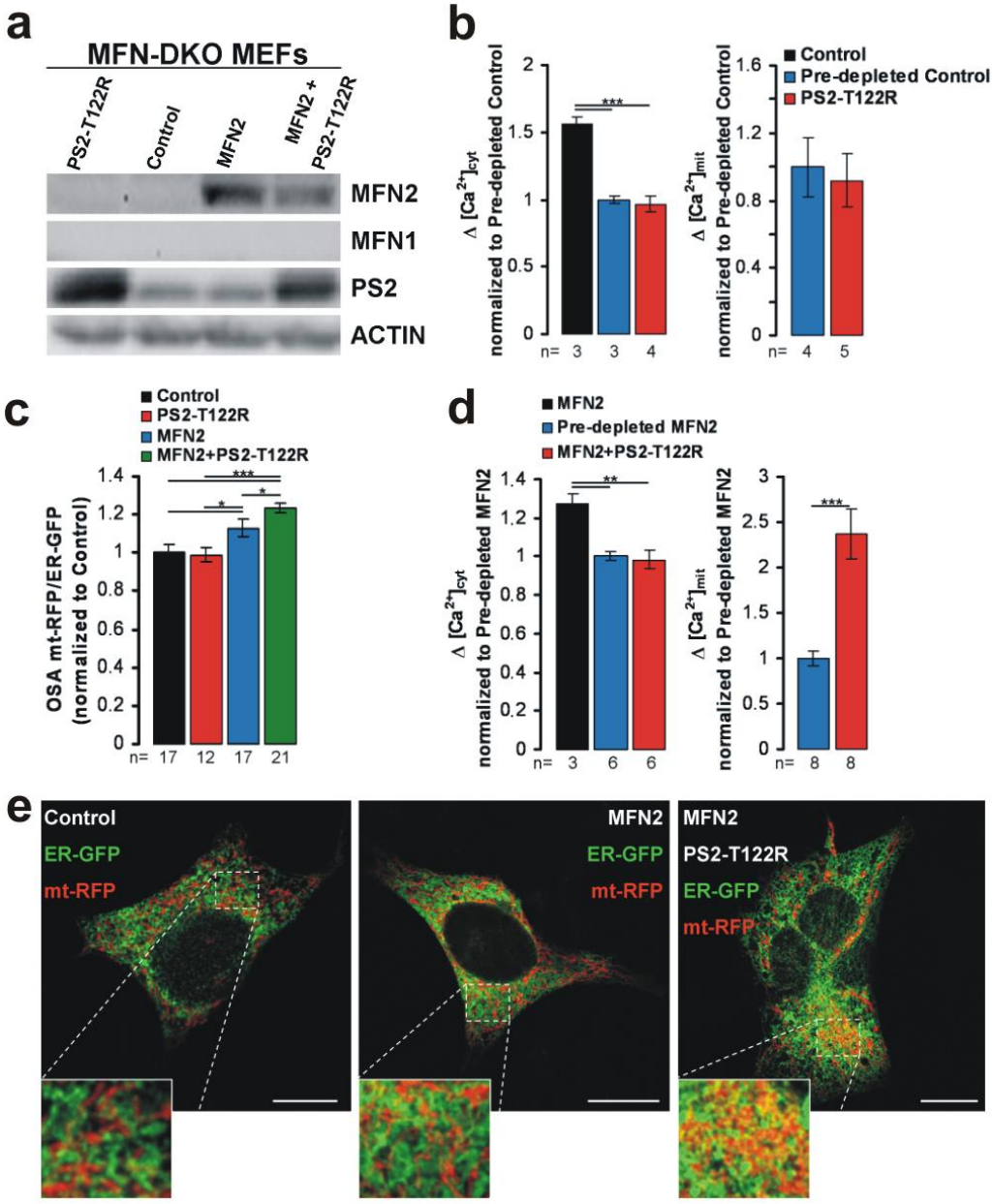

Fig.22: a) Mfn-DKO MEFs, transfected with the empty vector, with PS2-T122R alone, with Mfn2 alone or with both, were analysed for $[Ca^{2+}]c$ and $[Ca^{2+}]m$ changes b), d) by mit- and cyt-Aeq. Pre-depleted control cells were treated as described in Figure 18 to reach a cytosolic Ca^{2+} release similar to that observed in PS2 (or PS2+Mfn2) over-expressing cells. b), d) Bars represent mean $[Ca^{2+}]c$ (left) and $[Ca^{2+}]m$ (right) peaks upon stimulation, as described in Figure 18, in Mfn-DKO MEFs in the different conditions. c), e) ER–mitochondria interactions in Mfn-DKO MEFs in the different conditions, as revealed by e) confocal images of cells co-expressing mt-RFP and ER-GFP. Scale bar: 10 μm. c) OSA quantification, calculated from single confocal images, for each condition.

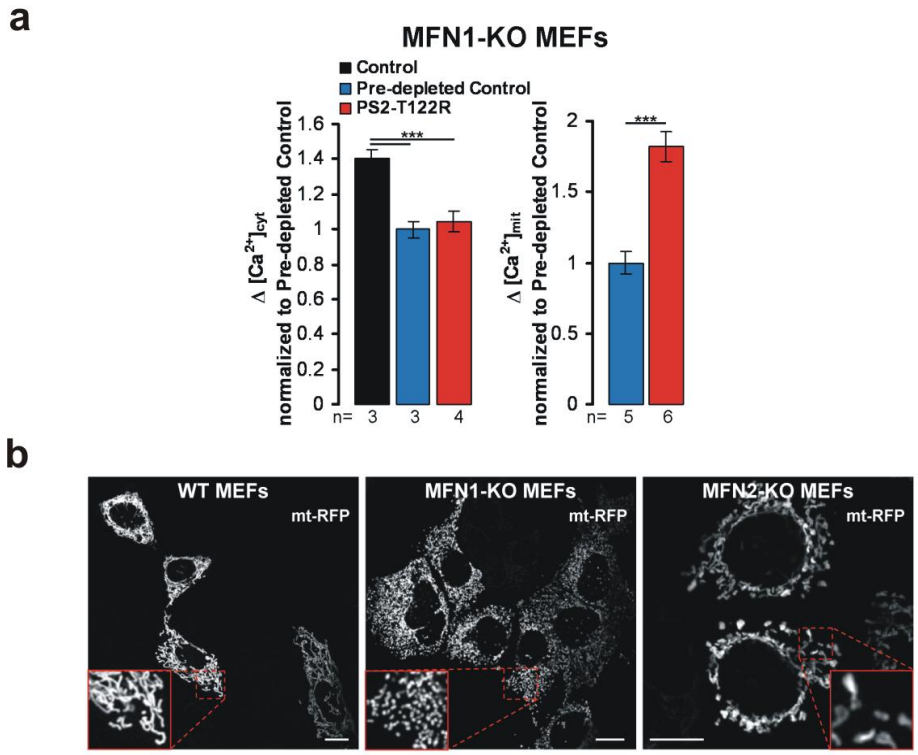

Fig.23: a) Mfn1-KO MEFs, transfected with the empty vector or with PS2-T122R, were analysed for $[Ca^{2+}]_c$ and $[Ca^{2+}]_m$ changes by mit-Aeq and cyt-Aeq. Bars represent mean $[Ca^{2+}]_c$ (left) and $[Ca^{2+}]_m$ (right) peaks upon cell stimulation in Ca^{2+}-free, EGTA-containing medium with ATP (200 μM). b) Mitochondrial morphology of wt and Mfn1- or Mfn2-KO MEFs, expressing mt-RFP, as revealed by confocal microscopy (Scale bar: 10 μm).

Mfn2 needs PS2, but not PS1, to exert its effect on ER-mitochondria tethering

Mfn2 has been proposed to mediate ER-mitochondria coupling in mammalian cells (de Brito O.M. and Scorrano L., 2008). We here demonstrate that PS2 effect on organelles' tethering depends on the presence of Mfn2, we have wondered if also Mfn2 needs PS2 to exert its function. To this purpose, we have applied the reciprocal approach, using MEFs wt and KO for both PS1 and PS2 (PS-DKO; Fig. 24a). In wt cells, Mfn2 over-expression resulted, upon stimulation, in reduced $[Ca^{2+}]$c rises (as previously reported in other cell types, de Brito O.M. and Scorrano L., 2008), but higher $[Ca^{2+}]$m peaks when the amplitude of $[Ca^{2+}]$c peaks in controls was brought close to that of Mfn2-expressing cells (Fig. 24b). Similarly, the area of ER-mitochondria proximity is increased upon Mfn2 over-expression (Fig. 24d). Conversely, when the same experimental procedures were applied to PS-DKO MEFs, no effect of Mfn2 over-expression was observed (Fig. 24c,e). The re-introduction of PS2 in these cells (Fig. 24f) was sufficient to recover the Mfn2-dependent ER-mitochondria tethering effect (Fig. 24g,h). On the contrary, the re-introduction of PS1 (Fig. 24i) was ineffective on both parameters (Fig. 24j,k).

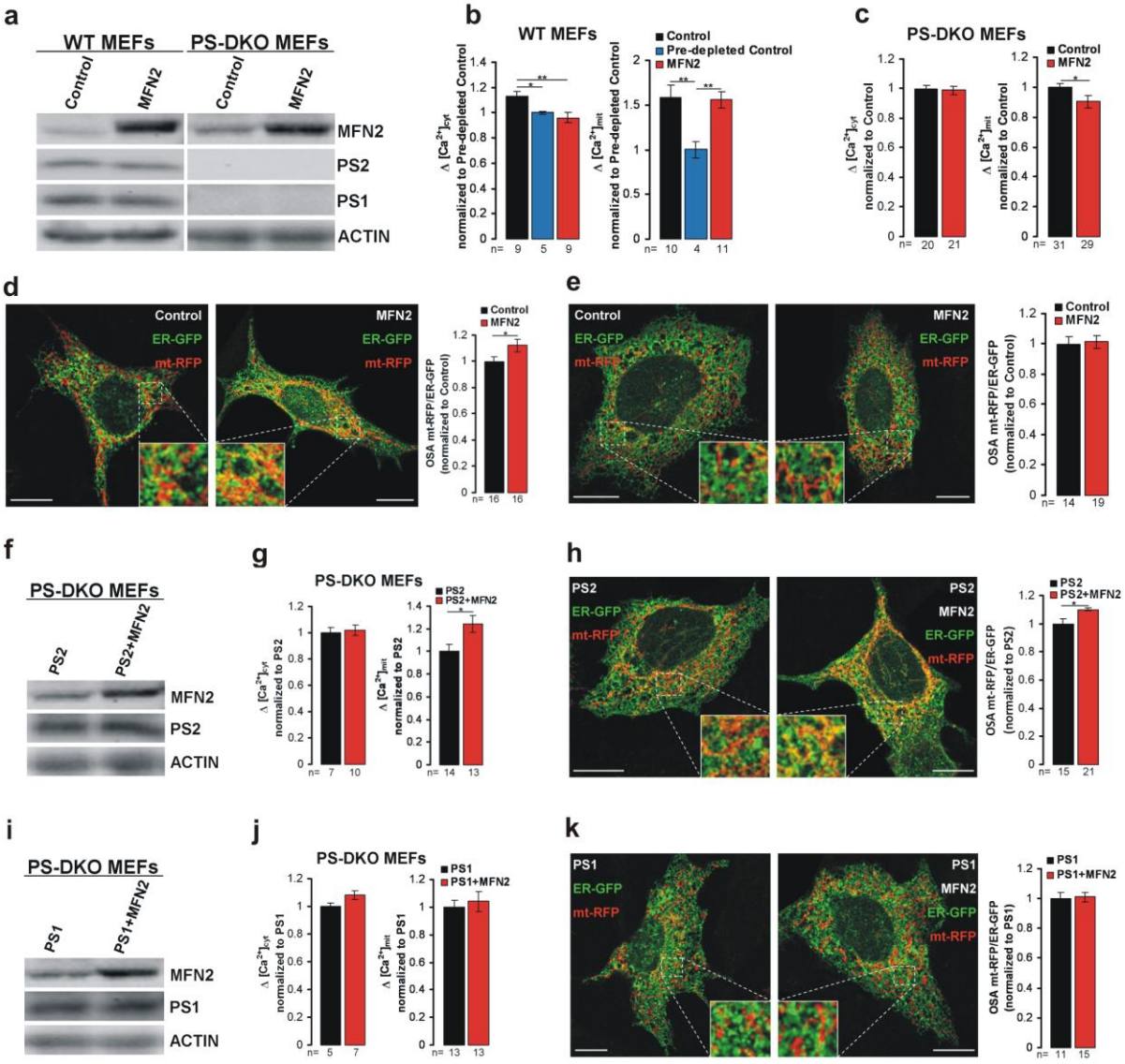

Fig.24: a) wt and PS-DKO MEFs, transfected with the empty vector or with Mfn2, were analysed for [Ca2+]c and [Ca2+]m changes b), c) by mit- and cyt-Aeq. Pre-depleted control cells were treated as described in Fig. 18 to reach a cytosolic Ca^{2+} release similar to that observed in Mfn2 over-expressing cells. b), c) Bars represent mean $[Ca^{2+}]$c (left) and $[Ca^{2+}]$m (right) peaks upon stimulation in wt b) and PS-DKO c) MEFs, respectively. d), e) ER–mitochondria interactions in wt d) and PS-DKO e) MEFs upon expression of Mfn2, as revealed by confocal images of cells co-expressing mt-RFP and ER-GFP. Scale bar: 10 μm. OSA quantification, calculated from single confocal images, is shown (right) for each condition. f-k) PS-DKO MEFs reconstituted with f) PS2 or i) PS1 and expressing Mfn2 were analysed for $[Ca^{2+}]$c and $[Ca^{2+}]$m changes (g,j, respectively), as well as for ER–mitochondria interactions (h,k, respectively, Scale bars: 10 μm), as described in panels b and d.

PS2 and Mfn2 physically interact

We then verified whether the functional interdependence of PS2 and Mfn2 requires a direct physical interaction between the two proteins. To this end we used an immunoprecipitation (IP) assay. In SH-SY5Y cells, expressing a tagged form of Mfn2 (Myc-Mfn2) and PS2-T122R, Myc-Mfn2 co-immunoprecipitates with the full length form of PS2 (Fig. 25a); at lower MW, and corresponding to the C-terminal fragment of PS2, a faint

band was also revealed, while no PS2 N-terminal fragment was ever found. Similarly, in Mfn2-KO MEFs co-expressing Myc-Mfn2 and PS2, either wt or T122R, Myc-Mfn2 co-immunoprecipitates with PS2 (Fig. 25c). Moreover, Myc-Mfn2 was still able to co-immunoprecipitate a truncated form of PS2 (PS2-Δ374-448; Fig. 25d), lacking the final part of its C-terminus (Fig. 25b), thus restricting the Mfn2-interacting domain of PS2 to its big cytosolic loop and the initial part of the trans-membrane domain 7. Noteworthy, PS2-Δ374-448 contains also the loss-of-function mutation D366A, indicating that the ability of PS2 to bind Mfn2 is independent from its enzymatic, γ-secretase activity (as demonstrated for other Ca^{2+}-related PS2 functions, Zampese E. et al., 2011; Brunello L. et al., 2009). Additional evidence for a direct PS2-Mfn2 molecular interaction comes also from the reciprocal experiment (Fig. 25e): in Mfn2-KO MEFs co-expressing Mfn2 and Myc-PS2 (wt or T122R; see Methods), IP of Myc-PS2 pulled down Mfn2, but not another highly expressed OMM protein, Tom20. Importantly, in cells over-expressing a tagged PS1 (V5-PS1), either wt or FAD-PS1-A246E, and a Myc-Mfn2, co-IP mediated by either anti-V5 (Fig. 25f) or anti-Myc (Fig. 25g) antibodies failed to pull down Mnf2 or PS1, respectively.

Since PS2 is an integral ER membrane protein found enriched in MAMs (Area-Gomez E. et al., 2009), as Mfn2 (de Brito O.M. and Scorrano L., 2008), the two proteins could interact both in *cis* and/or in *trans*. We thus carried out an IP assay in Mfn2-KO MEFs expressing Myc-PS2 wt and a Mfn2 mutant that is exclusively targeted to either the surface of mitochondria (Mfn2ActA) or the ER (Mfn2IYFFT) (descibed in de Brito O.M. and Scorrano L., 2008). IP of PS2 pulled down both proteins separately (Fig. 25h), or together, when the three proteins were co-expressed (Fig. 25i).

From a functional point of view, the increase in $[Ca^{2+}]$m peak, upon cell stimulation, was observed only when, in Mfn-DKO MEFs, PS2 was expressed together with both ER and mitochondrial Mfn2 (Fig. 26a). Neither Mfn2 on mitochondria (Fig. 26b) nor on the ER alone (Fig. 26c) were able to recover the PS2 tethering function. A similar result was also found when PS2-T122R was expressed together with the only ER-Mfn2 in Mfn2-KO MEFs, *i.e.*, a cell model endogenously expressing Mfn1 on mitochondria (Fig. 26d).

To further confirm the specificity of the interaction between Mfn2 and PS2, IP of PS2 failed to pull down Mfn1 in both wt and Mfn2-KO MEFs co-expressing Mfn1 and PS2 (Fig. 27). Moreover, we verified that endogenous Mfn2 physically interacts with endogenous PS2 (see below).

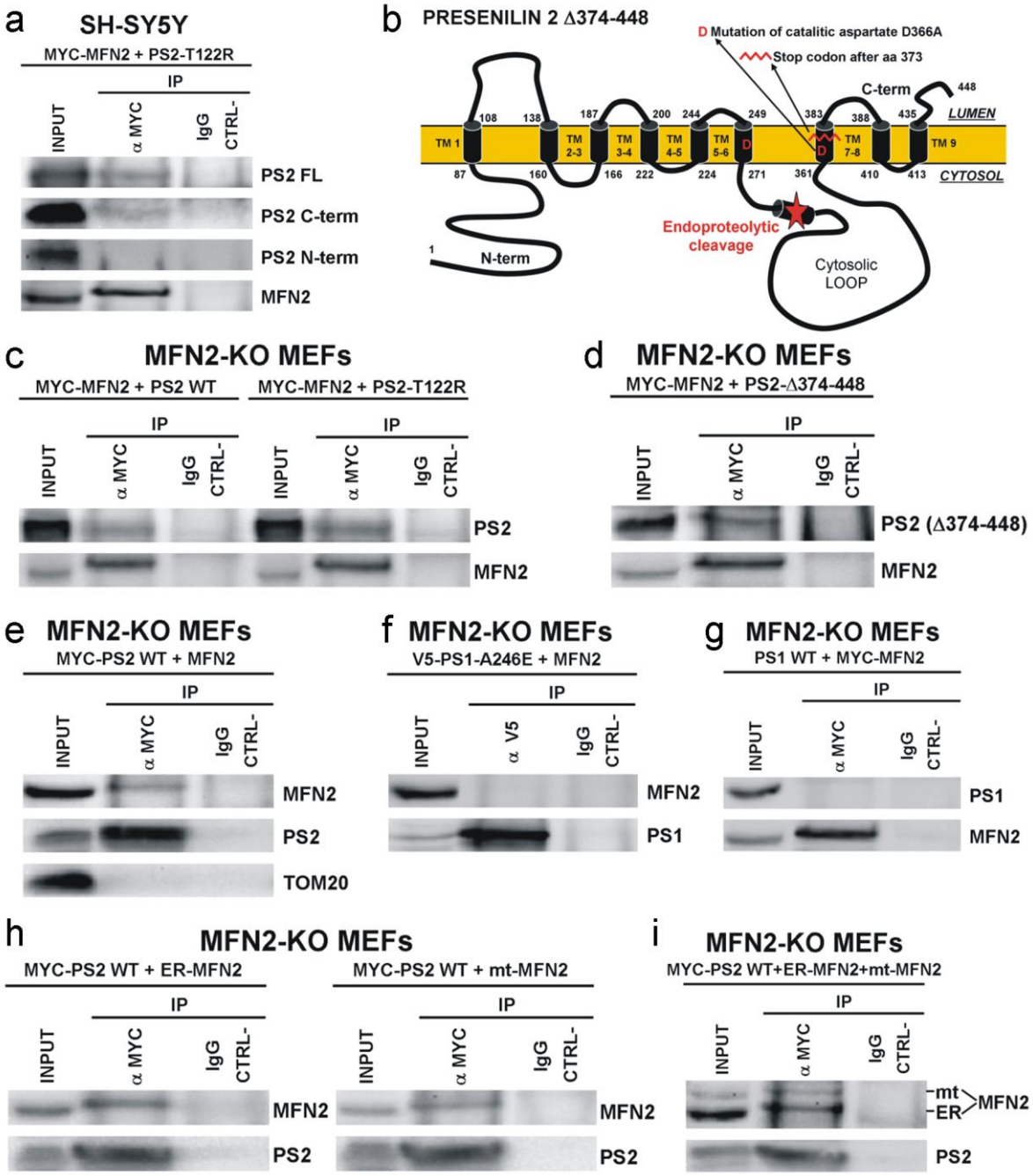

Fig.25: a) Immunoprecipitation assay of SH-SY5Y cells co-expressing Myc-Mfn2 and PS2-T122R. Cells were lysated and immunoprecipitated with an anti-Myc antibody or with irrelevant IgG, as a negative control (IgG CTRL-). Precipitates and lysate (input) were probed with specific antibodies for the indicated proteins. Note that the C-terminal fragment of PS2 was revealed in the precipitated fraction at longer blot exposure. b) PS2 topology representation indicating the position of the stop codon (374) in the PS2-Δ374-448 construct. Note also the presence of the D366A loss-of-function mutation in this truncated protein. Mfn2-KO MEFs co-expressing c) Myc-Mfn2 and PS2 (wt or T122R); d) Myc-Mfn2 and PS2-Δ374-448; e) Myc-PS2 wt and Mfn2; f) V5-PS1- A246E and Mfn2; g) PS1 wt and Myc-Mfn2; h) Myc-PS2 wt and either Mfn2IYFFT (ER-Mfn2), or Mfn2ActA (mt-Mfn2), or i) both Mfn2 variants, were lysated and immunoprecipitated with different specific antibodies (as indicated in each panel) or with irrelevant IgG, as a negative control (IgG CTRL-). Precipitates and lysates (input) were probed with specific antibodies for the indicated proteins.

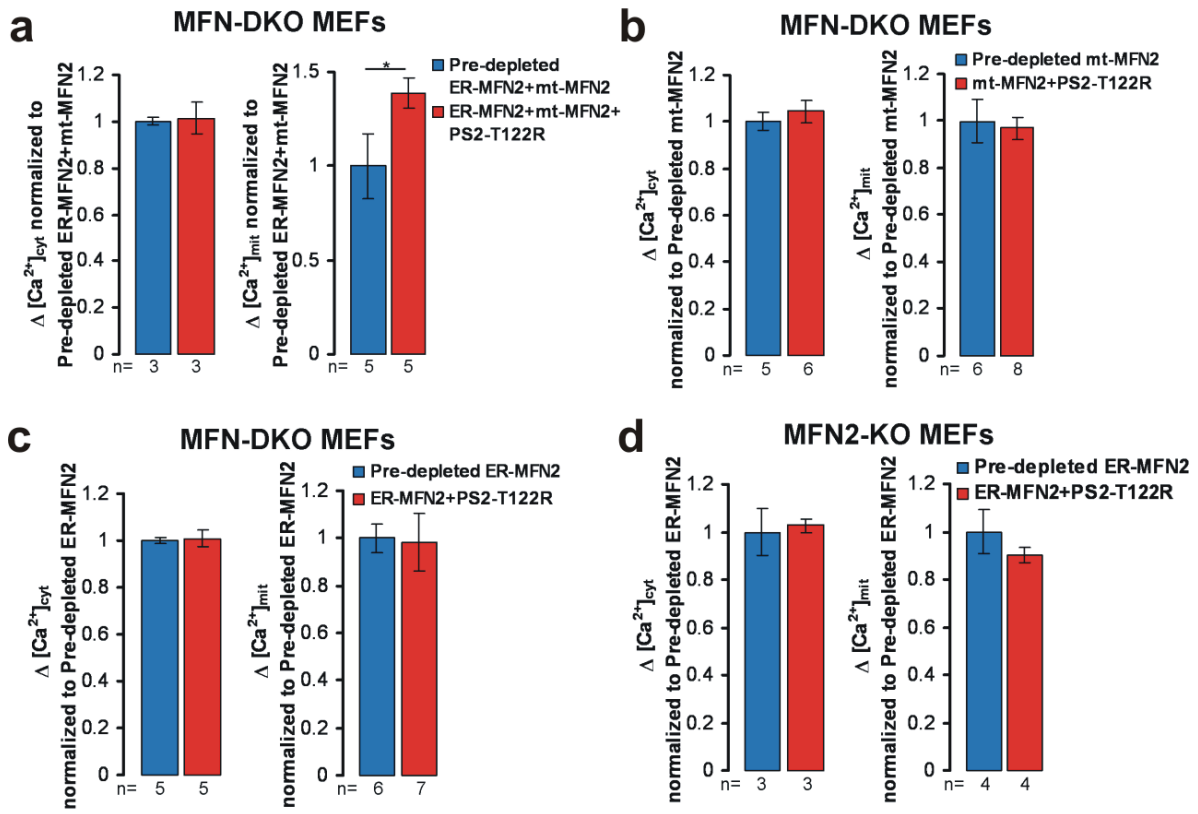

Fig.26: a-c) Mfn-DKO MEFs or d) Mfn2-KO MEFs, transfected with a) ER- and mt-Mfn2, b) mt-Mfn2, c), d) ER-Mfn2 together with PS2-T122R (or the void vector, as control) were analysed for $[Ca^{2+}]_c$ and $[Ca^{2+}]_m$ changes by mit-Aeq and cyt-Aeq. Pre-depleted control cells were preincubated in a Ca^{2+}-free, EGTA-containing medium for a fixed period of time to reach a cytosolic Ca^{2+} release similar to that observed in PS2-T122R expressing cells. Bars represent mean $[Ca^{2+}]_c$ (left) and $[Ca^{2+}]_m$ (right) peaks upon cell stimulation in Ca^{2+}-free, EGTA-containing medium with ATP (200 μM).

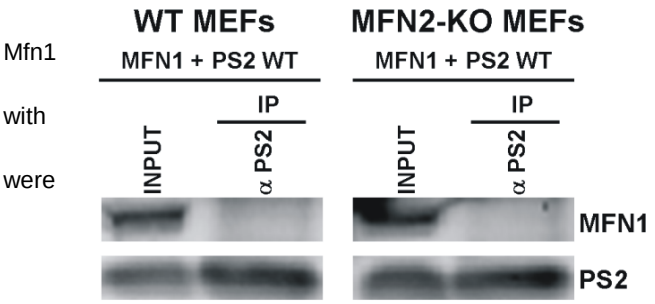

Mfn1 with were

Fig.27: wt or Mfn2-KO MEFs co-expressing and PS2 wt were lysated and immunoprecipitated with an anti-PS2 antibody or irrelevant IgG, as a negative control (IgG CTRL-). Precipitates and lysates (input) probed with specific antibodies for the indicated proteins.

We then investigated if the physical interaction between PS2 and Mfn2 occurs also in living cells. To address this possibility, fluorescence recovery after photobleaching experiments (FRAP) (Reits E.A. and Neefjes J.J., 2001) were performed. Figure 28 shows representative confocal images of a Mfn2-KO MEF expressing a CFP-PS2 (with a clear reticular ER pattern of expression) before (Fig. 28a) and after photobleaching (Fig. 28b,c) in a specific region of interest (ROI), and representative FRAP traces, within the same ROI, in

Mfn2-KO MEF cells expressing CFP-PS1wt, CFP-PS2wt or CFP-PS2-T122R alone (dotted traces) or together with Mfn2 (continuous traces). In CFP-PS1wt expressing cells (Fig. 28d) no difference in fluorescence recovery was found with or without Mfn2 co-expression; in MEFs expressing either CFP-PS2wt (Fig. 28e) or CFP-PS2-T122R (Fig. 28f), on the contrary, the fluorescence recovery was substantially lower when the two proteins were co-expressed with Mfn2, CFP-PS2-T122R being the most reduced.

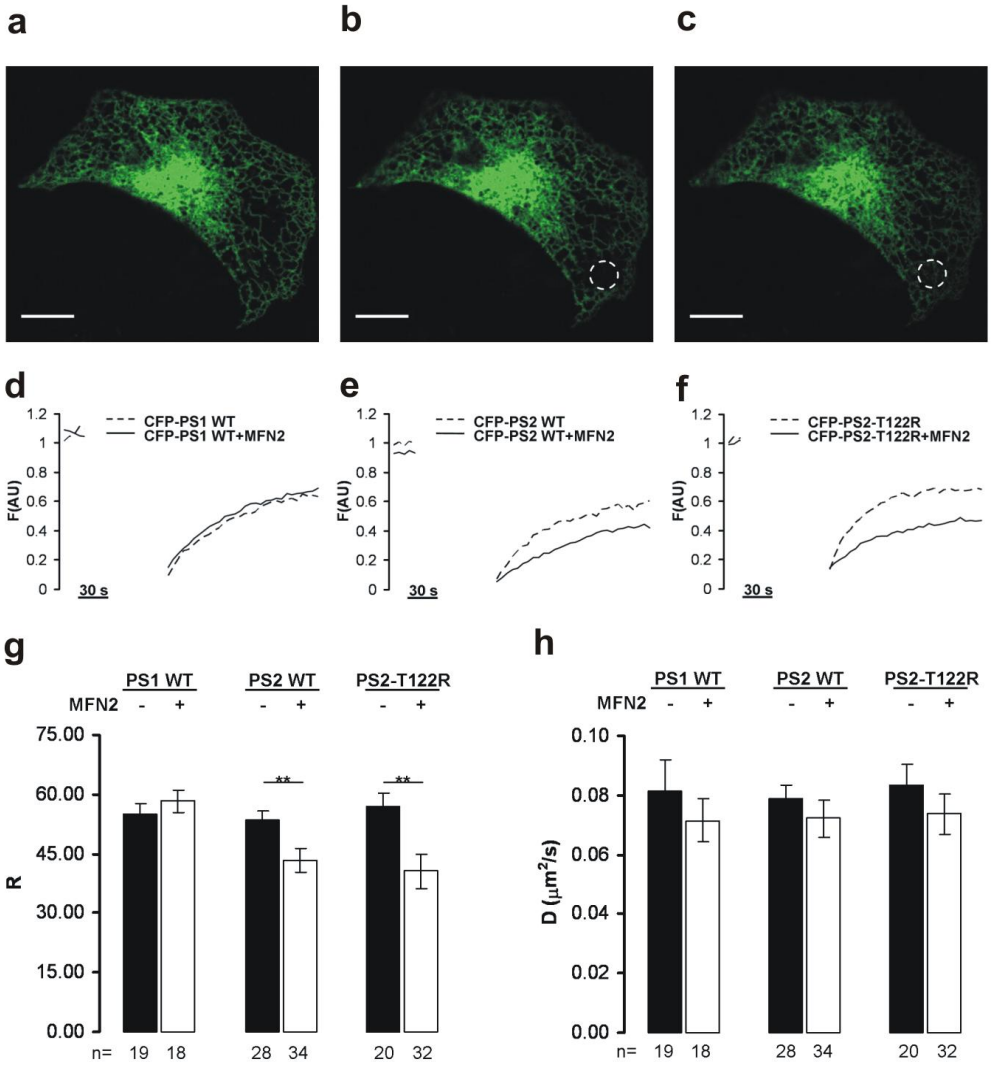

Fig.28: a-c) Confocal images of a Mfn2-KO MEF expressing CFP-PS2 before a) and after b), c) photobleaching in the drawn ROI. Scale bar: 10 μm. d-f) Representative FRAP traces of d) CFP-PS1wt, e) CFPPS2wt or f) CFP-PS2-T122R expressing Mfn2-KO MEFs, with (continuous trace) or without (dotted trace) co-expression of Mfn2. Traces show fluorescence intensities before and after photobleaching for the indicated time. Fluorescence values are normalized to prebleached ones and plotted over time. g), h) Bars represent mean values of g) the mobile fraction (R) and h) the diffusion constant (D) of each fluorescent protein (calculate as described in Methods) in the presence or absence of Mfn2.

Accordingly, the mobile fraction (R; see Methods) of fluorescent PS1 was independent from Mfn2 expression while, in the case of PS2 (wt or FAD), their mobile fractions were

reduced by the presence of Mfn2 with, again, PS2-T122R more affected (Fig. 28g). The diffusion constants of the fluorescent proteins were also calculated (D; see Methods) and no statistical difference in this parameter was found in the presence or absence of Mfn2 in the three conditions (Fig. 28h). To exclude any variation in membrane protein mobility due to possible ER structure modifications induced by PS2-Mfn2 interactions, the same cells expressing the chimeric ER protein GFP-sec61β and PS2 (wt or T122R), with or without Mfn2, were also analysed: no significant difference was found in GFP-sec61β mobile fraction and diffusion constant in the different conditions (Fig. 29).

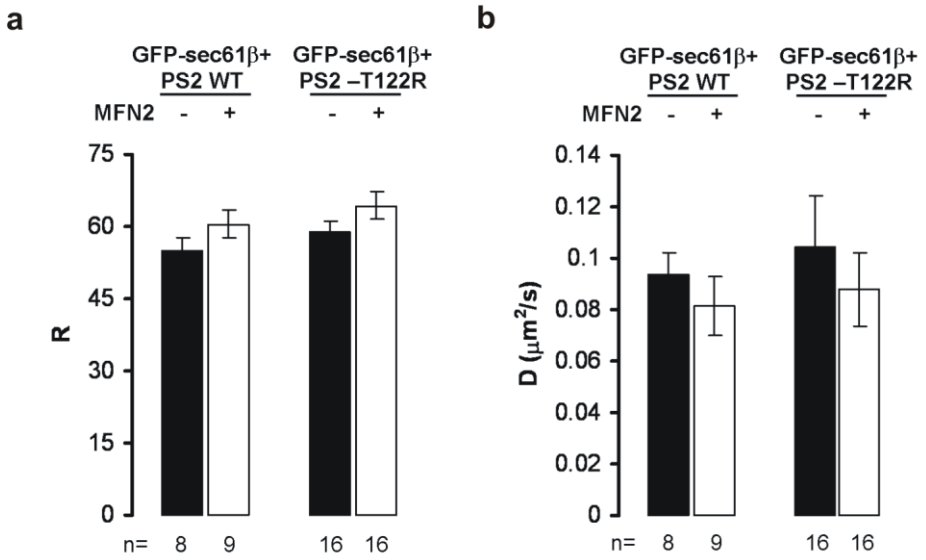

Fig.29: a), b) Bars represent mean values of a) the mobile fraction (R) and b) the diffusion constant (D) of GFP-sec61β (calculated as described in Methods) in Mfn2-KO MEFs expressing PS2 (wt or T122R) with or without Mfn2.

FAD-linked forms of PS2 markedly accumulate in MAMs, favouring Mfn2 recruitment

ER-mitochondria contacts are thought to occur in MAMs (see Introduction), membrane domains that can be purified and biochemically characterized using differential centrifugation of tissue homogenates. In order to verify whether the diverse ER-mitochondria tethering efficacy of wt and FAD-PS2 could depend from their differential MAM localization, we used brain homogenates from wt and PS2-N141I transgenic (Tg) mice (characterized in Kipanyula M.J. et al., 2012). Figure 30a shows that, in brain of wt mice, PS2 levels are similar between the generic ER/microsome fraction and MAMs. Conversely, in FAD-PS2 Tg mice, PS2 appears strongly enriched in the MAM fraction compared to total ER membranes. Interestingly, when Mfn2 was specifically revealed in the same fractions, its presence in MAMs, normalized to that in microsomes, was also increased in FAD-PS2 Tg

mice (2.56-fold ± 0.58) compared to controls (ratio MAMs/microsomes = 1.59 ± 0.16) (see also Fig. 30b).

These results are further confirmed by the finding that endogenous Mfn2 IP in the crude mitochondrial fractions (*i.e.*, mitochondria "contaminated" by MAMs) from brains of the two mice results in a much stronger co-precipitation of PS2 in the presence of FAD mutations (3.1-fold ± 0.71 compared to wt; $p<0.05$; n=3 independent experiments; Fig. 30c), again suggesting that in the fraction of ER membranes that contaminates crude mitochondria (*i.e.*, ER-MAMs) the mutant PS2 is more enriched compared to the wt protein and thus more able to bind to its partner Mfn2.

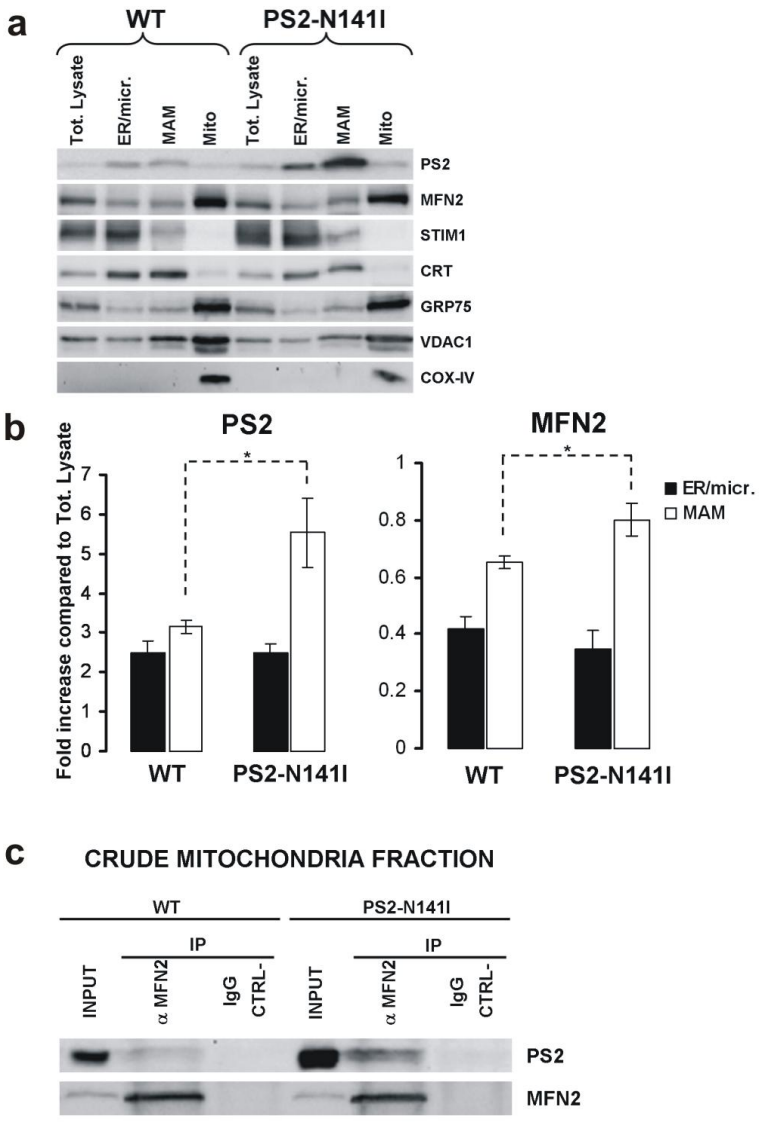

Fig.30: a) Western blot of the indicated proteins in brain sub-cellular fractions (35 µg/lane) from wt and FAD-PS2-N141I Tg mice. Tot. Lysate, total brain homogenates; ER/micr., microsomal fraction; MAM, mitochondria associated membrane fraction; Mito, pure mitochondrial fraction. Markers for sub-cellular fractions are: STIM1 and CRT (ER), GRP75 and VDAC1 (MAM/mitochondria), COXIV (mitochondria). b) Bars represent relative fold-increase, compared to total brain homogenates, of PS2 (left) and Mfn2 (right) levels in brain ER and MAM fractions of wt and PS2-N141I Tg mice (n = 4 independent experiments). c) Crude mitochondrial fractions from brain of wt and FAD-PS2-N141I Tg mice were immunoprecipitated with Mfn2 specific antibodies, or with irrelevant IgG, as a negative control (IgG CTRL-). Precipitated (IP) and total crude mitochondrial fractions (input) were probed with PS2 specific antibodies.

FAD-PS2 fibroblasts show increased ER-mitochondria tethering and Ca^{2+} *cross-talk*

The results here presented and those previously obtained (Zampese E. et al., 2011; Kipanyula M.J. et al., 2012) have been obtained mainly in PS2 over-expressing models; we have thus wondered whether FAD-PS2 is able to increase ER-mitochondria coupling also when it is expressed at endogenous level. For this purpose, we have analysed human fibroblasts from an AD patient carrying the FAD-PS2-N141I mutation in one of the two alleles.

Figure 31a shows a typical experiment in which fibroblasts from this patient and an healthy control (matched for age and sex) were analyzed, by Aeqs, for their Ca^{2+} responses as described above: upon stimulation with the IP3-generating agonist bradykinin, FAD-PS2 fibroblasts showed reduced $[Ca^{2+}]$m and $[Ca^{2+}]$c peaks compared to controls. However, when the amplitude of $[Ca^{2+}]$c peaks of controls was reduced to match that of FAD-PS2 cells, the $[Ca^{2+}]$m peaks in FAD-PS2 fibroblasts were larger than those of pre-depleted controls (Fig. 31b). As shown in other cell types (Zampese E. et al., 2011), the increased $[Ca^{2+}]$m peaks were not due to a direct effect of FAD-PS2 on the mitochondrial Ca^{2+} uptake machinery, since control and FAD fibroblasts showed comparable $[Ca^{2+}]$m increases upon permeabilization and perfusion with an intracellular-like medium at fixed $[Ca^{2+}]$ (for control and FAD fibroblasts perfused with 2.5 μM $[Ca^{2+}]$: 60 ± 3.7 μM, and 62 ± 5.3 μM $[Ca^{2+}]$m peaks, respectively; for control and FAD fibroblasts perfused with 5 μM $[Ca^{2+}]$: 99 ± 16 μM, and 105 ± 12 μM $[Ca^{2+}]$m peaks, respectively; n = 4). We have also investigated the driving force that controls mitochondrial Ca^{2+} uptake (*i.e.*, mitochondrial $\Delta\Psi$), loading mitochondria in living cells with TMRM: the staining of the organelles in control and FAD-PS2N141I fibroblasts was similar, suggesting that not significant differences on basal mitochondrial $\Delta\Psi$ are present (Fig. 31c).

The increase in mitochondrial Ca^{2+} uptake was observed also when $[Ca^{2+}]$c and $[Ca^{2+}]$m peaks were measured in the very same single cell co-expressing two GFP-based Ca^{2+} indicators (Fig. 31d), the mitochondrial 4mtD1cpv (to measure $[Ca^{2+}]$m) and the nuclear H2BD1cpv (as a surrogate to monitor $[Ca^{2+}]$c) (Giacomello M. et al., 2010; Zampese E. et al., 2011). For nuclear Ca^{2+} rises in the same range (0.2–0.55 nucΔR/R0), the mitochondrial responses of FAD-PS2 fibroblasts were significantly larger than those obtained in controls. The ratio between the mitochondrial and nuclear peak values, measured within this interval, was significantly higher in FAD-PS2 cells compared to controls (Fig. 31e).

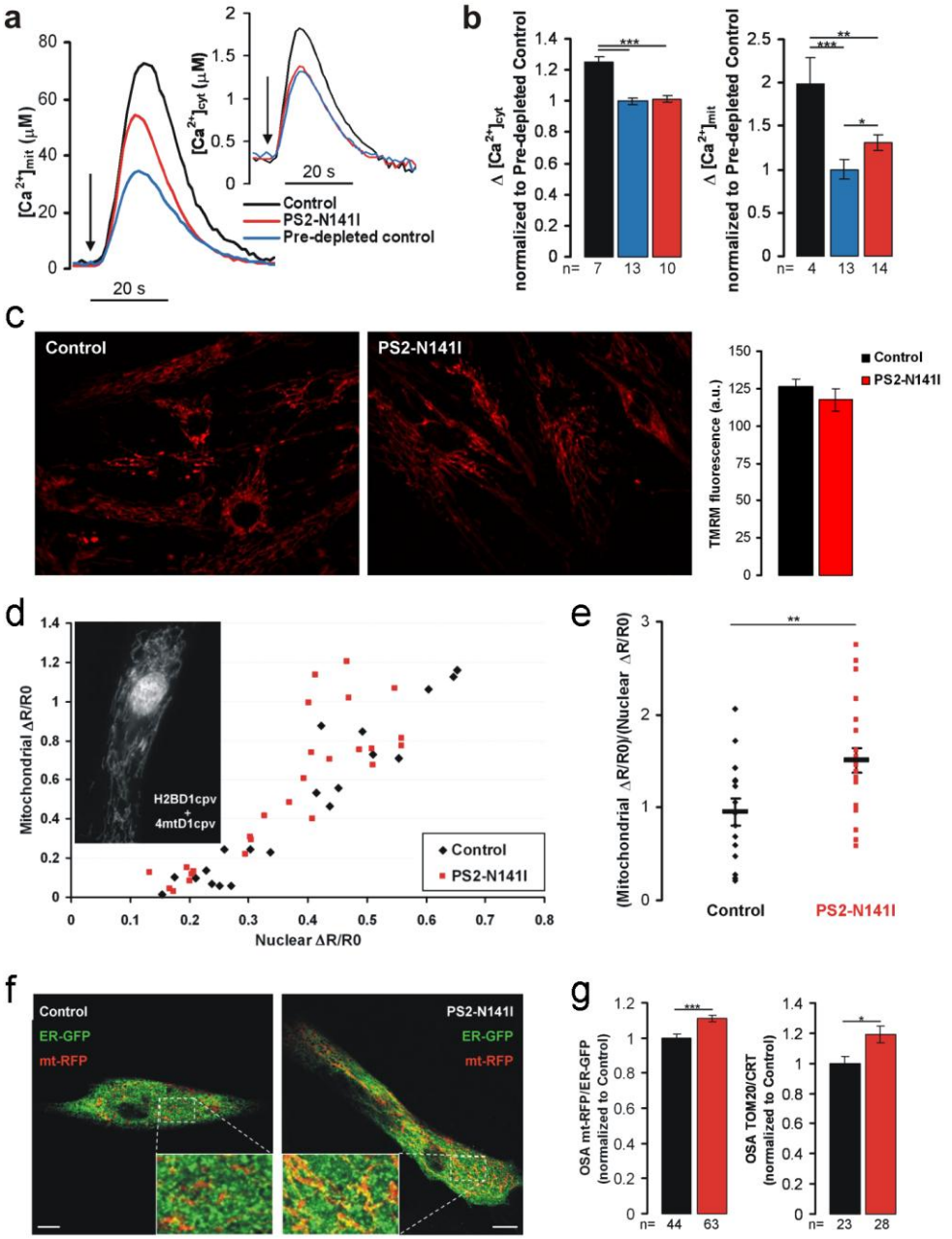

Fig. 31: a), b) $[Ca^{2+}]c$ and $[Ca^{2+}]m$ changes in control and FAD-PS2-N141I fibroblasts expressing mit- or cyt-Aeq. Pre-depleted control cells were pre-incubated in a Ca^{2+}-free, EGTA-containing medium for a fixed period of time to reach a cytosolic Ca^{2+} release similar to that observed in FAD fibroblasts. a) Representative cytosolic (inset) and mitochondrial Ca^{2+} traces in control (black), pre-depleted control (blue) and FAD-PS2-N141I (red) fibroblasts bathed in Ca^{2+}-free, EGTA-containing medium and challenged with BK (100 nM). b) Bars represent mean $[Ca^{2+}]c$ (left) and $[Ca^{2+}]m$ (right) peaks upon stimulation in the different conditions. c) Control and FAD-PS2-N141I fibroblasts were loaded with TMRM (10nM) and the basal fluorescence evaluated (right) to estimate mitochondrial $\Delta\Psi$. d) $[Ca^{2+}]m$ and $[Ca^{2+}]n$ peaks in single control and FAD fibroblasts, as revealed by specific cameleon Ca^{2+} probes. Cells co-expressing H2BD1cpv and 4mtD1cpv (inset) were stimulated as described in panel a. The increase in $[Ca^{2+}]m$ (mitochondrial ΔR/R0) is plotted as a function of the corresponding increase in $[Ca^{2+}]n$ (nuclear ΔR/R0) in the same cell. Each symbol represents one cell. e) Ratio between mitochondrial and nuclear peak values, measured as described in panel d within the nuclear 0.2–0.55 ΔR/R0 interval, in controls and FAD-PS2 fibroblasts. The mean ratio value results significantly higher in FAD-PS2 cells compared to controls (1.5 ± 0.13, n = 21 and 0.95 ± 0.14, n = 15 for FAD and control cells, respectively; $p<0.01$). f), g) ER–mitochondria interactions in control and FAD-PS2-N141I fibroblasts. f) Confocal images of cells co-expressing mt-RFP and ER-GFP. Scale bar: 10 μm. g) OSA quantification, calculated from single confocal images, for mt-RFP/ER-GFP (left) and TOM20/CRT immunofluorescence (right) for each condition.

As for FAD-PS2 over-expressing cells (Zampese E. et al., 2011) and neurons from FAD-PS2 Tg mice (Kipanyula M.J. et al., 2012), the increased $[Ca^{2+}]$m peak upon ER Ca^{2+} release observed in human FAD-PS2 fibroblasts depends on closer interactions between the two organelles: the co-localization area between the mt-RFP and ER-GFP signals (Fig. 31f) was significantly increased in human FAD-PS2 fibroblasts compared to controls (Fig. 31g, left). Co-localization coefficients confirm the significant increase in the ER–mitochondria juxtaposition in PS2-N141I fibroblasts (Manders' coefficients: 0.384 ± 0.006 and 0.42 ± 0.01; Pearson's coefficients: 0.217 ± 0.009 and 0.255 ± 0.011 for wt (n=30) and FAD-PS2 (n=28) fibroblasts, respectively; $p<0.01$). Similar results were obtained measuring the co-localization of two endogenous markers: the ER protein calreticulin and the mitochondrial protein Tom20 (Fig. 31g, right).

3. DISCUSSION

It is now firmly established that the correct organization and the dynamic interactions between ER and mitochondria, and particularly their Ca^{2+} cross-talk, coordinate and modulate key aspects of cell physiology, death and survival (Contreras L. et al., 2010; de Brito O.M. and Scorrano L., 2010; Filadi R. et al., 2012).

Impairment of mitochondrial functions have been observed in different neurodegenerative diseases and, among them, in AD patients as well as in different experimental models of AD (for a review, see Ankarcrona M. et al., 2010). In particular, alterations in mitochondrial Ca^{2+} handling seems to be a common feature among a wide spectrum of neurophatological conditions (Calì T. et al., 2012).

MAMs are specific ER membrane sub-domains closely coupled to mitochondria that modulate Ca^{2+} homeostasis and the metabolism of lipid, glucose and cholesterol (Hayashi T. et al., 2009). Interestingly, all these processes are altered in AD (Schon E.A. and Area-Gomez E., 2010).

We have recently described that PS2, and particularly its FAD mutants, is able to modulate ER-mitochondria coupling (Zampese E. et al., 2011), although the molecular mechanism of this feature has not been clarified yet.

The data here presented demonstrate, by crossed genetic complementation and ablation experiments, that PS2 requires the expression of Mfn2 in order to modulate ER-mitochondria coupling. In particular, the modulation of the tethering between the two organelles and their coupled Ca^{2+} transfer require the presence of the two proteins. Indeed, the previously reported ER-mitochondria tethering function of Mfn2 (de Brito O.M. and Scorrano L., 2008) is abolished in cells KO for both PS2 and PS1 and can be rescued completely by re-expression of PS2 alone, while PS1 is totally ineffective. Functional and biochemical evidence indicates that, to modulate ER-mitochondria vicinity, PS2 (wt and FAD) needs to physically interact, via its big cytosolic loop, with Mfn2 at both sides of MAM domains, likely forming, or stabilizing, a triple complex made by itself, ER-Mfn2 and mitochondrial Mfn2. On the contrary, Mfn1 seems to be dispensable for this PS2 tethering function. The latter observation suggests also that the lack of the PS2-mediated tethering effect in the absence of Mfn2 is not due to mitochondrial morphology alterations observed in Mfn2-KO cells, since a similar (or even stronger) fragmentation of the mitochondrial network is

observed also in Mfn1-KO cells. Thus, the leader function of Mfn2 as a molecular tether between ER and mitochondria has to be shared with PS2.

On the other hand, the previously described PS2 effect on intracellular Ca^{2+} stores (Brunello L. et al., 2009; Giacomello M. et al., 2005; Zatti G. et al., 2006; Zatti G. et al., 2004) is Mfn2-independent, since, upon PS2 over-expression, a reduction in cytosolic Ca^{2+} peak (a parameter that indirectly represents the Ca^{2+} content of intracellular stores) is observed also in Mfn2-KO cells. Noteworthy, the latter effect seems to be even more strong, compared to that observed in wt MEFs, probably because the expressed PS2 is not engaged in Mfn2 binding. In contrast, the reported ER Ca^{2+} depletion caused by Mfn2 over-expression (de Brito O.M. and Scorrano L., 2008), here confirmed, was observed only in the presence of PS2. Interestingly, the well known Mfn-mediated effect on mitochondria fusion seems, instead, to be independent from the presence of PS2. Thus, both proteins show distinct and multiple physiological roles, some similar to those exerted also by their homolog proteins (PS1 and Mfn1, respectively) and others completely divergent.

In addition to the effects described above regarding physiological cell functions, PS mutations are involved in the pathogenesis of FAD. The previously obtained results (demonstrating an increased PS2-mediated ER-mitochondria coupling in the presence of FAD-PS2 mutations) have been mainly obtained in over-expressing experimental models (Zampese E. et al., 2011; Kipanyula M.J. et al., 2012); to directly address this criticism we here demonstrate that, in human fibroblasts bearing the PS2-N141I mutation, ER-mitochondria interactions are clearly increased, compared to control cells. Similarly, both single-cell FRET data and cell-population Aeq-based Ca^{2+} measurements indicate that, in a "non over-expressing" cell model, FAD-PS2 mutants, despite reducing the maximal $[Ca^{2+}]_c$ peaks (due to partial depletion of the ER Ca^{2+} content) significantly increase Ca^{2+} transfer from ER to mitochondria. From the mechanistic point of view, the most important finding is that the FAD-PS2 effect on ER-mitochondria juxtaposition and Ca^{2+} cross-talk is, both quantitatively and qualitatively, very similar in transiently or stably over-expressing cells and in cells from a FAD patient, *i.e.*, a condition in which the PS2 mutation exerts its action independently of any artefact due to its over-expression.

Recently, an increased ER–mitochondria connectivity was observed also in human fibroblasts from individuals carrying FAD mutations in PS1 or APP, as well as in fibroblasts from sporadic AD patients (Area-Gomez E. et al., 2012). The increased coupling resulted in up-regulated MAM functions, as shown by an enhanced phospholipid and cholesterol

metabolism. On the same line, we have recently partecipated to a study (see the attached paper Hedskog L. et al., 2013) that shows how in human AD brains, as well as in a $APP_{Swe/Lon}$ mouse model, the levels of some MAMs related proteins were altered. Of note, in the mouse model the alteration was observed before the appearance of Aβ plaques. Moreover, the exposure to nanomolar [Aβ] induced in primary hippocampal neurons an increased number of ER-mitochondria contact points positive for VDAC1 and IP3R3, and, in SH-SY5Y cells, an increased ER-mitochondria Ca^{2+} transfer.

Both these studies, however, do not propose a possible molecular mechanism at the basis of their observations. In particular, as far as the first study is concerned, it is not clear why both sporadic and familial forms of AD display the same MAM phenotype. Are MAM alterations the consequence of specific mutations in PS or APP? What about the sporadic forms of the disease, in which these proteins are not mutated? To all these questions an answer is still lacking. Regard the possibility that Aβ peptides are responsible for these MAM alterations, a topological problem exists. Indeed, once generated, the majority of the Aβ peptide is released in the extracellular environment, thus it appears unlikely that it could come in contact with MAMs modulating their composition, at least directly. Although Aβ has been found in mitochondria (Manczak M. et al., 2006; Caspersen C. et al., 2005) and has been proposed to be actively imported into the organelle through Tom40 (Hansson Petersen C.A. et al., 2008), there is no agreement on this point, since substantial topological concerns still remain without an answer. In particular: how can Aβ reach the cytosol in order to be imported into mitochondria?

We here provide molecular evidence for a PS2 specific effect on ER-mitochondria coupling, through a direct physical interaction with Mfn2. In our hands, PS1 lacks to show this functionality; moreover, our IP and FRAP experiments clearly exclude the possibility of an interaction between PS1 and Mfn2. Concerning the molecular mechanism through which FAD-linked PS2 mutants are more efficient than their wt counterparts at modulating ER-mitochondria coupling, the tendency of mutated CFP-PS2, compared to the wt form, to display a more marked FRAP reduction in living cells expressing Mfn2 supports the idea that FAD-PS2 mutants are more efficient in engaging Mfn2. Indeed, our data show that FAD-PS2 mutants result much more enriched in MAMs than the wt form, thus here recruiting more Mfn2, by physically interacting with it both in *cis* and in *trans*, and forming more PS2-Mfn2 complexes critical for determining the apposition between the two organelles.

The mechanism by which FAD mutants preferentially localize at the MAM level within ER membranes, compared to the wt form, might be multiple, *e.g.*, PS2 conformation (full-length or processed form), differential post-translational protein modifications (for example, palmitoylation or ubiquitination, as shown for other MAM proteins Lynes E.M. et al., 2012; Sugiura A. et al., 2013), differential protein-protein interaction with other molecular anchor partners, etc, and additional investigations are required to clarify this point.

The mitochondrial abnormalities that have been described so far in AD are difficult to reconcile in a single clear scenario, because of the lacking of a clear and common molecular mechanism responsible for such alterations. However, it seems reasonable that they could be likely a consequence of a primary key insult, *e.g.*, the increased Aβ42 peptide production. In the case of PS2-linked FAD, however, mitochondrial alterations may represent a direct effect of the expression of PS2 mutants, accordingly to the mechanism here described. The increased physical and functional ER–mitochondria coupling could have diverse consequences relevant for FAD pathogenesis. For example, the strengthened Ca^{2+} cross-talk between the two organelles may have, under certain conditions and over very long periods of time, important and sometimes dramatic consequences, such as alterations of bioenergetic functions (*e.g.*, ATP or oxygen radical production, Ca^{2+} buffering, etc) or even an increase in mitochondria-dependent cell death (Contreras L. et al., 2010; Pizzo P. et al., 2012).

To date, increasing evidence is accumulating on the existence of early alterations in the functionality of the ER-mitochondria axis in AD. The outcome of these alterations is not completely clear and its understanding needs further investigations, in order to cast new light on AD pathogenesis.

The novel PS2-Mfn2 inter-dependency in modulating the physical/functional ER-mitochondria coupling here described adds further complexity to this scenario. Future studies will be required to verify the intriguing possibility that some Mfn2 mutations linked to Charcot-Marie-Tooth neuropathy type 2A (Cartoni R. and Martinou J.C., 2009), known to alter ER-mitochondria tethering, can act similarly to the FAD-PS2 forms, perhaps preventing or reinforcing their physical interaction and/or stabilization with PS2 at MAMs. If this is the case, the multi-protein complex formed by PS2 and Mfn2 at MAMs will be critical in the modulation of the ER-mitochondria axis, that represents a key, convergent step in the pathogenesis of different neurological diseases.

4. METHODS

Cell Culture and Transfection

Human fibroblasts (from Coriell Institute for medical research: FAD-PS2-N141I (AG09908); control fibroblasts (AG08525)) were grown in DMEM containing 15% FCS, supplemented with L-glutamine (2 mM), penicillin (100 U/ml) and streptomycin (100 µg/ml), in a humidified atmosphere containing 5% CO_2. Transfection was performed by electroporation using the Neon™ Transfection System (Life Technologies), according to manufacturer instruction. MEFs (wt, Mfn2-KO, Mfn1-KO, Mfn-DKO) were grown as previously described (de Brito O.M. and Scorrano L., 2008), as well as wt and PS-DKO MEFs (Brunello L. et al., 2009). SH-SY5Y cells were grown in DMEM containing 10% FCS, supplemented with L-glutamine (2 mM), penicillin (100 U/ml) and streptomycin (100 µg/ml), in a humidified atmosphere containing 5% CO_2. Cells were seeded onto glass coverslips (13 or 24-mm diameter) and transfection was performed at 60% confluence using Lipofectamine™ 2000 Transfection Reagent (Life Technologies). Aequorin and FRET measurements were usually performed 24 h after transfection.

For RNAi experiments, the growth medium was replaced 1 h before transfection with antibiotic-free medium. siRNAs (mouse PS2, target sequence: GAUAUACUCAUCUGCCAUG; siGENOME RISC-Free Control siRNA) (Dharmacon Research) were added to the transfection mixes to a final concentration of 20 nM.

Aequorin Ca^{2+} Measurements

MEF cells (0.5×10^5) were plated on coverslips (13 mm diameter), after 24 h were transfected and used for Ca^{2+} measurements the day after transfection (or 2 d after transfection for siRNA experiments). Human fibroblasts were plated after electroporation (0.5×10^5 cells/coverslip) and used for Ca^{2+} measurements after 24 h. Cells were incubated at 37°C with coelenterazine (5 µM) for 1 h in a modified Krebs–Ringer buffer (mKRB, in mM:140 NaCl, 2.8 KCl, 2 $MgCl_2$, 1 $CaCl_2$, 10 HEPES, 11 glucose, pH 7.4) and then transferred to the perfusion chamber. All the luminescence measurements were carried out in mKRB at 37°C. The experiments were terminated by cell permeabilization with digitonin (100 µM) in a hypotonic Ca^{2+}-rich solution (10 mM $CaCl_2$ in H_2O) to discharge the remaining unused aequorin pool. The light signal was collected as previously described (Brini M. et al., 1995).

To deplete the ER Ca^{2+} content partially, the following pre-depleting protocol was applied: after aequorin reconstitution, cells were pre-incubated for fixed time intervals (5–15 min) in Ca^{2+}-free, EGTA-containing medium (600 μM) at RT.

For cytosolic and mitochondrial Ca^{2+} measurements upon Capacitative Ca^{2+} Entry (CCE) activation, cells were pre-treated with the SERCA inhibitor cyclopiazonic acid (CPA, 20 μM) for 6 min in a Ca^{2+}-free, EGTA (600 μM)-containing medium; cells were then perfused with the same medium without the inhibitor and challenged with $CaCl_2$ (5 mM).

For permeabilization, cells were exposed for 1 min to digitonin (100 μM) in an intracellular-like medium containing (in mM): 130 KCl, 10 NaCl, 1 KH_2PO_4, 2 succinic acid, 1 $MgSO_4$, 20 Hepes, 0.05 EGTA, pH 7.0, at 37 °C. After digitonin removal by 2-min washing, mitochondrial Ca^{2+} uptake was estimated by mitochondria-targeted aequorin following cell perfusion with the same intracellular solution without EGTA and containing Ca^{2+} at different concentrations (2.5 and 5 μM).

Fluorescence Ca^{2+} Imaging

Human fibroblasts expressing fluorescent probes (H2BD1cpv and 4mtD1cpv) were analyzed using a DM6000 inverted microscope (Leica, Wetzlar, Germany) with a 40X oil objective (HCX Plan Apo, NA 1.25). Excitation light produced by a 410nm LED (Led Engin LZ1-00UA00 LED) was filtered at the appropriate wavelength (425 nm) through a band pass filter, and the emitted light was collected through a beamsplitter (OES s.r.l., Padua, Italy) (emission filters HQ 480/40M (for CFP) and HQ 535/30M (for cpV-YFP) and a dichroic mirror 515 DCXR). The beamsplitter permits the collection of the two emitted wavelengths at the same time, thus preventing any artefact due to movement of the organelles. All filters and dichroics were from Chroma Technologies (Bellow Falls, VT, USA). Images were acquired using an IM 1.4C cool camera (Jenoptik Optical Systems) attached to a 12-bit frame grabber. Synchronization of the excitation source and cool camera was performed through a control unit ran by a custom-made software package, Roboscope (developed by Catalin Cubotaru at VIMM, Padua, Italy); this software was also used for image analysis. Images were collected in continuous illumination with 150-ms exposure per image.

Cells were mounted into an open-topped chamber and maintained in an extracellular medium (modified Krebs-Ringer buffer). Classical experiments started in 1 mM $CaCl_2$; after perfusion with 300 μM EGTA, cells were stimulated by applying bradykinin (BK, 100nM); thereafter, the Ca^{2+} ionophore ionomycin (1 μM) was applied to completely discharge the

stores (or, without BK, as the only stimulus); finally digitonin (50 μM, to obtain plasma membrane permeabilization) in Ca^{2+}-free medium and then a saturating $CaCl_2$ concentration (10 mM) were applied, in order to verify the dynamic range of the probe.

Off-line analysis of FRET experiments was performed with ImageJ (Wayne Rasband, Bethesda, USA). CpV-YFP and CFP images were subtracted of background signals and distinctly analyzed after selecting proper regions of interest (ROIs) on each cell; subsequently, a ratio between cpV-YFP and CFP emissions was calculated (R=F530/F480). Data are presented as a $\Delta R/R_0$ values (where ΔR is the change of the cpV-YFP/CFP emission intensity ratio at any time, R_0 is the value at time of drug addition).

Confocal Analysis

Cells expressing endoplasmic reticulum (ER)-GFP and mitochondrial (mit)-RFP were analyzed with a Leica SP5 confocal system (DM IRE2) using the Ar/ArKr 488-nm laser line (GFP) and He/Ne 543-nm laser line (RFP). Co-localization analysis for the two markers was performed on z-stacks acquired with steps of 0.5 μm. For co-localization analyses, green and red channel images were acquired independently, and photomultiplier gain for each channel was adjusted to minimize background noise and saturated pixels. Once acquired, images were not modified further.

To estimate the overlapping signal area (OSA), analyses were carried out on single-plane images using ImageJ plug-ins. A threshold (based on the average intensity inside the analyzed cells) was applied to each channel, and the overlapping area was normalized to the total area occupied by both signals. In each condition, the OSA value was expressed as the percentage change over that measured in control cells (100%). Similarly, ER and mitochondria surface extension were estimate on the same single-plane images after application of a threshold (corresponding to the mean intensity of each signal within the analyzed cell). The area occupied by each signal was normalized to the total area occupied by the cell. Manders' and Pearson's coefficient[55-56] were calculated on z-stacks applying the ImageJ Co-localization Analysis plug-in.

Electron microscopy analysis

For conventional electron microscopy, cells grown in 35mm plastic dishes were fixed with 2% glutaraldehyde buffered with 0.1 M sodium cacodylate at pH 7.4 for 2h at room temperature. The fixed cells were carefully detached using a plastic cell scraper, collected

into eppendorf tubes and centrifuged to obtain the pellet. All samples were then washed three times in 0.1 M sodium cacodylate at pH 7.4 and post-fixed in 1% OsO_4 at room temperature in the same buffer. They were then washed three times in distilled water and stained with 0.5% uranyl acetate over night at 4°C. The pellets were dehydrated in graded steps of ethanol (50%, 70%, 90%, 100%), 2 times with 100% of acetone and embedded into Epon. Section (60 nm thick) were cut on a Leica UC7 ultramicrotome and examined with a Fei Tecnai 12 BioTwin Spirit transmission electron microscope.

Immunoprecipitation assay

Cells were harvested and solubilized in modified RIPA buffer (150mM NaCl, 25mM Tris-HCl, 1% NP40, 0.01% SDS, 0.05% Na-DOC, 1mM Na_2EDTA, protease inhibitor cocktail, pH 7.4). 300 μg of protein lysate (or 1 mg of crude mitochondria) were pre-cleared by adding 1 μg of irrelevant mouse or rabbit IgG together with 20 μl of protein A/G PLUS-Agarose (sc-2003 Santa Cruz Biotechnology) and incubated at 4°C for 45 min on a rocker platform. Cleared extracts were then incubated overnight with the indicated antibody (α-Myc, 05-724 Millipore; α-PS2, 1987-1 Epitomics; α-V5, R960-25 Life Technologies; α-Mfn2, ab56889 Abcam) and then adsorbed on 20 μl of protein A/G PLUS-Agarose at 4°C for 3h. Immunoprecipitates were collected by centrifugation at 2000 rpm and washed 4 times with 0.1M NaCl plus protease inhibitor cocktail. Beads were re-suspended in 30 μl of Loading Buffer and incubated at 37°C for 10 min. Protein were separated by SDS-PAGE and immunoblotted with the indicated antibody.

Subcellular fractionation and MAM purification

To isolate MAM, mouse brains from adult C57B6/J wt or FAD-PS2-N141I Tg mice (Kipanyula M.J. et al., 2012) were treated as previously described in Wieckowski M.R. et al., 2009. Briefly, mouse brains were cut into small pieces and homogenized using a Teflon pestle. The homogenate (total lysate) was centrifuged twice at 800g to remove nuclei and debris. After 9000 x g centrifugation, crude mitochondria pellet and a first supernatant were collected. This latter was further centrifuged at 100000 x g to generate the ER/microsome fraction. The crude mitochondrial fraction was uploaded to a Percoll gradient and centrifuged at 100000 x g, separating pure mitochondria and MAMs. The lower band, containing the pure mitochondria fraction, and the upper band, containing the MAM fraction, were collected and further washed to remove Percoll and mitochondria contamination from MAMs. The

fractions were then re-suspended in RIPA buffer, separated by SDS-PAGE (35 μg/lane) and immunoblotted with different antibodies.

Preparation of Protein Extracts and Western Blot Analysis

MEF and SH-SY5Y cells over-expressing PSs or Mfns, or transfected with specific siRNA, were harvested and treated as previously reported[30]. Briefly, cellular pellets were solubilized in RIPA buffer (50 mM Tris, 150 mM NaCl, 1% Triton X-100, 0.5% deoxycholic acid, 0,1% SDS, protease inhibitor cocktail, pH 7.5) and incubated on ice for 30 min. Unsolubilized material was spun down at 4000 x g for 5 min at 4°C. 35 μg of protein were loaded onto polyacrylamide gels (10-12%) and immunoblotted.

Western blot analyses were carried out with: α-PS2 C-term (1987-1 Epitomics); α-PS1 (anti-αPS1 loop; 529592 Calbiochem); α-mitofusin 2 (ab50838; Abcam); α-Myc (05-724 Millipore); α-PS2 N-term (Covance MMS-359S); α-actin (A4700; Sigma-Aldrich); α-CRT (PA3-900 Thermo Scientific); α-STIM1 (610954 BD Biosciences); α-VDAC1 (ab14734 Abcam); α-Grp75 (sc-13967 Santa Cruz Biotechnology).

The proteins were visualized by the chemiluminescence reagent ECL (Amersham, GE Healthcare, U.K. Ltd.). The intensity of the bands was analyzed using Image J software program.

CFP-PS Constructs

cDNAs for PS1 wt, PS2 wt, PS2-T122R and ECFP were amplified by PCR with specific primers to insert new restriction sites respectively at 5’ and 3’ of the sequences. After enzymatic digestion, the ECFP and PS fragments were ligated together into the pcDNA3 vector (Invitrogen) to obtain ECFP fused to the N-terminal of PSs.

To obtain Myc-PS2 constructs, cDNA for PS2 wt and PS2-T122R were amplified by PCR with specific primers (forward primer: 5'- CGC GGA TCC ATG CTC ACA TTC ATG GCC -3' and reverse primer: 5’-CCG GAA TTC TCA CAG GTC TTC TTC AGA GAT CAG TTT CTG TTC GAT GTA GAG CTG ATG GGA -3') to insert the Myc-tag at 3’ of the sequence. After enzymatic digestion PS fragments were ligated into the pcDNA3 vector (Invitrogen) to obtain the Myc-tag fused to the C-terminus of PS2.

FRAP experiments

FRAP experiments were carried out in Mfn2-KO MEFS upon transfection with the cDNA encoding CFP-PS (PS1wt, PS2wt or PS2-T122R) and Mfn2 (or the void vector), using lipofectamine 2000 (Invitrogen). For control experiments, GFP-sec61β (kindly provided by Gia K. Voeltz) was used as fluorescent protein. FRAP experiments were conducted, 24 h after transfection, with cells bathed in mKRB on a Leica SP5 confocal system using a 100X/1.4 oil objective and the Argon 458-nm laser line. Images were taken at 5 s intervals (25 s for the pre-bleaching period; 150 s for the recovery period).

The fluorescence intensity of the region of interest, the background and the whole cell fluorescence were measured with ImageJ and normalized curves were obtained as described previously (Phair R.D. et al., 2004), using the following formula: $I\,norm(t) = [I_{2pre}/(I_{2post\,(t)} - I_{3post(t)})]\ X[(I_{1(t)} - I_{3(t)}) / I_{1pre}]$, where ($I_1$) is the fluorescence value of the photobleached region, (I_2) is the whole cell fluorescence value, and (I_3) is the background value, before (*pre*) and after (*post*) bleaching.

The mobile fraction R is defined as $R = (F_\infty - F_0)/(F_i - F_0)$, where ($F_\infty$) is the fluorescence in the bleached region after full recovery, (F_i) is the fluorescence before bleaching and (F_0) is the fluorescence just after bleaching (Reits E.A. and Neefjes J.J., 2001).

The diffusion constant D is calculated according to Axelrod et al. (Axelrod D. et al., 1976), as $D = \gamma_D (R^2 / 4\tau_{1/2})$, where γ_D is a constant (0.88) referred to the circular region of interest (ROI) homogeneously bleached, R is the ROI radius and $\tau_{1/2}$ is the time needed for half fluorescence recovery after bleaching.

Materials

Restriction and modification enzymes were purchase from NEB Inc. (Ipswich, MA). BK, ATP and digitonin were purchased from Sigma-Aldrich, while ionomycin from Calbiochem. All other materials were analytical or of the highest available grade.

Statistical analysis

All data are representative of at least three different experiments. Data were analyzed using Origin 7.5 SR5 (OriginLab Corporation) and ImageJ (National Institutes of Health,). Unless otherwise stated, numerical values presented throughout the text refer to mean ± SEM

(n=number of independent experiments or cells; ∗ = p < 0.05, ∗∗=p<0.01, ∗∗∗ = p < 0.001, unpaired Student's *t* test).

5. REFERENCES

- Ankarcrona, M., Mangialasche, F. and Winblad, B. Rethinking Alzheimer's disease therapy: are mitochondria the key? J Alzheimers Dis 20(Suppl 2):S579–S590 (2010).
- Area-Gomez, E., de Groof, A.J., Boldogh, I., Bird, T.D., Gibson, G.E., Koehler, C.M., Yu, W.H., Duff, K.E., Yaffe, M.P., Pon, L.A. and Schon, E.A. Presenilins are enriched in endoplasmic reticulum membranes associated with mitochondria. Am J Pathol. 175(5):1810-1816 (2009).
- Area-Gomez, E., Del Carmen Lara Castillo, M., Tambini, M.D., Guardia-Laguarta, C., de Groof, A.J., Madra, M., Ikenouchi, J., Umeda, M., Bird, T.D., Sturley, S.L. and Schon, E.A. Upregulated function of mitochondria-associated ER membranes in Alzheimer disease. EMBO J. 31(21):4106-4123 (2012).
- Axelrod, D., Koppel, D.E., Schlessinger, J., Elson, E. and Webb, W. Mobility measurement by analysis of fluorescence photobleaching recovery kinetics. Biophysical J. 16, 1055-1069 (1976).
- Baughman, J.M., Perocchi, F., Girgis, H.S., Plovanich, M., Belcher-Timme, C.A., Sancak, Y., Bao, X.R., Strittmatter, L., Goldberger, O., Bogorad, R.L., Koteliansky, V. and Mootha, V.K. Integrative genomics identifies MCU as an essential component of the mitochondrial calcium uniporter. Nature 476, 341-345 (2011).
- Bernardi, P. and Azzone, G.F. Regulation of Ca2+ efflux in rat liver mitochondria. Role of membrane potential. Eur J Biochem 134:377–383 (1983).
- Bernardi, P. Mitochondrial transport of cations: channels, exchangers, and permeability transition. Physiol Rev 79:1127–1155 (1999).
- Berridge, M.J. Neuronal calcium signalling. Neuron 21: 13-26 (1998).
- Berridge, M.J., Bootman, M.D., Roderick, H.L. Calcium signalling: dynamics, homeostasis and remodelling. Nat Rev Mol Cell Biol. 4 (7): 517-529 (2003).
- Berridge, M.J., Lipp, P. and Bootman, M.D. The versatility and universality of calcium signalling. Nat Rev Mol Cell Biol. 1: 11-21 (2000).
- Beutner, G., Sharma, V.K., Giovannucci, R., Yule, D.I., and Sheu, S.S. Identification of a ryanodine receptor in rat heart mitochondria. J Biol Chem 276:21482–21488 (2001).
- Blaustein, M.P. and Lederer, W.J. Sodium/calcium exchange: its physiological implications. Physiol Rev. 79 (3): 763-854 (1999).
- Bojarski, L., Herms, J. and Kuznicki, J. Calcium dysregulation in Alzheimer's disease. Neurochem Int. 52: 621-633 (2008).
- Boyman, L., Williams, G.S., Khananshvili, D., Sekler, I. and Lederer, W.J. NCLX: the mitochondrial sodium calcium exchanger. J Mol Cell Cardiol. 59:205-213 (2013).
- Bragadin, M., Pozzan, T., and Azzone, G.F. Kinetics of Ca2+ carriers in rat liver mitochondria. Biochemistry 18, 5972-5978 (1979).
- Bravo, R., Vicencio, J.M., Parra, V., Troncoso, R., Munoz, J.P., Bui, M., Quiroga, C., Rodriguez, A.E., Verdejo, H.E., Ferreira, J., Iglewski, M., Chiong, M., Simmen, T., Zorzano, A., Hill, J.A., Rothermel, B.A., Szabadkai, G. and Lavandero, S. Increased ER-mitochondrial coupling promotes mitochondrial respiration and bioenergetics during early phases of ER stress. J Cell Sci. 124(Pt 13):2143-2152 (2011).
- Brini, M. Calcium-sensitive photoproteins. Methods 46: 160-166 (2008).
- Brini, M., Marsault, R., Bastianutto, C., Alvarez, J., Pozzan, T. and Rizzuto, R. Transfected aequorin in the measurement of cytosolic Ca2+ concentration ([Ca2+]c). A critical evaluation. J Biol Chem.; 270: 9896-9903 (1995).
- Brookes, P.S., Parker, N., Buckingham, J.A., Vidal-Puig, A., Halestrap, A.P., Gunter, T.E., Nicholls, D.G., Bernardi, P., Lemasters, J.J. and Brand, M.D. UCPs—unlikely calcium porters. Nat Cell Biol 10:1235–1237, author reply 1237–1240 (2008).

- Brunello, L., Zampese, E., Florean, C., Pozzan, T., Pizzo, P. and Fasolato, C. Presenilin-2 dampens intracellular Ca2+ stores by increasing Ca2+ leakage and reducing Ca2+ uptake. Journal of Cellular and Molecular Medicine 13: 3358–3369 (2009).
- Brunkan, A.L. and Goate, A.M. Presenilin function and gamma-secretase activity. Journal of Neurochemistry 93:769–792 (2005).
- Cali, T., Ottolini, D. and Brini, M. Mitochondrial Ca(2+) and neurodegeneration. Cell Calcium *52*, 73-85 (2012).
- Carafoli, E. Historical review: mitochondria and calcium: ups and downs of an unusual relationship. Trends in Biochemical Sciences 28, 175–181 (2003).
- Carafoli, E. The release of calcium from heart mitochondria by sodium. J Mol Cell Cardiol 6: 361–371 (1974).
- Cardenas, C., Miller, R.A., Smith, I., Bui, T., Molgo, J., Muller, M., Vais, H., Cheung, K.H., Yang, J., Parker, I., Thompson, C.B., Birnbaum, M.J., Hallows, K.R. and Foskett, J.K. Essential regulation of cell bioenergetics by constitutive InsP3 receptor Ca2+ transfer to mitochondria. Cell 142:270–283 (2010).
- Cartoni, R. and Martinou, J.C. Role of mitofusin 2 mutations in the physiopathology of Charcot-Marie-Tooth disease type 2A. Exp. Neurol. 218, 268-273 (2009).
- Caspersen, C., Wang, N., Yao, J., Sosunov, A., Chen, X., Lustbader, J.W., Xu, H.W., Stern, D., McKhann, G. and Yan, S.D. Mitochondrial Abeta: a potential focal point for neuronal metabolic dysfunction in Alzheimer's disease. FASEB J. 19(14):2040-2041 (2005).
- Celsi, F., Pizzo, P., Brini, M., Leo, S., Fotino, C., Pinton, P. and Rizzuto, R. Mitochondria, calcium and cell death: a deadly triad in neurodegeneration. Biochim Biophys Acta 1787: 335-344 (2009).
- Chang, K.T., Niescier, R.F. and Min, K.T. Mitochondrial matrix Ca2+ as an intrinsic signal regulating mitochondrial motility in axons. Proc Natl Acad Sci USA 108(37):15456–15461 (2011).
- Chen, Y.R. and Glabe, C.G. Distinct early folding and aggregation properties of Alzheimer amyloid-β peptides Aβ40 and Aβ42: stable trimer or tetramer formation by Aβ42. J. Biol. Chem. 281: 24414–24422 (2006).
- Cheung, K.H., Shineman, D., Muller, M., Cardenas, C., Mei, L., Yang, J., Tomita, T., Iwatsubo, T., Lee, V.M. and Foskett, J.K..et al. Mechanism of Ca2+ disruption in Alzheimer's disease by presenilin regulation of InsP3 receptor channel gating. Neuron 58:871–883 (2008).
- Chyung, J.H., Raper, D.M. and Selkoe, D.J. Gamma-secretase exists on the plasma membrane as an intact complex that accepts substrates and effects intramembrane cleavage. J Biol Chem. 280 (6): 4383-4392 (2005).
- Citron, M., Westaway, D., Xia, W., Carlson, G., Diehl, T., Levesque, G., Johnson-Wood, K., Lee, M., Seubert, P., Davis, A., Kholodenko, D., Motter, R., Sherrington, R., Perry, B., Yao, H., Strome, R., Lieberburg, I., Rommens, J., Kim, S., Schenk, D., Fraser, P., St George Hyslop, P. and Selkoe, D.J. Mutant presenilins of Alzheimer's disease increase production of 42-residue amyloid beta-protein in both transfected cells and transgenic mice. Nat Med. 3 (1): 67-72 (1997).
- Clapham, D.E. Calcium signalling. Cell 131 (6): 1047-1058 (2007).
- Contreras, L., Drago, I., Zampese, E. and Pozzan, T. Mitochondria: the calcium connection. Biochim. Biophys. Acta 1797, 607-618 (2010).
- Cosson, P., Marchetti, A., Ravazzola, M. and Orci, L. Mitofusin-2 independent juxtaposition of endoplasmic reticulum and mitochondria: an ultrastructural study. PLoS One 7(9):e46293 (2012).
- Crompton, M., Kunzi, M. and Carafoli, E. The calcium-induced and sodium-induced effluxes of calcium from heart mitochondria. Evidence for a sodium-calcium carrier. Eur J Biochem 79:549–580 (1977).
- Crompton, M., Moser, R., Ludi, H. and Carafoli, E. The interrelations between the transport of sodium and calcium in mitochondria of various mammalian tissues. Eur J Biochem 82:25–31 (1978).
- Csordas, G., Golenar, T., Seifert, E.L., Kamer, K.J., Sancak, Y., Perocchi, F., Moffat, C., Weaver, D., de la Fuente Perez, S., Bogorad, R., Koteliansky, V., Adijanto, J., Mootha, V.K. and Hajnoczky, G. MICU1 controls both the threshold and cooperative activation of the mitochondrial Ca2+ uniporter. Cell Metab 17, 976-987 (2013).

- Csordas, G., Renken, C., Varnai, P., Walter, L., Weaver, D., Buttle, K.F., Balla, T., Mannella, C.A. and Hajnoczky, G. Structural and functional features and significance of the physical linkage between ER and mitochondria. J Cell Biol 174(7): 915–921 (2006).
- Csordas, G., Thomas, A. P., and Hajnoczky, G. Quasi-synaptic calcium signal transmission between endoplasmic reticulum and mitochondria. *EMBO J.* 18, 96–108 (1999).
- Csordas, G., Varnai, P., Golenar, T., Roy, S., Purkins, G., Schneider, T.G., Balla, T., Hajnoczky, G. Imaging interorganelle contacts and local calcium dynamics at the ER-mitochondrial interface. Mol Cell 39(1):121–132 (2010).
- David, G., Barrett, J. N., and Barrett, E. F. Evidence that mitochondria buffer physiological Ca2+ loads in lizard motor nerve terminals. *J. Physiol.* 509, 59–65 (1998).
- de Brito, O.M. and Scorrano, L. An intimate liaison: spatial organization of the endoplasmic reticulum-mitochondria relationship. EMBO J. 29, 2715-2723 (2010).
- de Brito, O.M. and Scorrano, L. Mitofusin 2 tethers endoplasmic reticulum to mitochondria. Nature 456:605–610 (2008).
- De Marchi, U., Castelbou, C. and Demaurex, N. Uncoupling rotein 3 (UCP3) modulates the activity of sarco/endoplasmic reticulum Ca2+ -ATPase (SERCA) by decreasing mitochondrial ATP production. J Biol Chem 286:32533–32541(2011).
- De Stefani, D., Bononi, A., Romagnoli, A., Messina, A., De Pinto, V., Pinton, P. and Rizzuto, R.VDAC1 selectively transfers apoptotic Ca2+ signals to mitochondria. Cell Death Differ. 19(2):267-273 (2012).
- De Stefani, D., Raffaello, A., Teardo, E., Szabo, I., and Rizzuto, R. A forty-kilodalton protein of the inner membrane is the mitochondrial calcium uniporter. Nature 476, 336-340 (2011).
- De Strooper B. Loss-of-function presenilin mutations in Alzheimer disease. Talking Point on the role of presenilin mutations in Alzheimer disease. EMBO Rep. 8 (2): 141-146 (2007).
- De Strooper, B. and Annaert, W. Novel Research Horizons for Presenilins and gamma-Secretases in Cell Biology and Disease. Annu Rev Cell Dev Biol. 1-26 (2010).
- De Strooper, B., Iwatsubo, T. and Wolfe, M.S. Presenilins and gamma-secretase: structure, function, and role in Alzheimer disease. Cold Spring Harbor Perspectives in Medicine 2:a006304 (2012).
- Del Arco, A., Agudo, M. and Satrustegui, J. Characterization of a second member of the subfamily of calcium-binding mitochondrial carriers expressed in human non-excitable tissues. Biochem J 345(Pt 3):725–732 (2000).
- DeLuca, H. F. & Engstrom, G. W. Calcium uptake by rat kidney mitochondria. Proc.Natl Acad. Sci. USA 47, 1744–1750 (1961).
- Denton, R.M. Regulation of mitochondrial dehydrogenases by calcium ions. Biochim Biophys Acta 1787:1309–1316 (2009).
- Drago, I., De Stefani, D., Rizzuto, R. and Pozzan, T. Mitochondrial Ca2+ uptake contributes to buffering cytoplasmic Ca2+ peaks in cardiomyocytes. Proc Natl Acad Sci U S A 109, 12986-12991 (2012).
- Drago, I., Pizzo, P. and Pozzan, T. After half a century mitochondrial calcium in- and efflux machineries reveal themselves. EMBO J 30, 4119-4125 (2011).
- Dreses-Werringloer, U., Lambert, J.C., Vingtdeux, V., Zhao, H., Vais, H., Siebert, A., Jain, A., Koppel, J., Rovelet-Lecrux, A., Hannequin, D., Pasquier, F., Galimberti, D., Scarpini, E., Mann, D., Lendon, C., Campion, D., Amouyel, P., Davies, P., Foskett, J.K., Campagne, F. and Marambaud, P. A polymorphism in CALHM1 influences Ca2+ homeostasis, Abeta levels, and Alzheimer's disease risk. Cell 133: 1149-1161 (2008).
- Emilsson, L., Saetre, P. and Jazin, E. Alzheimer's disease: mRNA expression profiles of multiple patients show alterations of genes involved with calcium signaling. Neurobiol Dis. 21: 618-625 (2006).
- Ertekin-Taner, N. Genetics of Alzheimer's disease: a centennial review. Neurol Clin. 25: 611-667 (2007).
- Etcheberrigaray, R., Hirashima, N., Nee, L., Prince, J., Govoni, S., Racchi, M., et al. Calcium responses in fibroblasts from asymptomatic members of Alzheimer's disease families. Neurobiology of Disease 5: 37–45 (1998).

- Fiala, J.C. Mechanisms of amyloid plaque pathogenesis. Acta Neuropathol. 114: 551-571 (2007).
- Fieni, F., Lee, S.B., Jan, Y.N., Kirichok, Y. Activity of the mitochondrial calcium uniporter varies greatly between tissues. Nat Commun 3:1317 (2012).
- Filadi, R., Zampese, E., Pozzan, T., Pizzo, P. and Fasolato, C. Endoplasmic Reticulum-Mitochondria Connections, Calcium Cross-Talk and Cell Fate: A Closer Inspection. In "Endoplasmic Reticulum Stress in Health and Disease" Agostinis, P. and Samali, A. Springer Edition, Part 1, 75-106 (2012).
- Fill, M. and Copello, J.A. Ryanodine receptor calcium release channels. Physiol Rev 82 (4):893-922 (2002).
- Florean, C., Zampese, E., Zanese, M., Brunello, L., Ichas, F., De Giorgi, F. and Pizzo, P. High content analysis of gamma-secretase activity reveals variable dominance of presenilin mutations linked to familial Alzheimer's disease. Biochim Biophys Acta. 1783 (8):1551-1560 (2008).
- Förstl, H. and Kurz, A. Clinical features of Alzheimer's disease. Eur Arch Psychiatry Clin Neurosci.; 249 (6): 288-290 (1999).
- Foskett, J.K., White, C., Cheung, K.H. and Mak, D.O. Inositol trisphosphate receptor Ca2+ release channels. Physiol Rev. 87 (2): 593-658 (2007).
- Friedman, J.R., Lackner, L.L., West, M., DiBenedetto, J.R., Nunnari, J. and Voeltz, G.K. ER tubules mark sites of mitochondrial division. Science 334, 358-362 (2011).
- Gandy, S. The role of cerebral amyloid beta accumulation in common forms of Alzheimer disease. J Clin Invest. 115: 1121-1129 (2005).
- Giacomello, M., Barbiero, L., Zatti, G., Squitti, R., Binetti, G., Pozzan, T., Fasolato, C., Ghidoni, R. and Pizzo, P. Reduction of Ca2+ stores and capacitative Ca2+ entry is associated with the familial Alzheimer's disease presenilin-2 T122R mutation and anticipates the onset of dementia. Neurobiol Dis. 18 (3): 638-648 (2005).
- Giacomello, M., Drago, I., Bortolozzi, M., Scorzeto, M., Gianelle, A., Pizzo, P. and Pozzan, T. Ca2+ hot spots on the mitochondrial surface are generated by Ca2+ mobilization from stores, but not by activation of store-operated Ca2+ channels. Mol Cell 38(2):280–290 (2010).
- Giorgi, C., De Stefani, D., Bononi, A., Rizzuto, R. and Pinton, P. Structural and functional link between the mitochondrial network and the endoplasmic reticulum. Int J Biochem Cell Biol. 41(10):1817-1827 (2009).
- Giorgio, V., von Stockum, S., Antoniel, M., Fabbro, A., Fogolari, F., Forte, M., Glick, G.D., Petronilli, V., Zoratti, M., Szabó, I., Lippe, G. and Bernardi, P. Dimers of mitochondrial ATP synthase form the permeability transition pore. Proc Natl Acad Sci U S A 110 (15): 5887-5892 (2013).
- Goedert, M. and Spillantini, M.G. A century of Alzheimer's disease. Science 314: 777-781 (2006).
- Haass, C. and Selkoe, D.J. Soluble protein oligomers in neurodegeneration: lessons from the Alzheimer's amyloid beta-peptide. Nat Rev Mol Cell Biol. 8:101-112 (2007).
- Hamasaki, M., Furuta, N., Matsuda, A., Nezu, A., Yamamoto, A., Fujita, N., Oomori, H., Noda, T., Haraguchi, T., Hiraoka, Y., Amano, A. and Yoshimori, T. Autophagosomes form at ER-mitochondria contact sites. Nature 495, 389-393 (2013).
- Hansson Petersen, C.A., Alikhani, N., Behbahani, H., Wiehager, B., Pavlov, P.F., Alafuzoff, I., Leinonen, V., Ito, A., Winblad, B., Glaser, E. and Ankarcrona, M. The amyloid beta-peptide is imported into mitochondria via the TOM import machinery and localized to mitochondrial cristae. Proc Natl Acad Sci USA 105(35):13145–13150 (2008).
- Hardy, J. and Selkoe, D.J.: The amyloid hypothesis of Alzheimer's disease: progress and problems on the road to therapeutics. Science 297: 353-356 (2002).
- Hayashi, T. and Su, T.P. Sigma-1 receptor chaperones at the ER-mitochondrion interface regulate Ca(2+) signaling and cell survival. Cell 131(3):596–610 (2007).
- Hayashi, T., Rizzuto, R., Hajnoczky, G. and Su, T.P. MAM: more than just a housekeeper. Trends Cell Biol. 19(2):81-88 (2009).
- Hedskog, L., Pinho, C.M., Filadi, R., Rönnbäck, A., Hertwig, L., Wiehager, B., Larssen, P., Gellhaar, S., Sandebring, A., Westerlund, M., Graff, C., Winblad, B., Galter, D., Behbahani, H., Pizzo, P., Glaser, E. and

Ankarcrona, M. Modulation of the endoplasmic reticulum-mitochondria interface in Alzheimer's disease and related models. Proc Natl Acad Sci U S A 110(19):7916-7921 (2013).

- Herms, J., Schneider, I., Dewachter, I., Caluwaerts, N., Kretzschmar, H. and Van Leuven, F. Capacitive calcium entry is directly attenuated by mutant presenilin-1, independent of the expression of the amyloid precursor protein. J Biol Chem 278: 2484-2489 (2003).
- Herreman, A., Serneels, L., Annaert, W., Collen, D., Schoonjans, L. and De Strooper, B. Total inactivation of gamma-secretase activity in presenilin-deficient embryonic stem cells. Nat Cell Biol. 2: 461-462 (2000).
- Honarnejad, K. and Herms, J. Presenilins: role in calcium homeostasis. Int J Biochem Cell Biol. 44(11):1983-1986 (2012).
- Ito, E., Oka, K., Etcheberrigaray, R., Nelson, T.J., McPhie, D.L., Tofel-Grehl, B., et al. Internal Ca2+ mobilization is altered in fibroblasts from patients with Alzheimer disease. Proc Natl Acad Sci USA 91:534–853 (1994).
- Iwasawa R., Mahul-Mellier, A.L., Datler, C., Pazarentzos, E., and Grimm, S. Fis1 and Bap31 bridge the mitochondria-ER interface to establish a platform for apoptosis induction. EMBO J. 30(3):556-68 (2011).
- Jiang, D., Zhao, L. and Clapham, D.E. Genome-wide RNAi screen identifies Letm1 as a mitochondrial Ca2+/H + antiporter. Science 326:144–147 (2009).
- Kaether, C., Haass, C. and Steiner, H. Assembly, trafficking and function of gamma-secretase. Neurodegener Dis.; **3** (4-5): 275-283 (2006).
- Kaether, C., Schmitt, S., Willem, M. and Haass, C. Amyloid precursor protein and Notch intracellular domains are generated after transport of their precursors to the cell surface. Traffic. 7 (4): 408-415 (2006).
- Kasri, N.N., Kocks, S.L., Verbert, L., Hébert, S.S., Callewaert, G., Parys, J.B., Missiaen, L. and De Smedt, H. Up-regulation of inositol 1,4,5-trisphosphate receptor type 1 is responsible for a decreased endoplasmic-reticulum Ca2+ content in presenilin double knock-out cells. Cell Calcium 40 (1): 41-51 (2006).
- Kessels, H.W., Nguyen, L.N., Nabavi, S. and Malinow, R.: The prion protein as a receptor for amyloid-beta. Nature 466: E3-4 (2010).
- Kim, J., Kleizen, B., Choy, R., Thinakaran, G., Sisodia, S.S. and Schekman, R.W. Biogenesis of gamma-secretase early in the secretory pathway. J Cell Biol. 179 (5): 951-963 (2007).
- Kim, T.W., Pettingell, W.H., Hallmark, O.G., Moir, R.D., Wasco, W. and Tanzi, R.E. Endoproteolytic cleavage and proteasomal degradation of presenilin 2 in transfected cells. Journal of Biological Chemistry 272:11006–11010 (1997).
- Kimberly, W.T., Xia, W., Rahmati, T., Wolfe, M.S. and Selkoe, DJ. The transmembrane aspartates in presenilin 1 and 2 are obligatory for gamma-secretase activity and amyloid beta-protein generation. J Biol Chem. 275 (5): 3173-3178 (2000).
- Kipanyula, M.J., Contreras, L., Zampese, E., Lazzari, C., Wong, A.K., Pizzo, P., Fasolato, C. and Pozzan, T. Ca2+ dysregulation in neurons from transgenic mice expressing mutant presenilin 2. Aging Cell 11(5): 885-993 (2012).
- Kornmann, B., Currie, E., Collins, S.R., Schuldiner, M., Nunnari, J., Weissman, J.S. and Walter, P. An ER-mitochondria tethering complex revealed by a synthetic biology screen. Science 325(5939):477–481 (2009).
- Korobova, F., Ramabhadran, V. and Higgs, H.N. An actin-dependent step in mitochondrial fission mediated by the ER-associated formin INF2. Science 339, 464-467 (2013).
- LaFerla, F.M. Calcium dyshomeostasis and intracellular signalling in Alzheimer's disease. Nat Rev Neurosci. 3: 862-872 (2002).
- LaFerla, F.M., Green, K.N. and Oddo, S. Intracellular amyloid-beta in Alzheimer's disease. Nat Rev Neurosci. 8: 499-509 (2007).
- Laurén, J., Gimbel, D.A., Nygaard, H.B., Gilbert, J.W. and Strittmatter, S.M. Cellular prion protein mediates impairment of synaptic plasticity by amyloid-beta oligomers. Nature 457: 1128-1132 (2009).
- Lehninger, A. L., Rossi, C. S., and Greenawalt, J. W. Respiration dependent accumulation of inorganic phosphate and Ca ions by rat liver mitochondria. Biochem. Biophys. Res. Commun. 10, 444–448 (1963).

- Lewis, R.S. The molecular choreography of a store-operated calcium channel. Nature 446: 284-287 (2007).
- Li, W., Shariat-Madar, Z., Powers, M., Sun, X., Lane, R.D. and Garlid, K.D. Reconstitution, identification, purification, and immunological characterization of the 110-kDa Na+/Ca2+ antiporter from beef heart mitochondria. J Biol Chem 267:17983–17989 (1992).
- Lissandron, V., Podini, P., Pizzo P. and Pozzan, T. Unique characteristics of Ca^{2+} homeostasis of the trans-Golgi compartment. Proc Natl Acad Sci USA 107 (20):9198-9203 (2010).
- Lynes, E.M., Bui, M., Yap, M.C., Benson, M.D., Schneider, B., Ellgaard, L., Berthiaume, L.G. and Simmen, T. Palmitoylated TMX and calnexin target to the mitochondria-associated membrane. EMBO J. 31, 457-470 (2012).
- Ma, Q.H., Futagawa, T., Yang, W.L., Jiang, X.D., Zeng, L., Takeda, Y., Xu, R.X., Bagnard, D., Schachner, M., Furley, A.J., Karagogeos, D., Watanabe, K., Dawe, G.S. and Xiao, Z.C. A TAG1-APP signalling pathway through Fe65 negatively modulates neurogenesis. Nat Cell Biol. 10: 283-294 (2008).
- MacAskill, A.F. and Kittler, J.T. Control of mitochondrial transport and localization in neurons. Trends Cell Biol 20(2):102–112 (2010).
- Mallilankaraman, K., Cardenas, C., Doonan, P.J., Chandramoorthy, H.C., Irrinki, K.M., Golenar, T., Csordas, G., Madireddi, P., Yang, J., Muller, M., Miller, R., Kolesar, J.E., Molgo, J., Kaufman, B., Hajnoczky, G., Foskett, J.K. and Madesh, M. MCUR1 is an essential component of mitochondrial Ca2+ uptake that regulates cellular metabolism. Nat Cell Biol 14, 1336-1343 (2012b).
- Mallilankaraman, K., Doonan, P., Cardenas, C., Chandramoorthy, H.C., Muller, M., Miller, R., Hoffman, N.E., Gandhirajan, R.K., Molgo, J., Birnbaum, M.J., Rothberg, B.S., Mak, D.O., Foskett, J.K. and Madesh, M. MICU1 is an essential gatekeeper for MCU-mediated mitochondrial Ca(2+) uptake that regulates cell survival. Cell 151, 630-644 (2012).
- Manczak, M., Anekonda, T.S., Henson, E., Park, B.S., Quinn, J. and Reddy, P.H. Mitochondria are a direct site of A beta accumulation in Alzheimer's disease neurons: implications for free radical generation and oxidative damage in disease progression. Hum Mol Genet. 15(9):1437-1449 (2006).
- Marchi, S., and Pinton, P. The mitochondrial Calcium uniporter complex: molecular components, structure and physiopathological implications. J Physiol. (2013).
- Marchi, S., Lupini, L., Patergnani, S., Rimessi, A., Missiroli, S., Bonora, M., Bononi, A., Corra, F., Giorgi, C., De Marchi, E., Poletti, F., Gafa, R., Lanza, G., Negrini, M., Rizzuto, R. and Pinton, P. Downregulation of the Mitochondrial Calcium Uniporter by Cancer-Related miR-25. Curr Biol 23, 58-63 (2013).
- Martell, J.D., Deerinck, T.J., Sancak, Y., Poulos, T.L., Mootha, V.K., Sosinsky, G.E., Ellisman, M.H. and Ting, A.Y. Engineered ascorbate peroxidase as a genetically encoded reporter for electron microscopy. Nat Biotechnol 30, 1143-1148 (2012).
- Mattson M.P. Pathways towards and away from Alzheimer's disease. Nature 430: 631–639 (2004).
- McCarthy, J.V., Twomey, C. and Wujek, P. "Presenilin-dependent regulated intramembrane proteolysis and gamma-secretase activity". Cell Mol Life Sci. 66 (9):1534-1555 (2009).
- McCombs, J.E., Gibson, E.A. and Palmer, A.E. Using a genetically targeted sensor to investigate the role of presenilin-1 in ER Ca2+ levels and dynamics. Molecular Biosystems 6:1640–1649 (2010).
- Michalak, M., Groenendyk, J., Szabo, E., Gold, L.I. and Opas, M. Calreticulin, a multi-process calcium-buffering chaperone of the endoplasmic reticulum. The Biochemical journal 417 (3): 651-666 (2009).
- Mitchell, P., and Moyle, J. Chemiosmotic hypothesis of oxidative phosphorylation. Nature 213, 137–139 (1967).
- Morré, D.J., Merritt, W.D. and Lembi, C.A. Connections between mitochondria and endoplasmic reticulum in rat liver and onion stem. Protoplasma 73(1):43–49 (1971).
- Nicholls, D.G. and Crompton, M. Mitochondrial calcium transport. FEBS Lett 111, 261-268 (1980).
- Nicholls, D.G.and Chalmers, S. The integration of mitochondrial calcium transport and storage. J Bioenerg Biomembr 36: 277–281 (2004).
- Nowikovsky, K., Pozzan, T., Rizzuto, R., Scorrano, L. and Bernardi, P. Perspectives on: SGP Symposium on Mitochondrial Physiology and Medicine: The pathophysiology of LETM1. J Gen Physiol 139(6):445–454 (2012).

- Ogura, T., Mio, K., Hayashi, I., Miyashita, H., Fukuda, R., Kopan, R., Kodama, T., Hamakubo, T., Iwatsubo, T., Tomita, T., et al. Three-dimensional structure of the g-secretase complex. Biochem Biophys Res Commun 343: 525–534 (2006).
- Osenkowski, P., Li, H., Ye, W., Li, D., Aeschbach, L., Fraering, P.C., Wolfe, M.S., Selkoe, D.J. and Li, H. Cryoelectron microscopy structure of purified g-secretase at 12 A° resolution. J Mol Biol 385: 642–652 (2009).
- Pagliarini, D. J., Calvo, S. E., Chang, B., Sheth, S. A., Vafai, S. B., Ong, S. E., Walford, G. A., Sugiana, C., Boneh, A., Chen, W. K., Hill, D. E., Vidal, M., Evans, J. G., Thorburn, D. R., Carr, S. A., and Mootha, V. K. A mitochondrial protein compendium elucidates complex I disease biology. *Cell* 134, 112–123 (2008).
- Palmer, A.E., Giacomello, M., Kortemme, T., Hires, S.A., Lev-Ram, V., Baker, D. and Tsien, R.Y.Ca2+ indicators based on computationally redesigned calmodulin-peptide pairs. Chem Biol. 13 (5): 521-530 (2006).
- Palty R, Sekler I. The mitochondrial Na2+/Ca2+ exchanger. Cell Calcium 52(1):9-15 (2012).
- Palty, R., Ohana, E., Hershfinkel, M., Volokita, M., Elgazar, V., Beharier, O., Silverman, W.F., Argaman, M. and Sekler, I. Lithium-calcium exchange is mediated by a distinct potassium-independent sodium-calcium exchanger. J Biol Chem 279: 25234–25240 (2004).
- Palty, R., Silverman, W.F., Hershfinkel, M., Caporale, T., Sensi, S.L., Parnis, J., Nolte, C., Fishman, D., Shoshan-Barmatz, V., Herrmann, S., Khananshvili, D. and Sekler, I. NCLX is an essential component of mitochondrial Na+/Ca2+ exchange. Proc Natl Acad Sci USA 107: 436–441 (2010).
- Pan, X., Liu, J., Nguyen, T., Liu, C., Sun, J., Teng, Y., Fergusson, M.M., Rovira, I.I., Allen, M., Springer, D.A., Aponte, A.M., Gucek, M., Balaban, R.S., Murphy, E. and Finkel, T. The physiological role of mitochondrial calcium revealed by mice lacking the mitochondrial calcium uniporter. Nat Cell Biol 15, 1464-1472 (2013).
- Panfili, E., Sandri, G., Sottocasa, G.L., Lunazzi, G., Liut, G., and Graziosi, G. Specific inhibition of mitochondrial Ca2+ transport by antibodies directed to the Ca2+-binding glycoprotein. Nature 264, 185-186 (1976).
- Paredes, R.M., Etzler, J.C., Watts, L.T., Zheng, W. and Lechleiter, J.D. Chemical calcium indicators. Methods 46(3):143-151 (2008).
- Parihar, M.S. and Hemnani, T. Alzheimer's disease pathogenesis and therapeutic interventions. J Clin Neurosci. 11(5): 456-467 (2004).
- Patron, M., Raffaello, A., Granatiero, V., Tosatto, A., Merli, G., De Stefani, D., Wright, L., Pallafacchina, G., Terrin, A., Mammucari, C., and Rizzuto, R. The Mitochondrial Calcium Uniporter (MCU): Molecular Identity and Physiological Roles. J. Biol. Chem. 288: 10750-10758 (2013).
- Perl, P.D. Neuropathology of Alzheimer's disease. Mt Sinai J Med. 77: 32-42 (2010).
- Perocchi, F., Gohil, V.M., Girgis, H.S., Bao, X.R., McCombs, J.E., Palmer, A.E.and Mootha, V.K. MICU1 encodes a mitochondrial EF hand protein required for Ca(2+) uptake. Nature 467, 291-296 (2010).
- Perrin, R.J., Fagan, A.M. and Holtzman, D.M. Multimodal techniques for diagnosis and prognosis of Alzheimer's disease. Nature 461: 916-922 (2009).
- Phair, R.D., Gorski, S.A. and Misteli, T. Measurement of dynamic protein binding to chromatin in vivo, using photobleaching microscopy. Methods Enzymol. 375, 393-414 (2004).
- Pinton, P., Giorgi, C., Siviero, R., Zecchini, E. and Rizzuto, R. Calcium and apoptosis: ER-mitochondria Ca2+ transfer in the control of apoptosis. Oncogene 27:6407–6418 (2008).
- Pinton, P., Pozzan, T. and Rizzuto, R. The Golgi apparatus is an inositol 1,4,5-trisphosphate-sensitive Ca^{2+} store, with functional properties distinct from those of the endoplasmic reticulum. EMBO J 17 (18):5298-5308 (1998).
- Pizzo, P., Drago, I., Filadi, R. and Pozzan, T. Mitochondrial Ca2+ homeostasis: mechanism, role, and tissue specificities. Pflugers Arch - Eur J Physiol 464:3–17 (2012).
- Pizzo, P., Lissandron, V., Capitanio, P. and Pozzan, T. Ca2+ signalling in the Golgi apparatus. Cell Calcium 50(2):184-192 (2011).

- Plovanich, M., Bogorad, R.L., Sancak, Y., Kamer, K.J., Strittmatter, L., Li, A.A., Girgis, H.S., Kuchimanchi, S., De Groot, J., Speciner, L., Taneja, N., Oshea, J., Koteliansky, V., and Mootha, V.K. MICU2, a paralog of MICU1, resides within the mitochondrial uniporter complex to regulate calcium handling. PLoS One 8, e55785 (2013).
- Pozzan, T., Mongillo, M. and Rudolf, R. The Theodore Bücher lecture. Investigating signal transduction with genetically encoded fluorescent probes Eur J Biochem. 270(11):2343-52 (2003).
- Qiu, J., Tan, Y.W., Hagenston, A.M., Martel, M.A., Kneisel, N., Skehel, P.A., Wyllie, D.J., Bading, H., and Hardingham, G.E. Mitochondrial calcium uniporter Mcu controls excitotoxicity and is transcriptionally repressed by neuroprotective nuclear calcium signals. Nat Commun 4, 2034 (2013).
- Querfurth, H.W. and LaFerla, F.M. Alzheimer's disease. N Engl J Med. 362: 329-344 (2010).
- Raffaello, A., De Stefani, D., and Rizzuto, R. The mitochondrial Ca2+ uniporter. Cell Calcium 52, 16-21 (2012).
- Raffaello, A., De Stefani, D., Sabbadin, D., Teardo, E., Merli, G., Picard, A., Checchetto, V., Moro, S., Szabo, I., and Rizzuto, R. The mitochondrial calcium uniporter is a multimer that can include a dominant-negative pore-forming subunit. EMBO J 32, 2362-2376 (2013).
- Rapizzi, E., Pinton, P., Szabadkai, G., Wieckowski, M.R., Vandecasteele, G., Baird, G., Tuft, R.A., Fogarty, K.E., and Rizzuto, R. Recombinant expression of the voltage-dependent anion channel enhances the transfer of Ca2+ microdomains to mitochondria. *J Cell Biol* 159: 613–624 (2002).
- Rasola, A. and Bernardi, P. Mitochondrial permeability transition in Ca2+-dependent apoptosis and necrosis. Cell Calcium 50: 222– 233 (2011).
- Raturi, A. and Simmen T. Where the endoplasmic reticulum and the mitochondrion tie the knot: the mitochondria-associated membrane (MAM). Biochim Biophys Acta. 1833(1):213-224 (2013).
- Reits, E.A. and Neefjes, J.J. From fixed to FRAP: measuring protein mobility and activity in living cells. Nat. Cell Biol. 3, E145-147 (2001).
- Rizzuto, R. and Pozzan, T. Microdomains of intracellular Ca2+: molecular determinants and functional consequences. Physiol Rev. 86 (1): 369-408 (2006).
- Rizzuto, R., Brini, M., Murgia, M. and Pozzan, T. Microdomains with high Ca2+ close to IP3- sensitive channels that are sensed by neighboring mitochondria. Science 262 (5134):744–747 (1993).
- Rizzuto, R., Pinton, P., Brini, M., Chiesa, A., Filippin, L. and Pozzan, T. Mitochondria as biosensors of calcium microdomains. Cell Calcium 26(5):193–199 (1999).
- Rizzuto, R., Pinton, P., Carrington, W., Fay, F. S., Fogarty, K. E., Lifshitz, L. M., Tuft, R. A., and Pozzan, T. Close contacts with the endoplasmic reticulum as determinants of mitochondrial Ca2+ responses. *Science* 280, 1763–1766 (1998).
- Rizzuto, R., Simpson, A. W., Brini, M., and Pozzan, T. Rapid changes of mitochondrial Ca2+ revealed by specifically targeted recombinant aequorin. *Nature* 358, 325–327 (1992).
- Robertson, J.D. The molecular structure and contact relationships of cell membranes. Prog Biophys Mol Biol 10:343–418 (1960).
- Rowland, A.A. and Voeltz, G.K. Endoplasmic reticulum-mitochondria contacts: function of the junction. Nat Rev Mol Cell Biol. 13(10):607-265 (2012).
- Ruby, J.R., Dyer, R.F. and Skalko, R.G. Continuities between mitochondria and endoplasmic reticulum in the mammalian ovary. Z Zellforsch Mikrosk Anat 97(1):30–37 (1969).
- Rudolf, R., Mongillo, M., Rizzuto, R. and Pozzan, T. Looking forward to seeing calcium. Nat Rev Mol Cell Biol. 4 (7): 579-586 (2003).
- Rudolf, R., Mongillo, M., Rizzuto, R., and Pozzan, T. Looking forward to seeing calcium. Nat Rev Mol Cell Biol 4, 579-586 (2003).
- Sancak, Y., Markhard, A.L., Kitami, T., Kovacs-Bogdan, E., Kamer, K.J., Udeshi, N.D., Carr, S.A., Chaudhuri, D., Clapham, D.E., Li, A.A., Calvo, S.E., Goldberger, O. and Mootha, V.K. EMRE Is an Essential Component of the Mitochondrial Calcium Uniporter Complex. Science 342, 1379-1382 (2013).

- Saris, N.E., Sirota, T.V., Virtanen, I., Niva, K., Penttila, T., Dolgachova, L.P. and Mironova, G.D. Inhibition of the mitochondrial calcium uniporter by antibodies against a 40-kDa glycoproteinT. J Bioenerg Biomembr 25, 307-312 (1993).
- Scheuner, D., Eckman, C., Jensen, M., Song, X., Citron, M., Suzuki, N., Bird, T.D., Hardy, J., Hutton, M., Kukull, W., Larson, E., Levy-Lahad, E., Viitanen, M., Peskind, E., Poorkaj, P., Schellenberg, G., Tanzi, R., Wasco, W., Lannfelt, L., Selkoe, D., and Younkin, S. Secreted amyloid beta-protein similar to that in the senile plaques of Alzheimer's disease is increased in vivo by the presenilin 1 and 2 and APP mutations linked to familial Alzheimer's disease. Nat Med. 2 (8): 864-870 (1996).
- Schon, E.A. and Area-Gomez, E. Is Alzheimer's disease a disorder of mitochondria-associated membranes? J Alzheimers Dis 20(Suppl 2):S281–S292 (2010).
- Schwaller, B. The continuing disappearance of "pure" Ca2+ buffers. Cell Mol Life Sci. 66 (2): 275-300 (2009).
- Shilling, D., Mak, D.O., Kang, D.E. and Foskett, J.K. Lack of evidence for presenilins as endoplasmic reticulum Ca2+ leak channels. J Biol Chem. 287(14):10933-10944 (2012).
- Shimojo, M., Sahara, N., Murayama, M., Ichinose, H. and Takashima, A. Decreased Abeta secretion by cells expressing familial Alzheimer's disease-linked mutant presenilin 1. Neurosci Res. Mar; 57 (3): 446-53 (2007).
- Sottocasa, G., Sandri, G., Panfili, E., De Bernard, B., Gazzotti, P., Vasington, F.D., and Carafoli, E. Isolation of a soluble Ca2+ binding glycoprotein from ox liver mitochondria. Biochem Biophys Res Commun 47, 808-813 (1972).
- Stone, S. J. and Vance, J. E. Phosphatidylserine synthase-1 and -2 are localized to mitochondria-associated membranes. J. Biol. Chem. 275, 34534–34540 (2000).
- Streb, H., Irvine, R. F., Berridge, M. J., and Schulz, I. Release of Ca2+ from a nonmitochondrial intracellular store in pancreatic acinar cells by inositol-1,4,5-trisphosphate. *Nature* 306, 67–69 (1983).
- Strehler, E.E., Caride, A.J., Filoteo, A.G., Xiong, Y., Penniston, J.T. and Enyedi, A. Plasma membrane Ca2+ ATPases as dynamic regulators of cellular calcium handling. Ann N Y Acad Sci. 1099: 226-236 (2007).
- Sugiura, A., Nagashima, S., Tokuyama, T., Amo, T., Matsuki, Y., Ishido, S., Kudo, Y., McBride, H.M., Fukuda, T., Matsushita, N., Inatome, R., Yanagi, S. MITOL Regulates Endoplasmic Reticulum-Mitochondria Contacts via Mitofusin2. Mol Cell. 51, 20-34 (2013).
- Supnet, C. and Bezprozvanny, I. The dysregulation of intracellular calcium in Alzheimer disease. Cell Calcium 47: 183-189 (2010).
- Szabadkai, G. and Duchen, M. R. Mitochondria: The Hub of Cellular Ca2+ Signaling. Physiology 23: 84-94 (2008).
- Thinakaran, G. and Koo, E.H. Amyloid precursor protein trafficking, processing, and function. J Biol Chem. 283: 29615-29619 (2008).
- Tolia, A. and De Strooper, B. Structure and function of gamma-secretase. Semin Cell Dev Biol. 20: 211-218 (2009).
- Toyoshima, C. How Ca2+-ATPase pumps ions across the sarcoplasmic reticulum membrane. Biochim Biophys Acta. 1793 (6): 941-946 (2009).
- Trenker, M., Malli, R., Fertschai, I., Levak-Frank, S. and Graier, W.F. Uncoupling proteins 2 and 3 are fundamental for mitochondrial Ca2+ uniport. Nat Cell Biol 9:445–452 (2007).
- Tsien, R.Y. New calcium indicators and buffers with high selectivity against magnesium and protons: design, synthesis, and properties of prototype structures. Biochemistry. 19 (11): 2396-404 (1980).
- Tu, H., Nelson, O., Bezprozvanny, A., Wang, Z., Lee, S.F., Hao, Y.H., et al. Presenilins form ER Ca2+ leak channels a function disrupted by familial Alzheimer's disease-linked mutations. Cell 126: 981–993 (2006).
- Vance, J.E. Phospholipid synthesis in a membrane fraction associated with mitochondria. J Biol Chem 265(13):7248–7256 (1990).

- Vasington, F. D. and Murphy, J. V. Ca ion uptake by rat kidney mitochondria and its dependence on respiration and phosphorylation. J. Biol. Chem. 237, 2670–2677 (1962).
- Villa, A., Garcia-Simon, M.I., Blanco, P., Sese, B., Bogonez, E. and Satrustegui, J. Affinity chromatography purification of mitochondrial inner membrane proteins with calcium transport activity. Biochim Biophys Acta 1373:347–359 (1998).
- Waldeck-Weiermair, M., Malli, R., Naghdi, S., Trenker, M., Kahn, M.J. and Graier, W.F. The contribution of UCP2 and UCP3 to mitochondrial Ca(2+) uptake is differentially determined by the source of supplied Ca(2+). Cell Calcium 47:433–440 (2010).
- Walker, E.S., Martinez, M., Brunkan, A.L. and Goate, A. Presenilin 2 familial Alzheimer's disease mutations result in partial loss of function and dramatic changes in Abeta 42/40 ratios. J Neurochem. 92 (2): 294-301 (2005).
- Walsh, D.M., Klyubin, I., Fadeeva, J.V., Cullen, W.K., Anwyl, R., Wolfe, M.S., Rowan, M.J. and Selkoe, D.J. Naturally secreted oligomers of amyloid beta protein potently inhibit hippocampal long-term potentiation in vivo. Nature 416: 535-539 (2002).
- Wang, Y., Deng, X. and Gill, D.L. Calcium signaling by STIM and Orai: intimate coupling details revealed. Sci Signal 3 (148): pe42 (2010).
- Westermann, B. Mitochondrial fusion and fission in cell life and death. Nat. Rev. Mol. Cell Biol. 11, 872-884 (2010).
- Wieckowski, M.R., Giorgi, C., Lebiedzinska, M., Duszynski, J. and Pinton, P. Isolation of mitochondria-associated membranes and mitochondria from animal tissues and cells. Nat. Protoc. 4, 1582-1590 (2009).
- Wojda, U., Salinska, E. and Kuznicki, J. Calcium ions in neuronal degeneration. IUBMB Life 60: 575-590 (2008).
- Wolfe, M.S. and Guénette, S.Y. APP at a glance. J Cell Sci. 120: 3157-3161 (2007).
- Wong, A.K., Capitanio, P., Lissandron, V., Bortolozzi, M., Pozzan, T. and Pizzo, P. Heterogeneity of Ca2+ handling among and within Golgi compartments. J Mol Cell Biol. 5(4):266-276 (2013).
- Yi, M., Weaver, D. and Hajnoczky, G. Control of mitochondrial motility and distribution by the calcium signal: a homeostatic circuit. J Cell Biol 167(4):661–672 (2004).
- Yoo, A.S., Cheng, I., Chung, S., Grenfell, T.Z., Lee,,H., Pack-Chung, E., Handler, M., Shen, J., Xia, W., Tesco, G., Saunders, A.J., Ding, K., Frosch, M.P., Tanzi, R.E., Kim and T.W. Presenilin-mediated modulation of capacitative calcium entry. Neuron. 27: 561-572 (2000).
- Yu, J.T., Chang, R.C. and Tan, L. Calcium dysregulation in Alzheimer's disease: from mechanisms to therapeutic opportunities. Prog Neurobiol. 89: 240-255 (2009).
- Zampese, E. and Pizzo, P. Intracellular organelles in the saga of Ca^{2+} homeostasis: different molecules for different purposes? Cell Mol Life Sci. 69 (7): 1077:1104 (2012).
- Zampese, E., Fasolato, C., Kipanyula, M.J., Bortolozzi, M., Pozzan, T. and Pizzo, P. Presenilin 2 modulates endoplasmic reticulum (ER)-mitochondria interactions and Ca2+ cross-talk. Proc Natl Acad Sci U S A. 108(7):2777-2782 (2011).
- Zatti, G., Burgo, A., Giacomello, M., Barbiero, L., Ghidoni, R., Sinigaglia, G., Florean, C., Bagnoli, S., Binetti, G., Sorbi, S., Pizzo, P. and Fasolato, C. Presenilin mutations linked to familial Alzheimer's disease reduce endoplasmic reticulum and Golgi apparatus calcium levels. Cell Calcium 39 (6): 539-550 (2006).
- Zatti, G., Ghidoni, R., Barbiero, L., Binetti, G., Pozzan, T., Fasolato, C. and Pizzo, P. The presenilin 2 M239I mutation associated with familial Alzheimer's disease reduces Ca2+ release from intracellular stores. Neurobiol Dis. 15 (2): 269-278 (2004).
- Zazueta, C., Holguin, J.A., and Ramirez, J. Calcium transport sensitive to ruthenium red in cytochrome oxidase vesicles reconstituted with mitochondrial proteins. J Bioenerg Biomembr 23, 889-902 (1991).
- Zheng, H. and Koo, E.H. The amyloid precursor protein: beyond amyloid. Mol Neurodegener. 3: 1-5 (2006).

AKNOWLEDGEMENTS

I am grateful to Gabriele Turacchio and Elisa Greotti for performing EM and FRAP experiments, respectively. Thanks to Prof. Tullio Pozzan for the opportunity to work in his lab and to Dr. Paola Pizzo for leading my project and continuous support.

Finally, special thanks to my family and friends.

ATTACHMENTS